

DISSERTATION

THE ECOLOGICAL AND EVOLUTIONARY MECHANISMS BEHIND THE
PERSISTENCE OF HIGHLY VIRULENT PATHOGENS: PLAGUE AS A CASE STUDY

Submitted by

Michael G. Buhnerkempe

Department of Biology

In partial fulfillment of the requirements

For the Degree of Doctor of Philosophy

Colorado State University

Fort Collins, Colorado

Spring 2013

Doctoral Committee:

Advisor: Colleen T. Webb

N. LeRoy Poff

Rebecca J. Eisen

Jennifer A. Hoeting

ABSTRACT

THE ECOLOGICAL AND EVOLUTIONARY MECHANISMS BEHIND THE PERSISTENCE OF HIGHLY VIRULENT PATHOGENS: PLAGUE AS A CASE STUDY

The persistence of emerging infectious diseases is the result of eco-evolutionary feedbacks between a pathogen and its novel host. Spatial structure both within and between host populations (i.e., a metapopulation) in particular can have a large effect on the establishment and subsequent coevolution of a host and pathogen. Here, my colleagues and I explore how differing metapopulation structures in a host and pathogen affect the coevolutionary maintenance of high virulence and low resistance in an emerging infectious disease. We use the relatively recent emergence of plague, caused by the bacterium *Yersinia pestis*, in North America as a case study to both understand how spatial structure in the pathogen may differ from that of its host and how these differences may affect coevolutionary trajectories.

Host responses to *Y. pestis* infection are highly variable with some species, like black-tailed prairie dogs (*Cynomys ludovicianus*), experiencing massive population declines upon introduction of the plague bacterium (i.e., epizootics), while others, like the California ground squirrel (*Spermophilus beecheyi*), exhibit enzootic maintenance of *Y. pestis*. These species in particular have markedly different spatial structures, but it is unclear how regional transmission of plague may structure the pathogen population. To understand transmission more fully, we developed a mechanistic model of plague infection in a single population that incorporated multiple routes of transmission and parameterized the model for the two species mentioned above. We found that transmission in the epizootic system is driven largely through on-host

cycling of fleas (i.e., a booster-feed infection cycle). In contrast, enzootics are driven by an off-host, questing flea reservoir.

The potential for off-host fleas to drive plague dynamics reveals the potential for non-overlapping host and pathogen metapopulation structures. The effect of such a structure on coevolution is not well-understood, particularly for quantitative traits where no theoretical methods exist to study coevolution in a metapopulation. Consequently, we also developed a novel theoretical framework for studying quantitative trait coevolution in a metapopulation. This new framework reveals that coevolutionary outcomes for resistance and virulence depend on the interaction between host and pathogen dispersal strategies with local reproduction and transmission dynamics favoring a diversity of resistance-virulence combinations. Host-pathogen coevolution is also affected by the shape of life-history trade-offs for both the host and the pathogen. We predicted coevolutionary outcomes under different host and pathogen dispersals assuming three different trade-off functions when resistance comes at the cost of reproduction and virulence increases transmission while decreasing the infectious period: accelerating, linear, and decelerating costs. We found that selection on resistance is most sensitive to concave trade-off functions, and selection on virulence was most sensitive to convex functions, although coevolutionarily stable strategies were only predicted when both resistance and virulence had accelerating cost trade-off functions. Predictions from the model also differ from those observed in well-mixed and spatially structured single populations indicating that eco-evolutionary dynamics do not scale directly with space.

Implications for future models of plague coevolution are also discussed.

ACKNOWLEDGEMENTS

Funding for this work was provided by NSF-IGERT Grant DGE-#0221595, administered by the PRIMES program at Colorado State University; Foreign Animal Disease Modeling Program, Science and Technology Directorate, U. S. Department of Homeland Security (Grant ST-108-000017); and USDA Cooperative Agreements 11-9208-0269-CA 11-1 and 09-9208-0235-CA. I also acknowledge support from a Centers for Disease Control and Prevention Regular Fellowship. I would like to thank the Webb Lab, especially Clint Leach, Andrew Kanarek, and Greg Ames, for useful discussions on conceptual and methodological issues related to this work. Additionally, I would like to thank my committee members, Rebecca Eisen, LeRoy Poff, and Jennifer Hoeting, and especially my advisor, Colleen Webb, for the useful feedback on this manuscript and work in general. Finally, I am deeply grateful for the continued support of my family and especially to my wife, Billie Buhnerkempe, for her love and encouragement without which this would not have been possible.

TABLE OF CONTENTS

ABSTRACT.....	ii
ACKNOWLEDGEMENTS.....	iv
CHAPTER 1 – Emerging infectious diseases: establishment and persistence.....	1
CHAPTER 2 – Transmission shifts underlie variability in population responses to <i>Yersinia pestis</i> infection	13
CHAPTER 3 – Dispersal strategies alter coevolutionary trajectories for host resistance and pathogen virulence in a metapopulation	45
CHAPTER 4 – The interaction of resistance-reproduction and virulence-transmission trade-offs, coevolution, and spatial structure in a metapopulation.....	79
CHAPTER 5 – General conclusions.....	104

CHAPTER 1

EMERGING INFECTIOUS DISEASES: ESTABLISHMENT AND PERSISTENCE

Emerging infectious diseases are a growing problem around the world (Daszak et al. 2010; Cunningham et al. 2012). These previously unobserved pathogens are of particular concern because emergence is often associated with cross-species jumps into naïve hosts that often experience high mortality (Cunningham et al. 2012). In particular, wildlife and domestic animal reservoirs for many emerging pathogens allow for repeated introductions into novel host populations (e.g., Hendra [Murray et al. 1995a, 1995b], Nipah [Chua et al. 1999, 2000] and Ebola viruses [Guenno et al. 1995; Towner et al. 2008]), but this spillover does little to explain the likelihood of establishment and potential endemic maintenance of highly virulent pathogens (i.e., causing high mortality in the host). Many ecological mechanisms have been thought to promote establishment and endemic maintenance of highly virulent pathogens (e.g., host birth pulses [Altizer et al. 2006; George et al. 2011], seasonal host mixing patterns [Grenfell 1992; Altizer et al. 2006; George et al. 2011]), but spatial structure in host populations has received considerable support as a viable mechanism underlying pathogen persistence.

Theoretical studies have shown that the division of a host population into a large number of sub-populations (i.e., a metapopulation) can promote persistence of pathogen (Grenfell and Harwood 1997; Swinton 1998; Park et al. 2002). Long-term persistence due to the spatial subdivision of the susceptible population has been observed in measles (Grenfell 1992; Bolker and Grenfell 1995), phocine distemper in harbour seals (*Phoca vitulina*; Swinton et al. 1998), and plant/pathogen associations (Burdon and Thrall 1999). Additionally, spatial structure in the pathogen population as a result epidemiological coupling between spatially distinct patches can

impact pathogen persistence with the longest persistence times observed at intermediate levels of coupling (Grenfell and Harwood 1997; Keeling 2000; Hagenaars et al. 2004). Spatial effects in the pathogen population were seen in the varying transmission mechanisms for schistosomiasis both within and between sub-Saharan African villages with a combination of mechanisms creating sustained regional persistence in the absence of village-level persistence (Gurarie and Seto 2008). However, ecological persistence does not by itself explain why some spatially structured host-pathogen systems have failed to coevolve away from the high virulence and low resistance that characterize emergence (e.g., bubonic plague in black-tailed prairie dogs towns; Cully and Williams 2001), while other spatially structured host-pathogen systems have seen reductions in virulence coupled with increases in resistance (e.g., myxomatosis in European rabbit warrens; Fenner and Ratcliffe 1965; Levin and Pimental 1981). Thus, it is crucial to understand how spatial structure in hosts and pathogens mediate coevolutionary pressures that allow for long-term maintenance of highly virulent pathogens in wholly susceptible hosts.

Attempts to study the effects of spatial structure on host/pathogen coevolution have explored a range of potential spatial structures from metapopulations to single, structured populations. Metapopulation studies of coevolution have made use of gene-for-gene models (Thrall and Burdon 2002) or matching allele models (Gandon et al. 1996; Gandon 2002). In both of these approaches, the genetic basis for resistance and virulence is specifically modeled with phenotypes for the host and pathogen dependent on the genotype of the other. These explicit genetic models point to an interaction between host and pathogen dispersal in determining coevolutionary outcomes (Thompson and Burdon 1992; Gandon et al. 1996; Gandon 2002; Thrall and Burdon 2002; Nuismer 2006). Here, when pathogen dispersal is higher than host dispersal, the pathogen remains virulent as it is more locally adapted to the host (Gandon et al.

1996; Gandon 2002; Nuismer 2006), while hosts become more resistant to local pathogen populations when host dispersal is higher (Gandon et al. 1996; Gandon 2002). Consequently, greater genotypic diversity for both resistance and virulence is observed when dispersal is local (Thrall and Burdon 2002). These types of models have been used to understand several natural systems including plant-pathogen interactions (Thompson and Burdon 1992; Burdon and Thrall 1999; Thrall et al. 2002; Thrall and Burdon 2003) and laboratory studies of bacteria and their associated bacteriophages (Buckling and Rainey 2002; Morgan et al. 2005; Vogwill et al. 2008). Despite the insights gained into these relatively simple host-pathogen systems, gene-for-gene and matching allele models are not readily generalizable across mammalian disease systems, where the genetic architecture underlying host resistance and parasite virulence can become considerably more complex (Sorci et al. 1997). Consequently, models of quantitative trait coevolution within a metapopulation are needed to further our understanding of the ecological impacts of spatial structure and dispersal on coevolutionary dynamics of emerging infectious diseases.

To this point, the only models to incorporate spatial structure with quantitative trait evolution have focused on single, structured populations (Boots and Sasaki 1999; Haraguchi and Sasaki 2000; Boots et al. 2004; Lion and Boots 2010; Best et al. 2011). These studies used nearest-neighbor networks of individuals placed on a grid to represent spatial structure and found that increased spatial structure due to local transmission selects for decreased virulence (Boots and Sasaki 1999; Haraguchi and Sasaki 2000; Boots et al. 2004; Lion and Boots 2010; Best et al. 2011). Similarly, local transmission and local host reproduction on the grid, which both promote spatial structure, select for higher resistance and lower virulence (Best et al. 2011). This coevolutionary outcome can be altered, however, by changing the relative scaling between local-

global reproduction and local-global transmission resulting in interactions between host and pathogen dispersal strategies (Best et al. 2011). Additionally, evolutionary outcomes in even simple systems can be altered according to the life-history trade-offs experienced by the pathogen (Alizon et al. 2009). Specifically, virulence is commonly assumed to increase the transmissibility of a pathogen, and the shape of the trade-off function underlying this relationship can alter evolutionary trajectories (Kamo et al. 2007). While promising, it is unclear how to compare this body of work to previous gene-for-gene models at the metapopulation scale to determine how coevolutionary effects scale across hierarchical levels of structure. Consequently, the work on quantitative trait coevolution needs to be extended to include metapopulation dynamics in order to capture a wide variety of host-pathogen systems (Sorci et al. 1997). However, no models of quantitative trait coevolution in a metapopulation currently exist highlighting the need for theoretical as well as empirical advancements in studying the effects of spatial structure on resistance-virulence coevolution.

Bubonic plague in North America provides a useful empirical system to begin to develop and combine ideas about the coevolutionary effects of host and pathogen metapopulation structure. Plague is caused by the bacterium *Yersinia pestis* which is a highly virulent pathogen that is spread primarily via infectious fleas. It was introduced to the United States in the early 20th century, and since that time, it has spread through much of the western U.S (Barnes 1982; Eskey and Haas 1940). *Y. pestis* affects numerous mammal species in the U.S. and responses to *Y. pestis* infection are highly variable (Gage and Kosoy 2005). Some species, like the California ground squirrel (*Spermophilus beecheyi*), exhibit relatively high levels of resistance (Williams et al. 1979), while others, like the black-tailed prairie dog (*Cynomys ludovicianus*) exhibit little resistance to *Y. pestis* infection and experience nearly 100% mortality (Cully and Williams

2001). Although the genetic mechanisms underlying host resistance to plague are not entirely clear, multiple genes are usually assumed to underlie host resistance to infectious diseases (Sorci et al. 1997). Resistance in plague hosts has long been thought to exhibit polygenic inheritance (Hubbert and Goldenberg 1970), and more recent QTL mapping of genetic differences in hosts between plague free and endemic areas in Madagascar has identified 22 loci that may be under selection due to *Y. pestis* infection (Tollenaere et al. 2010). Additionally, virulence of the plague bacterium is determined by multiple virulence factors making it a good candidate for the study of quantitative trait evolution (Gage and Kosoy 2005).

Although the ecological mechanisms underlying plague persistence in the western U.S. are not completely understood, the plague bacterium is most commonly hypothesized to persist in maintenance host populations that show high resistance to plague infection with epizootics caused by spill-over events to highly susceptible species (Gage and Kosoy 2005). However, specifying hosts as the primary pathogen reservoir completely ignores the role of the flea vector in long-term persistence and spread. Additionally, recent studies of plague dynamics in black-tailed prairie dogs support the notion that spatial structure in these populations could lead to regional persistence (Snäll et al. 2008; George 2009). Similarly, California ground squirrel populations exhibit spatial structure, but inter-patch distances are much smaller than in prairie dog populations (Evans and Holdenried 1943; Dobson 1979; Stapp et al. 2004). Smaller inter-patch distances may lead to greater dispersal rates and mixing, and indeed, California ground squirrels have been observed to quickly respond to local density fluctuations by moving to areas of low density (Dobson 1979). Thus, coevolutionary differences in pathogen virulence and host resistance between species like the black-tailed prairie dog and the California ground squirrel may be a result of differing spatial structures and host mixing patterns.

As other work has shown, coevolutionary outcomes are not only affected by the dispersal strategy of the host but of the pathogen as well (Gandon et al. 1996; Best et al. 2011). However, the dispersal strategy of the pathogen is dependent on the mode of transmission (Gurarie and Seto 2008). Blocked-flea transmission has long been the dominant paradigm for plague transmission (Bacot and Martin 1914), but this route has been shown to be ineffective at driving plague dynamics in prairie dogs (Webb et al. 2006). Transmission of the plague bacterium in the absence of blockage has been shown to be a viable alternative (Eisen et al. 2006), but its role in natural plague dynamics is not well understood. Additionally, *Y. pestis* is capable of persisting in infected carcasses and the surrounding soil for one to two weeks providing another potential transmission mechanism (Ber et al. 2003; Eisen et al. 2008). Determining the relative importance of these transmission mechanisms within local populations can help to determine the dispersal rate of the pathogen. In particular, carcass transmission would promote local transmission, while a flea reservoir underlying transmission may itself be spatially structured and not entirely dependent on the host for dispersal leading to more global dispersal (Brinkerhoff et al. 2011).

Here, I will explore the ecological effects of metapopulation structure and dispersal on the coevolution of host resistance and pathogen virulence loosely based on plague infection in black-tailed prairie dogs and California ground squirrels. In Chapter 2, I study the factors that give rise to differences in species-specific responses to *Y. pestis* infection at the subpopulation level (i.e., enzootic vs. epizootic dynamics) in order to better understand the epizootiologically relevant processes that scale up to determine transmission between subpopulations. Specifically, I construct a general model of plague dynamics parameterized both for prairie dogs and California ground squirrels that combines multiple transmission routes to identify if flea-borne transmission differs between these two species and how this may determine dispersal of the

pathogen between host populations. I then aim to determine how differing dispersal patterns driven by potential differences in flea-borne transmission and host movement affect the coevolutionary trajectories of host resistance and virulence of the plague bacterium in these two hosts. However, as mentioned previously, no methods currently exist to theoretically study quantitative trait coevolution in a metapopulation. Thus, in Chapter 3, I present a novel modeling framework to address this problem. This framework is inspired by the plague system, although it is not a plague-specific model. Consequently, it provides an intuitive understanding of coevolutionary processes under varying dispersal strategies on which to study specific host-pathogen systems. The intuition developed in Chapter 3 is expanded on in Chapter 4 by the inclusion of multiple different tradeoff functions between host resistance and reproduction and pathogen virulence and transmission. The functional form of these tradeoffs has been found to alter coevolutionary trajectories in single populations (Kamo et al. 2007), and thus, a better understanding of their effect in a metapopulation context is needed to fully understand ecological feedbacks on host-pathogen coevolution. I conclude with a discussion of the application of these novel methods to the plague system and other host-pathogen systems in general.

LITERATURE CITED

- Alizon, S., A. Hurford, N. Mideo, and M. Van Baalen. 2009. Virulence evolution and the trade-off hypothesis: history, current state of affairs and the future. *Journal of Evolutionary Biology* 22: 245-259.
- Altizer, S., A. Dobson, P. Hosseini, P. Hudson, M. Pascual, and P. Rohani. 2006. Seasonality and the dynamics of infectious diseases. *Ecology Letters* 9: 467-484.
- Bacot, A.W. and C.J. Martin. 1914. Observations on the mechanism of the transmission of plague by fleas. *Journal of Hygiene* 13: 423-439.
- Barnes, A.M. 1982. Surveillance and control of bubonic plague in the United States. *Symposia of the Zoological Society of London* 50: 237-270.
- Ber, R., E. Mamroud, M. Aftalion, A. Tidhar, D. Gur, Y. Flashner, and S. Cohen. 2003. Development of an improved selective agar medium for isolation of *Yersinia pestis*. *Applied and Environmental Microbiology* 69: 5787-5792.
- Best, A., S. Webb, A. White, and M. Boots. 2011. Host resistance and coevolution in spatially structured populations. *Proceedings of the Royal Society Series B* 278: 2216-2222.
- Bolker, B. and B. Grenfell. 1995. Space, persistence and dynamics of measles. *Philosophical Transactions of the Royal Society Series B* 348: 309-320.
- Boots, M. and A. Sasaki. 1999. 'Small worlds' and the evolution of virulence: infection occurs locally and at a distance. *Proceedings of the Royal Society Series B* 266: 1933-1938.
- Boots, M., P.J. Hudson, and A. Sasaki. 2004. Large shifts in pathogen virulence relate to host population structure. *Science* 303: 842-844.
- Brinkerhoff, R.J., A.P. Martin, R.T. Jones, and S.K. Collinge. 2011. Population genetic structure of the prairie dog flea and plague vector, *Oropsylla hirsuta*. *Parasitology* 138: 71-79.
- Buckling, A. and P.B. Rainey. 2002. Antagonistic coevolution between a bacterium and a bacteriophage. *Proceedings of the Royal Society Series B* 269: 931-936.
- Burdon, J.J. and P.H. Thrall. 1999. Spatial and temporal patterns in coevolving plant and pathogen associations. *American Naturalist* 153: S15-33.
- Chua, K.B., K.J. Goh, K.T. Wong, A. Kamarulzaman, P.S.K. Tan, T.G. Ksiazek, S.R. Zaki, G. Paul, S.K. Lam, and C.T. Tan. 1999. Fatal encephalitis due to Nipah virus among pig-farmers in Malaysia. *Lancet* 354: 1257-1259.
- Chua, K.B., W.J. Bellini, P.A. Rota, B.H. Harcourt, A. Tamin, S.K. Lam, T.G. Ksiazek, P.E. Rollin, S.R. Zaki, W.-J. Shieh, C.S. Goldsmith, D.J. Gubler, J.T. Roehrig, B. Eaton, A.R.

- Gould, J. Olson, H. Field, P. Daniels, A.E. Ling, C.J. Peters, L.J. Anderson, and B.W.J. Mahy. 2000. Nipah virus: a recently emergent deadly paramyxovirus. *Science* 288: 1432-1435.
- Cully, J.F. and E.S. Williams. 2001. Interspecific comparisons of sylvatic plague in prairie dogs. *Journal of Mammalogy* 82: 894-905.
- Cunningham, A.A., A.P. Dobson, and P.J. Hudson. 2012. Disease invasion: impacts on biodiversity and human health. *Philosophical Transactions of the Royal Society Series B* 367: 2804-2806.
- Daszak, P., A.A. Cunningham, and A.D. Hyatt. 2010. Emerging infectious diseases of wildlife – threats to biodiversity and human health. *Science* 287: 443-449.
- Dobson, F.S. 1979. An experimental study of dispersal in the California ground squirrel. *Ecology* 60: 1103-1109.
- Eisen, R.J., S.W. Bearden, A.P. Wilder, J.A. Montenieri, M.F. Antolin, and K.L. Gage. 2006. Early-phase transmission of *Yersinia pestis* by unblocked fleas as a mechanism explaining rapidly spreading plague epizootics. *PNAS* 103: 15380-15385.
- Eisen, R.J., J.M. Petersen, C.L. Higgins, D. Wong, C.E. Levy, P.S. Mead, M.E. Schriefer, K.S. Griffith, K.L. Gage, and C.B. Beard. 2008. Persistence of *Yersinia pestis* in soil under natural conditions. *Emerging Infectious Diseases* 14: 941-943.
- Eskey, C.R. and V.H. Haas. 1940. Plague in the western part of the United States. *Public Health Bulletin* 254: 1-82.
- Evans, F.C. and R. Holdenried. 1943. A population study of the Beechey ground squirrel in central California. *Journal of Mammalogy* 24: 231-260.
- Fenner, F. and F.N. Ratcliffe. 1965. *Myxomatosis*. Cambridge University Press: Cambridge, England.
- Gage, K.L. and M.Y. Kosoy. 2005. Natural history of plague: perspectives from more than a century of research. *Annual Review of Entomology* 50: 505-528.
- Gandon, S., Y. Capowiez, Y. Dubois, Y. Michalakis, and I. Olivieri. 1996. Local adaptation and gene-for-gene coevolution in a metapopulation model. *Proceedings of the Royal Society Series B* 263: 1003-1009.
- Gandon, S. 2002. Local adaptation and the geometry of host-parasite coevolution. *Ecology Letters* 5: 246-256.
- George, D. 2009 Pathogen persistence in wildlife populations: Case studies of plague in prairie dogs and rabies in bats. PhD Thesis, Colorado State University.

- George, D.B., C.T. Webb, M.L. Farnsworth, T.J. O'Shea, R.A. Bowen, D.L. Smith, T.R. Stanley, L.E. Ellison, and C.E. Rupprecht. 2011. Host and viral ecology determine bat rabies seasonality and maintenance. *PNAS* 108: 10208-10213.
- Grenfell, B. 1992. Chance and chaos in measles dynamics. *Journal of the Royal Statistical Society Series B* 54: 383-398.
- Grenfell, B., and J. Harwood. 1997. (Meta)population dynamics of infectious diseases. *Trends in Ecology and Evolution* 12: 395-399.
- Guenno, B.L., P. Formenty, M. Wyers, P. Gounon, F. Walker, and C. Boesch. 1995. Isolation and partial characterisation of a new strain of Ebola virus. *Lancet* 345: 1271-1274.
- Gurarie, D. and E.Y.W. Seto. 2008. Connectivity sustains disease transmission in environments with low potential for endemicity: modeling schistosomiasis with hydrologic and social connectivities. *Journal of the Royal Society Interface* 6: 495-508.
- Hagenaars, T.J., C.A. Donnelly, and N.M. Ferguson. 2004. Spatial heterogeneity and the persistence of infectious diseases. *Journal of Theoretical Biology* 229: 349-359.
- Haraguchi, Y. and A. Sasaki. 2000. The evolution of pathogen virulence and transmission rate in a spatially structured population. *Journal of Theoretical Biology* 203: 85-96.
- Hubbert, W.T., and M.I. Goldenberg. 1970. Natural resistance to plague: genetic basis in the vole (*Microtus californicus*). *American Journal of Tropical Medicine and Hygiene* 19: 1015-1019.
- Kamo, M., A. Sasaki, and M. Boots. 2007. The role of trade-off shapes in the evolution of parasites in spatial host populations: an approximate analytical approach. *Journal of Theoretical Biology* 244: 588-596.
- Levin, S., and D. Pimental. 1981. Selection of intermediate rates of increase in pathogen-host systems. *American Naturalist* 117: 308-315.
- Lion, S. and M. Boots. 2010. Are pathogens "prudent" in space? *Ecology Letters* 13: 1245-1255.
- Morgan, A.D., S. Gandon, and A. Buckling. 2005. The effect of migration on local adaptation in a coevolving host-parasite system. *Nature* 437: 253-256.
- Murray, K., R. Rogers, L. Selvey, P. Selleck, A. Hyatt, A. Gould, L. Gleeson, P. Hooper, and H. Westbury. 1995a. A novel morbillivirus pneumonia of horses and its transmission to humans. *Emerging Infectious Diseases* 1: 31-33.

- Murray, K., P. Selleck, P. Hooper, A. Hyatt, A. Gould, L. Gleeson, H. Westbury, L. Hiley, L. Selvey, B. Rodwell, and P. Ketterer. 1995b. A morbillivirus that caused fatal disease in horses and humans. *Science* 268: 94-97.
- Nuismer, S. 2006. Parasite local adaptation in a geographic mosaic. *Evolution* 60: 24-30.
- Park, A.W., S. Gubbins, and C.A. Gilligan. 2002. Extinction times for closed epidemics: the effects of host spatial structure. *Ecology Letters* 5: 747-755.
- Snäll, T., R.B. O'Hara, C. Ray, and S.K. Collinge. 2008. Climate-driven spatial dynamics of plague among prairie dog colonies. *American Naturalist* 171: 238-248.
- Sorci, G., A.P. Møller, and T. Boulinier. 1997. Genetics of host-parasite interactions. *Trends in Ecology and Evolution* 12: 196-200.
- Stapp, P., M.F. Antolin, and M. Ball. 2004. Patterns of extinction in prairie dog metapopulations: plague outbreaks follow El Niño events. *Frontiers in Ecology and the Environment* 2: 235-240.
- Swinton, J. 1998. Extinction times and phase transitions for spatially structured closed epidemics. *Bulletin of Mathematical Biology* 60: 215-230.
- Swinton, J., J. Harwood, B.T. Grenfell, and C.A. Gilligan. 1998. Persistence thresholds for phocine distemper virus infection in harbor seal *Phoca vitulina* metapopulations. *Journal of Animal Ecology* 67: 54-68.
- Thompson, J.N. and J.J. Burdon. 1992. Gene-for-gene coevolution between plants and parasites. *Nature* 360: 121-125.
- Thrall, P.H. and J.J. Burdon. 2002. Evolution of gene-for-gene systems in metapopulations: the effect of spatial scale of host and pathogen dispersal. *Plant Pathology* 51: 169-184.
- Thrall, P.H. and J.J. Burdon. 2003. Evolution of virulence in a plant host-pathogen metapopulation. *Science* 299: 1735-1737.
- Thrall, P.H., J.J. Burdon, and A. Young. 2002. Variation in resistance and virulence among demes of a plant host-pathogen metapopulation. *Journal of Ecology* 89: 736-748.
- Tollenaere, C., J.-M. Duplantier, L. Rahalison, M. Ranjalahy, and C. Brouat. 2010. AFLP genome scan in the black rat (*Rattus rattus*) from Madagascar: detecting genetic markers undergoing plague-mediated selection. *Molecular Ecology* 20: 1026-1038.
- Towner, J.S., T.K. Sealy, M.L. Khristova, C.G. Albariño, S. Conlan, S.A. Reeder, P.-L. Quan, W.I. Lipkin, R. Downing, J.W. Tappero, S. Okware, J. Lutwama, B. Bakamutumaho, J. Kayiwa, J.A. Comer, P.E. Rollin, T.G. Ksiazek, and S.T. Nichol. 2008. Newly discovered

- Ebola virus associated with hemorrhagic fever outbreak in Uganda. *PLoS Pathogens* 4: e1000212.
- Vogwill, T., A. Fenton, and M.A. Brockhurst. 2008. The impact of parasite dispersal on antagonistic host-parasite coevolution. *Journal of Evolutionary Biology* 21: 1252-1258.
- Webb, C.T., C.P. Brooks, K.L. Gage, and M.F. Antolin. 2006. Classic flea-borne transmission does not drive plague epizootics in prairie dogs. *PNAS* 103: 6236-6241.
- Williams, J.E., M.A. Moussa, and D.C. Cavanaugh. 1979. Experimental plague in the California ground squirrel. *Journal of Infectious Diseases* 140: 618-621.

CHAPTER 2

TRANSMISSION SHIFTS UNDERLIE VARIABILITY IN POPULATION RESPONSES TO *YERSINIA PESTIS* INFECTION^{1,2}

Summary

Host populations for the plague bacterium, *Yersinia pestis*, are highly variable in their response to plague ranging from near deterministic extinction (i.e., epizootic dynamics) to a low probability of extinction despite persistent infection (i.e., enzootic dynamics). Much of the work to understand this variability has focused on specific host characteristics, such as population size and resistance, and their role in determining plague dynamics. Here, however, we advance the idea that the relative importance of alternative transmission routes may vary causing shifts from epizootic to enzootic dynamics. We present a model that incorporates host and flea ecology with multiple transmission hypotheses to study how transmission shifts determine population responses to plague. Our results suggest enzootic persistence relies on infection of an off-host

¹This work was previously published in PLoS ONE and is reprinted here with minor formatting changes under the journal's open access agreement with permission from the authors. Please see:

Buhnerkempe, M.G., Eisen, R.J., Goodell, B., Gage, K.L., Antonin, M.F., and Webb, C.T. 2011. Transmission shifts underlie variability in population responses to *Yersinia pestis* infection. PLoS ONE 6: e22498.

²Co-authors for this chapter include:

Colleen T. Webb, Brandon Goodell, and Michael F. Antonin

Department of Biology, Colorado State University, Fort Collins, CO 80523, USA

Rebecca J. Eisen and Kenneth L. Gage

Division of Vector-Borne Infectious Diseases, Centers for Disease Control, Fort Collins, CO 80522, USA

flea reservoir and epizootics rely on transiently maintained flea infection loads through repeated infectious feeds by fleas. In either case, early-phase transmission by fleas (i.e., transmission immediately following an infected blood meal) has been observed in laboratory studies, and we show that it is capable of driving plague dynamics at the population level. Sensitivity analysis of model parameters revealed that host characteristics (e.g., population size and resistance) vary in importance depending on transmission dynamics, suggesting that host ecology may scale differently through different transmission routes enabling prediction of population responses in a more robust way than using either host characteristics or transmission shifts alone.

Introduction

Plague, caused by the bacterium *Yersinia pestis*, remains a public health concern because of its high virulence in multiple mammal species, including humans, and its role in past pandemics in humans. Despite its historical importance and the continued threat of human cases, plague is primarily a disease of rodents and their fleas. Consequently, humans are at greatest risk of exposure to *Y. pestis* during plague epizootics when rodent hosts die in large numbers increasing potential exposures to sick or dead animals and infectious fleas [1]. Thus, understanding outbreaks in rodents may aid in prediction, control and prevention of human cases.

However, rodent species show high variability in their population-level response to plague infection, and the mechanisms that determine outbreak conditions are not fully understood. The variability in host response can be compartmentalized into two classes: either enzootic (i.e., low probability of extinction despite persistent infection in a population) or epizootic (i.e., high probability of extinction due to plague). This classification enables

predictions that can be based on observable intra-population dynamics rather than invoking landscape-level maintenance mechanisms involving the interaction of plague dynamics in multiple species [2-4].

Previous research on plague dynamics depended on observation of host characteristics to differentiate between epizootic and enzootic populations. For example, enzootic hosts, such as great gerbils (*Rhombomys opimus*) in Kazakhstan, show high levels of prolonged resistance (40-60% of hosts; [4]) while epizootic hosts, like black-tailed prairie dogs (*Cynomys ludovicianus*), rarely survive plague infection [5]. In gerbils, disease prevalence also exhibits a threshold behavior with host abundance where plague fails to persist below the threshold [6,7] and prevalence increases with host abundance above the threshold [8]. While these observations aid in prediction, they largely ignore one of the key components in plague dynamics: fleas and their effect on transmission.

Here, we propose that shifts from enzootic to epizootic dynamics could be accounted for by variation in the relative strength of alternative transmission routes, an avenue of plague research that has received relatively little attention. Theoretical work supports the notion that heterogeneities in transmission rates determine population disease dynamics [9-11]. For almost a century, a single transmission route depending upon blocked fleas (i.e., formation of a biofilm in a flea's midgut resulting in continued feeding attempts and subsequent regurgitation of bacteria) has been the dominant transmission paradigm for plague [4,12]. This focus has left other transmission routes relatively unexplored, but a recent modeling study questioned the role of blocked-fleas in plague dynamics sparking interest in alternative transmission routes [13].

Experimentally studying transmission routes in natural systems is nearly impossible, but laboratory experiments have identified effective transmission routes that could also affect

population responses to plague infection. In particular, early-phase transmission by un-blocked fleas (i.e., transmission immediately following an infectious blood meal) has been shown to be a viable alternative to blocked-flea transmission in several flea species under laboratory conditions [14-19]. A “booster” feed infection cycle (i.e., continued blood meals on infectious hosts that boost the density of *Y. pestis* in the flea) allows for the maintenance of infection levels in fleas and increases infectious duration for early-phase transmission [20]. In addition, the role of transmission from external reservoirs, such as infected, questing (i.e., host-seeking) fleas [4,21,22] or infected carcasses [23], is largely unstudied but potentially important. Indeed, infected questing fleas have survived for over a year in the field [24-27], and viable *Y. pestis* has survived in carcasses and soil for several days under both field and laboratory conditions [28-30].

In order to simultaneously consider how multiple transmission routes interact to determine plague dynamics, we present a general model of *Y. pestis* dynamics that incorporates three routes of plague transmission: 1) the booster-feed infection cycle; 2) the build-up of infectious, questing fleas; and 3) contact with carcass-derived material. We parameterize the model for an epizootic host, the black-tailed prairie dog, and for an enzootic host, the California ground squirrel (*Spermophilus beecheyi*). We sequentially remove or reduce each transmission route to understand how the influence of each route may vary between characteristic epizootic and enzootic hosts. We also use sensitivity analysis of model parameters to quantify the importance of transmission routes across a broader range of species and to explore how previously identified host characteristics interact with transmission to improve prediction of plague dynamics.

Methods

We developed an ordinary differential equation (ODE) model consisting of both host and flea submodels (Eqs. 1-11; Figs. 2.4 and 2.5). Host and flea classes and model parameters are defined in tables 2.1 and 2.2, respectively.

Host Submodel

$$\frac{dS}{dt} = r(S + R) \left(1 - \frac{N}{K}\right) - \beta_E F_{EQ} S \left(1 - e^{-\frac{aN}{B}}\right) - \beta_L F_{LQ} S \left(1 - e^{-\frac{aN}{B}}\right) - \beta_R S \frac{M}{B} - \mu S + \phi R \quad (1)$$

$$\frac{dE}{dt} = \beta_E F_{EQ} S \left(1 - e^{-\frac{aN}{B}}\right) + \beta_L F_{LQ} S \left(1 - e^{-\frac{aN}{B}}\right) + \beta_R S \frac{M}{B} - E(\sigma + \mu) \quad (2)$$

$$\frac{dI}{dt} = \sigma(1 - p)E - \alpha I \quad (3)$$

$$\frac{dR}{dt} = p\sigma E - R(\phi + \mu) \quad (4)$$

$$\frac{dM}{dt} = \alpha I - \lambda M \quad (5)$$

Flea Submodel

$$\frac{dF_{SQ}}{dt} = \delta F_{SH} + r_F F_O \left(\frac{N}{1 + N + F_O}\right) - F_{SQ} \left[\mu_F + \left(1 - e^{-\frac{aN}{B}}\right) \right] \quad (6)$$

$$\frac{dF_{SH}}{dt} = F_{SQ} \left(1 - e^{-\frac{aN}{B}}\right) - F_{SH} \left(\mu_F + \delta + \gamma \frac{I}{N} \right) + \theta_L F_{LH} \frac{(S + E + R)}{N} \quad (7)$$

$$\frac{dF_{EQ}}{dt} = F_{EH} (\delta + \alpha) - F_{EQ} \left[\mu_F + \left(1 - e^{-\frac{aN}{B}}\right) \right] \quad (8)$$

$$\frac{dF_{EH}}{dt} = F_{EQ} \left(1 - e^{-\frac{aN}{B}} \right) - F_{EH} \left[\mu_F + \delta + \alpha + \theta_E \frac{(S + E + R)}{N} \right] + \gamma F_{SH} \frac{I}{N} + \gamma F_{LH} \frac{I}{N} \quad (9)$$

$$\frac{dF_{LQ}}{dt} = F_{LH} (\delta + \alpha) - F_{LQ} \left[\mu_F + \left(1 - e^{-\frac{aN}{B}} \right) \right] \quad (10)$$

$$\frac{dF_{LH}}{dt} = F_{LQ} \left(1 - e^{-\frac{aN}{B}} \right) + \theta_E F_{EH} \frac{(S + E + R)}{N} - F_{LH} \left[\mu_F + \delta + \alpha + \gamma \frac{I}{N} + \theta_L \frac{(S + E + R)}{N} \right] \quad (11)$$

We include three transmission routes in the model (Table 2.3). We separate fleas into questing (i.e., host seeking) and on-host classes to differentiate between the fleas in the questing reservoir and those fleas actively participating in the booster-feed infection cycle. Transmission from both the flea reservoir and the booster-feed infection cycle occurs via early-phase transmission (EP), which is divided into two-stages. EP stage 1 (EP1) defines transmission immediately following an infectious blood meal, with transmission efficiency quickly declining as a blood meal is taken from a non-infectious host (i.e. S , E , or R) causing fleas to transition to EP stage 2 (EP2; [20]). Another non-infectious blood meal is required to clear infection, and consequently, infectious questing fleas remain infectious indefinitely in our model (see Table 2.3 and Appendix 2.1 for a test of this assumption). Also, given that social structure within a local population may be important for transmission [31], some characterization of social segregation was needed. Rather than develop a fully spatial model, we introduced a correction factor, B , to the transmission terms to account for heterogeneous mixing between social groups. Due to the relative ineffectiveness of blocked-flea and pneumonic transmission in a similar model [13], we ignore these routes.

We developed a stochastic realization of our model using C++ based on Gillespie's Direct Algorithm [11,32]. The stochastic model was run for 300,000 events, which equates to 2-

5 years. All model runs were started with a host population close to carrying capacity. Results of 100 simulations were used to obtain extinction (i.e., host population goes extinct during the model run), enzootic (i.e., both the host population and plague persist throughout the model run), and disease fade probabilities (i.e., plague goes extinct despite persistence of host population).

To understand how transmission varies between epizootic and enzootic cycles, we parameterized the model to simulate both an epizootic and enzootic population (Table 2.2). Parameter values for the epizootic host were based on black-tailed prairie dogs and *Oropsylla hirsuta*, a common prairie dog flea [18,21,33]. The enzootic host parameter values reflected California ground squirrels and their dominant flea species, *O. montana* [1,34,35]. We also parameterized the flea sub-model for *O. tuberculata cynomuris*, another common prairie dog flea (Table 2.4, [18]), but the results for this species were similar to those for *O. hirsuta*. All parameter values were obtained from the literature or fit to observed data, but when data were not available, we substituted for the most closely related species available (for details of parameter estimation see Appendix 2.2).

To test the importance of transmission routes, we systematically removed them from both the epizootic and enzootic systems (Table 2.3). Because all flea-borne transmission is tied to early-phase transmission efficiency in our model, booster feeds cannot be removed without removing the flea reservoir. By comparing behavior with no flea-borne transmission to behavior when only infectious questing fleas were removed, we were able to determine the effect of the booster-feed infection cycle on plague dynamics. The simulations with flea-borne transmission began with five questing EP1 and EP2 fleas, and simulations with no flea-borne transmission began with one infectious carcass.

We also examined the relative importance of the transmission routes in a more general sense by performing sensitivity analysis on model parameters associated with each transmission route (Table 2.3). By extending this sensitivity analysis to include model parameters that represent characteristics of the hosts and fleas, we determined how previously identified host characteristics may interact with transmission routes to determine plague dynamics. We used a multi-parameter sensitivity analysis proposed by Blower and Dowlatabadi [36]. We constructed 100 random parameter sets using stratified random samples from uniform distributions spanning a range of potential values for host and flea species. The range was determined by increasing the largest value of a parameter found in our parameter sets (Tables 2.2 and 2.4) by an order of magnitude, which is a reasonable approximation of the range for most parameter values. Each parameter set was simulated 100 times in the full model. Partial-rank correlation coefficients (PRCCs) between each parameter and model output determined the relative importance of each parameter.

Results

The model showed clear enzootic and epizootic behavior for our two parameterizations (Fig. 2.1A and B respectively). In addition, model results for the prairie dog and ground squirrel parameterizations closely matched independent data (for detailed model results see Appendix 2.3). Parameter values for California ground squirrels created enzootic behavior for prolonged periods (>3 years; Fig. 2.1A) with 90% of surviving hosts found to be resistant to plague. Similarly, a natural population of California ground squirrels showed evidence of antibody responses to previous plague exposure in 11 of 13 years, accounting for 93% of the total population [35]. For the prairie dog parameter set, the model predicted high extinction

probabilities similar to areas where epizootics have been observed on black-tailed prairie dog towns [37], as well as others specifically studied by us on the Pawnee National Grassland where all 12 confirmed plague epizootics on towns from 2003 to 2008 resulted in severe population declines or extinction (Fig. 2.1B). The model also predicted short-lived epizootics with towns declining to near extinction after about 3 weeks with remnant hosts persisting for around 37.5 weeks (Fig. 2.1B), a range inclusive of the observed 6-8 week window from first detection of plague to apparent town extinction [13].

Looking at the role of our three transmission routes during enzootic cycles, infection potential from the booster-feed infection cycle declines during the majority of the model run (i.e., negative growth rate of infection potential), while the infectious, questing flea reservoir increases almost throughout (Fig. 2.1C). Infectious carcasses played little role in the enzootic cycle (Fig. 2.1C). In contrast, infection potential from booster-feeds showed a sharp increase during the early-stages of an epizootic, but then quickly declined as the epizootic progressed (Fig. 2.1D). Infection potential from the flea reservoir showed a similar pattern, although it continued to increase after infection from the booster-feed infection cycle crashed (Fig. 2.1D). The role of infectious carcasses paralleled that of the flea reservoir although the magnitude of change was not as great (Fig. 2.1D).

Systematic removal of transmission routes helped provide a clearer picture of each in plague dynamics, especially for epizootic behavior (Fig. 2.2). For the epizootic host parameterization, removing all flea-borne transmission (i.e., booster-feeds and the flea reservoir) resulted in a shift to enzootic behavior (Fig. 2.2A). However, when only the infectious, questing flea reservoir is removed, model behavior is again dominated by epizootics (Fig. 2.2A). Combined, these results suggest that booster-feed transmission plays an important role in

epizootics. Removal of the carcass reservoir still results in primarily epizootics, but disease fade is more likely (Fig. 2.2A). Removal of both reservoirs shows a significant increase in enzootic behavior with epizootics still dominating (Fig. 2.2A). Overall, this supports the idea that booster-feed transmission dominates but at least one type of reservoir transmission is needed to reach epizootic levels. In the enzootic host, removal of all flea-borne transmission resulted in a shift to disease fade-out (Fig. 2.2B). However, when booster-feeds were reinserted into the model and only the flea reservoir was removed, the shift to disease fade-out remained (Fig. 2.2B). Removal of the carcass reservoir alone has little impact on plague dynamics (Fig. 2.2B). Together, these results on enzootic probability suggest a consistent role for a flea reservoir in enzootic dynamics.

Our multi-parameter sensitivity analysis was consistent with the relative importance of transmission routes described above and revealed that model results were sensitive to parameters influential to both the booster-feed infection cycle and the infectious, questing flea reservoir (Table 2.3; Fig. 2.3). In particular, flea questing efficiency, a , was positively correlated with enzootic probability but had little effect on extinction probability. Increasing transmission efficiency from EP2, β_L , increased extinction probability as did an increase in the transition rate between EP1 and EP2 for fleas taking non-infectious blood meals, θ_E .

Population responses to plague infection were also sensitive to several host parameters in the model (Fig. 2.3). Among these, extinction probability was increased by higher rates of resistance loss, φ , and shorter host exposure periods (i.e., increased values of σ). However, increased host resistance, p , and increased host carry capacity, K , served to decrease epizootic behavior. In contrast, enzootic probability was increased by increasing host carrying capacity and declined with higher rates of resistance loss, shorter host exposure periods, and decreasing host

connectance (i.e., increased values of our of spatial correction factor, B). Sensitivities that are not reported were not significant.

Discussion

Our model produced characteristic enzootic and epizootic behaviors, and model behaviors for our specific parameterizations were consistent with empirical observations of plague activity in the hosts that they were based on, black-tailed prairie dogs and California ground squirrels. The agreement with natural systems highlights our ability to reliably compare the shifting roles of transmission routes in creating each dynamic. In particular, the booster-feed infection cycle is primarily responsible for epizootic behavior. While laboratory experiments have demonstrated that the booster feed infection cycle results in the maintenance of infection levels in fleas [20], we extend this result and show here that the booster-feed infection cycle can produce sustained transmission capable of initiating large scale epizootics (Figs. 2.1D and 2.2A). However, booster-feed infections may rapidly reduce the host population making prolonged periods in the booster-feed infection cycle unlikely due to host limitation. Consequently, an additional source of infection (i.e., infectious carcasses or infectious, questing fleas) is most likely needed to ensure extinction of remnant populations in epizootic hosts (Figs. 2.1D and 2.2A). In contrast, enzootic dynamics rely on a shift from the continuous maintenance of transmission chains through the booster-feed infection cycle seen in epizootic dynamics to the buildup of infectious, questing fleas (Figs. 2.1C and 2.2B).

Our sensitivity analysis supports the role of shifting transmission dynamics in determining plague dynamics in the host population. We found that epizootic behavior (i.e., higher extinction probability) was strongly affected by flea characteristics that determine both

the strength and turnover rate of the booster-feed infection cycle, while enzootic potential was strongly influenced by flea questing efficiency adding support to the involvement of a flea reservoir in the maintenance of plague at the population level [38]. While the strength of transmission routes varies between epizootics and enzootics, it is important to note that our sensitivity analysis suggests that transmission in general is tempered by heterogeneous mixing of individuals (i.e., higher values of our spatial correction factor, B ; Fig. 2.3). Understanding variation in the strength of transmission routes is thus highly contingent upon understanding the processes that determine epizootiologically relevant mixing of hosts. Recent modeling studies have revealed the potential for alternate hosts, like grasshopper mice, to serve as a link between spatially distinct prairie dog coterries [31]. Additionally, occasional non-local interactions between socially distinct groups of individuals could increase their epizootiological connection leading to more global connectivity as seen in a population of African lions [39]. The importance of a flea reservoir in plague dynamics also supports the idea that a questing flea reservoir could increase connectance between individuals by linking socially distinct units through transient interactions with a common infectious reservoir. However more research is needed to determine mechanisms governing connectivity and their role in determining the relative importance of transmission routes.

While the flea reservoir may be important in connecting spatially distinct groups of hosts, we also hypothesize that questing fleas may act as a bridge in enzootics, connecting temporally separated pools of susceptible hosts generated from a resistant refuge. This endogenously derived temporal bridge contrasts with more traditionally hypothesized exogenous sources of re-infection. Bat rabies virus may display a similar endogenous bridging mechanism by entering a quiescent state during host hibernation, thus creating a bridge between birth pulses that refresh

the susceptible pool [40,41]. Additionally, other systems are consistent with an endogenous temporal bridging mechanism including leptospirosis epizootics in California sea lions [42], overwintering dynamics in other vector-borne diseases like bluetongue virus in northern Europe [43] and West Nile Virus in the eastern United States [44], and transstadial transmission of Lyme disease spirochetes [45].

Most of the previous research on the variability in population responses to plague infection has focused on host traits, and our sensitivity analysis confirmed some of these observations, particularly the importance of host resistance and population size as observed in Asian great gerbils [4,6-8]. This result is not surprising given the extensive evidence for a critical community size in the theoretical disease literature (e.g., [9,10,46,47]) and seen in other systems, such as measles [48,49], phocine distemper [50], and cowpox virus [51].

However, while our analysis confirms previous observations on the role of host characteristics in determining disease dynamics, it is important to note that these traits do not act independently of transmission routes to determine population response and thus, the effects of host traits may depend on the specific transmission routes operating. For example, we found that increasing host carrying capacity generally increased enzootic potential in our sensitivity analysis. However, our specific results for prairie dogs and California ground squirrels exhibited the opposite of the expected responses with black-tailed prairie dogs having larger population sizes but higher probabilities of extinction. Here, knowledge of transmission shifts may be more informative. Specifically, the importance of booster-feeds in epizootics, a transmission route that relies on continued contact between hosts and fleas, may create a situation where increasing host abundance leads to large epizootic potential that cannot be maintained. This is in contrast to enzootic hosts where an endogenous bridging mechanism like infectious, questing fleas

overcomes issues of host limitation. The maintenance of infection potential in a flea reservoir may also alter the traditionally hypothesized role of resistance in promoting enzootics. In this case, resistance may primarily be important in avoiding epizootics and becomes important in promoting enzootics only when infectious, questing fleas dominate transmission. Thus, host and flea characteristics may scale up through transmission routes allowing for more robust predictions than when considering either host or flea characteristics alone.

Table 2.1: Host and flea variables.

Variable	Description
S	Susceptible host
E	Exposed host
I	Infectious host (i.e., bacteremia $\geq 10^6$ cfu/mL [52,53])
R	Resistant host
M	Infectious carcass reservoir
N	Population size (i.e., $S + E + I + R$)
F_{SQ}	Susceptible, questing flea
F_{SH}	Susceptible, on-host flea
F_{EQ}	EP1, questing flea reservoir
F_{EH}	EP1, on-host flea in booster-feed infection cycle
F_{LQ}	EP2, questing flea reservoir
F_{LH}	EP2, on-host flea in booster-feed infection cycle
F_0	Breeding, on-host fleas (i.e., $F_{SH} + F_{EH} + F_{LH}$)

Table 2.2: Parameter values.

Parameter	Epizootic host ¹	Enzootic host ²	Description ³	Reference
r	0.087	0.025	Intrinsic rate of increase	[54,55]
K	200	26	Carrying capacity	[54,55]
μ	0.0002	0.0005	Natural mortality rate	[54,56]
β_r	0.073	0.073	Transmission rate: infectious carcasses	[13]
B	20	50	Spatial correction factor to transmission	[13,55,56]
σ	0.22	0.169	(Exposed period) ⁻¹	[57,58]
α	0.5	0.5	Disease induced mortality rate	[53,57]
λ	0.091	0.091	Infectious carcass decay rate	[29]
p	0.01	0.412	Probability of gaining resistance	[58]
φ	0.011	0.002	Rate resistance is lost	[59]
β_E	0.044	0.082	Transmission rate: EP1	[14,18,19]
β_L	0.01	0.059	EP2 transmission rate	[18-20]
δ	0.059	0.059	Rate of leaving hosts	[60]
a	0.02	0.02	Questing efficiency	See Appendix 2.2
μ_F	0.01	0.01	Natural mortality rate	[61]
r_F	2.5	2.5	Conversion efficiency	See Appendix 2.2
γ	0.84	0.92	Transmission rate: hosts to vector	[14,18,19]
θ_E	1	0.25	Rate of transition from EP1 to EP2 while feeding	[18-20]
θ_L	1	0.33	Rate of transition from EP2 to susceptible while feeding	[18-20]

¹Parameterized for the black-tailed prairie dog and *Oropsylla hirsuta* system. ²Parameterized for the California ground squirrel and *O. montana* system. ³Units for rates are in (days)⁻¹

Table 2.3: Transmission routes.

Mechanism	Transmission Type ¹	Influential Parameters	Testing Method
Booster-feed infection cycle	Frequency-dependent	$\beta_E, \beta_L, \theta_E, \theta_L$	Set $\beta_E = \beta_L = 0$ ²
Infectious, questing flea reservoir	Frequency-dependent	a, μ_F, α, δ (and indirectly β_E and β_L)	Allow loss of infectiousness in questing fleas (see Appendix 2.1)
Infectious carcasses	Density-dependent	β_r, λ	Set $\beta_R = 0$

¹See [13]. ²Notice that the removal of booster-feed infections also requires removal of transmission from the flea reservoir.

Table 2.4: Alternate flea parameter values. Parameter values for the prairie dog flea *O. tuberculata cynomuris*. Other flea species are provided for comparison.

Parameter	<i>Oropsylla hirsuta</i>	<i>O. tuberculata cynomuris</i>	<i>O. montana</i>	Description ¹	Reference
β_E	0.044	0.147	0.082	Transmission rate: EP1	[14,18,19]
β_L	0.01	0.01	0.059	EP2 transmission rate	[18-20]
δ	0.059	0.059	0.059	Rate of leaving hosts	[60]
a	0.02	0.02	0.02	Questing efficiency	See Appendix 2.2
μ_F	0.01	0.01	0.01	Natural mortality rate	[61]
r_F	2.5	2.5	2.5	Conversion efficiency	See Appendix 2.2
γ	0.84	0.82	0.92	Transmission rate: hosts to vector	[14,18,19]
θ_E	1	1	0.25	Rate of transition from EP1 to EP2 while feeding	[18-20]
θ_L	1	1	0.33	Rate of transition from EP2 to susceptible while feeding	[18-20]

¹Units for rates are in days.

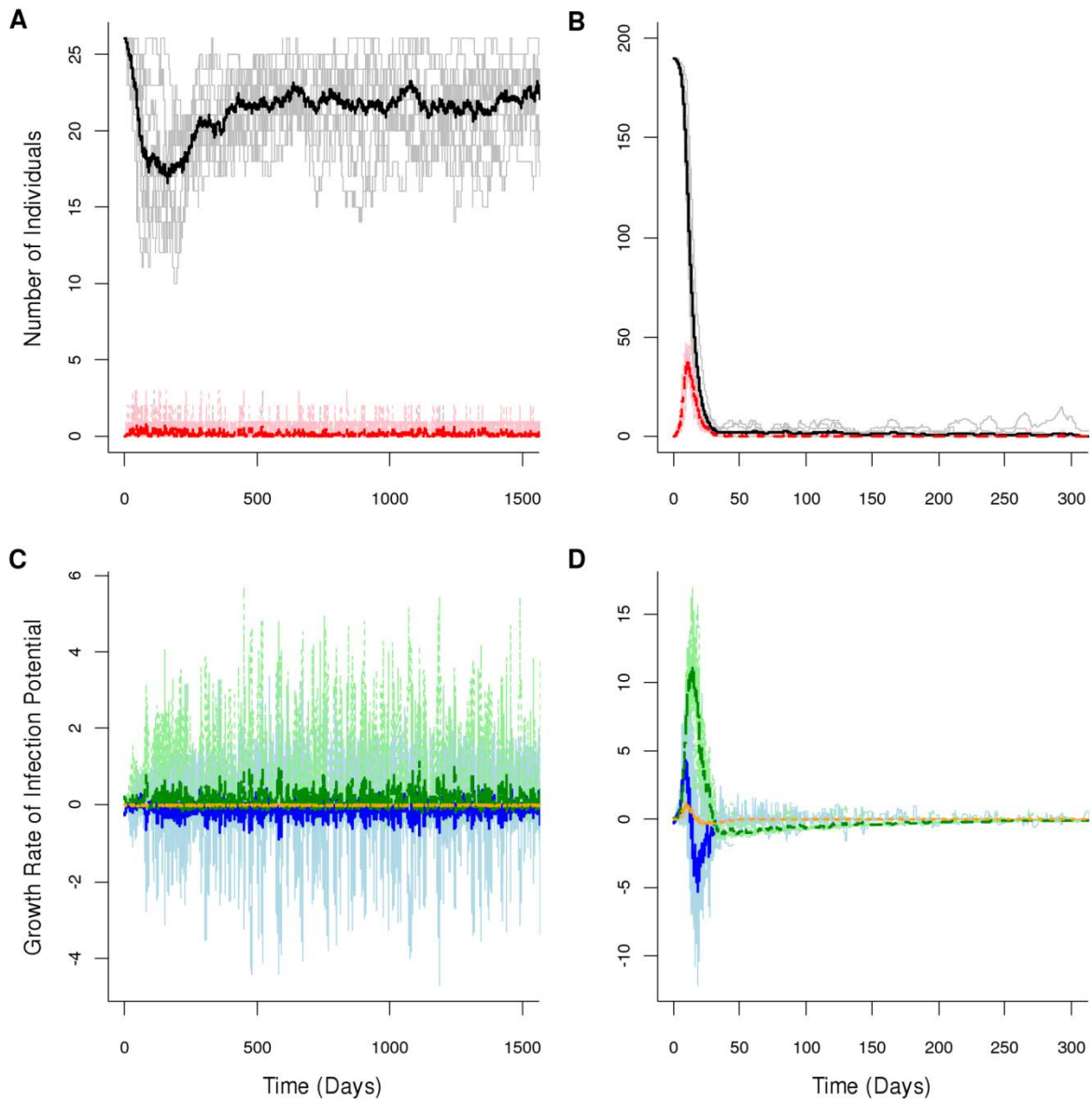


Figure 2.1: Enzootic and epizootic plague dynamics. Model behavior for given parameter values (Table 2.2) with light/bold lines giving results for independent model runs/average behavior. Total population size (gray/black) and number of infectious individuals (pink/red) are shown for the A) enzootic host and B) epizootic host. The growth rate of infection potential over time for the three transmission routes, booster-feed infections (light blue/blue), questing flea reservoir (light green/green), and carcass reservoir (light orange/orange) are shown for the C) enzootic host and D) epizootic host.

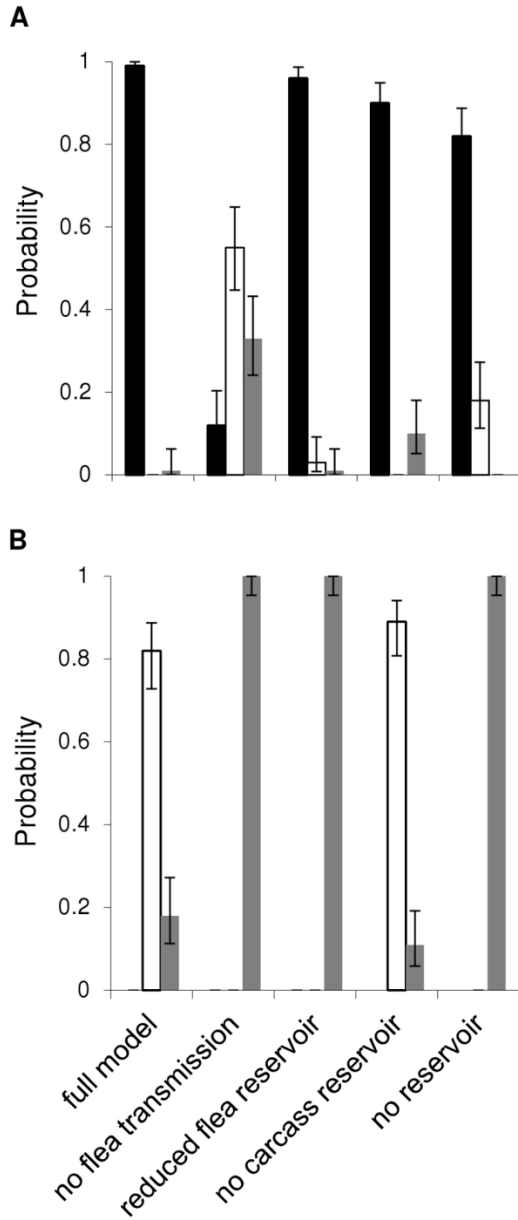


Figure 2.2: Transmission hypothesis testing. Testing was done using default parameter values for the (a) black-tailed prairie dog and (b) California ground squirrel. Each case represents the effect of removing either one or multiple transmission routes on extinction probability (black bars), enzootic probability (white bars), or disease fade probability (gray bars). 95% confidence intervals are also given.

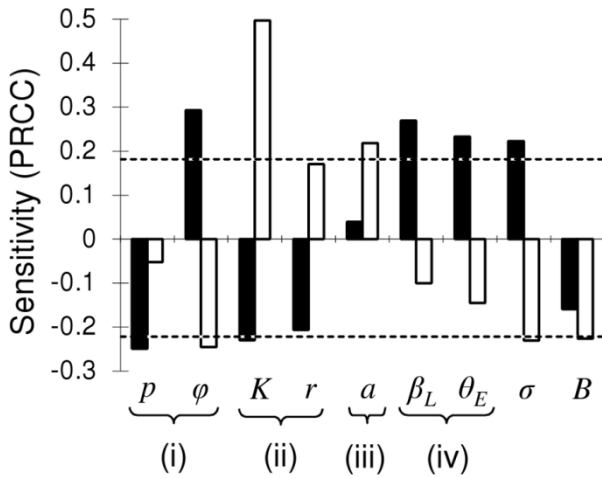


Figure 2.3: Multi-parameter sensitivity analysis. Partial rank correlation coefficients (PRCCs) between extinction (black bars) and enzootic (white bars) probabilities and model parameters. Dashed lines indicate the critical values for significance ($p < 0.05$). Parameters are grouped by the following: (i) host resistance, (ii) host population size, (iii) efficiency of the flea reservoir, and (iv) efficiency of the booster-feed infection cycle.

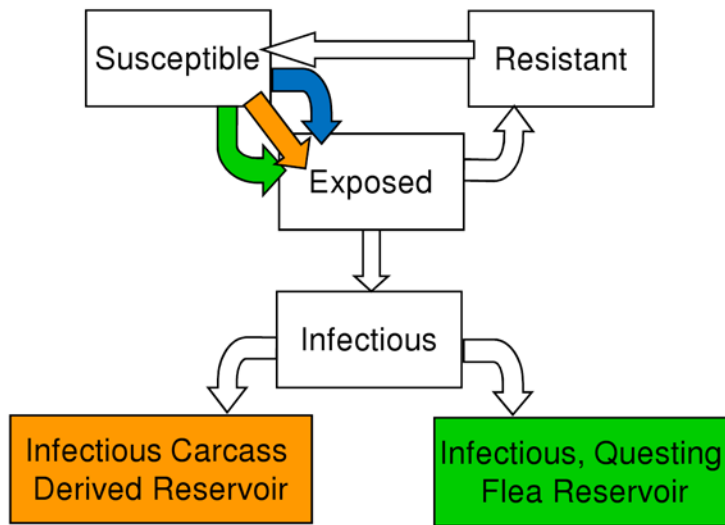


Figure 2.4: Flow chart for the host sub model. The three transmission routes included in the model are highlighted: booster-feed infection cycle (blue), infectious, questing flea reservoir (green), and infectious carcasses (orange).

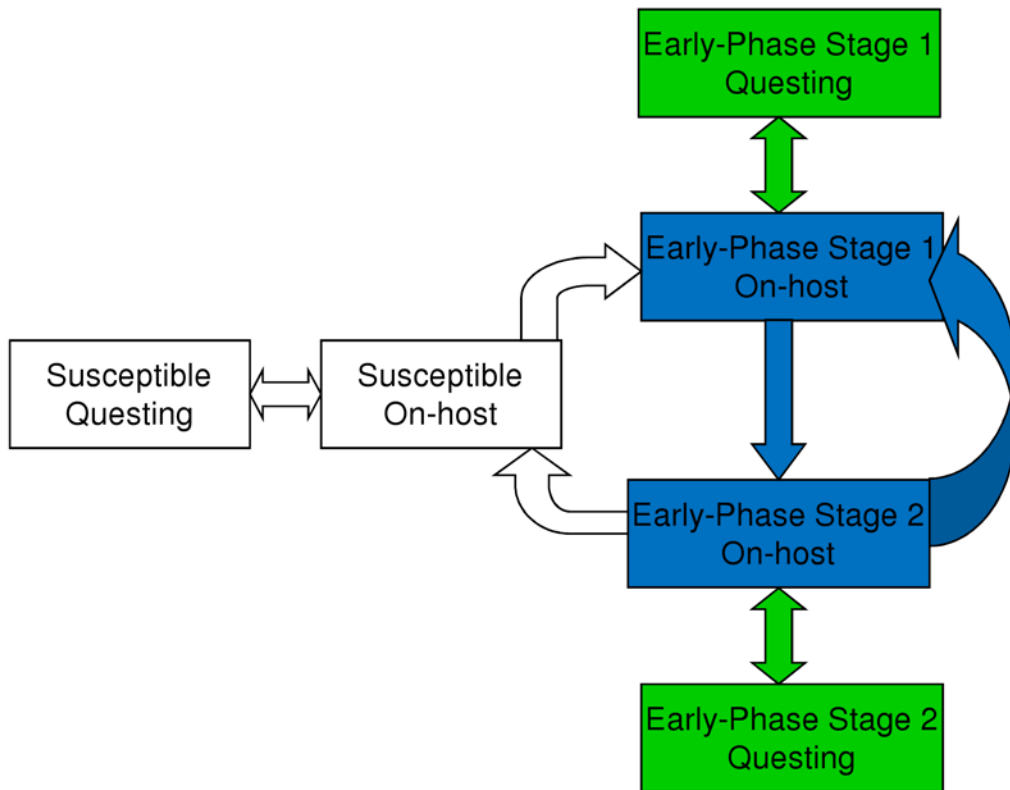


Figure 2.5: Flow chart for the flea submodel. The relationship between the booster-feed infection cycle (blue) and infectious flea reservoir (green) is highlighted.

LITERATURE CITED

1. Barnes AM (1982) Surveillance and control of bubonic plague in the United States. *Symp Zool Soc Lond* 50: 237-270.
2. Poland J, Barnes A (1979) Plague. In: Steele JH, Stoenner H, Kaplan W, editors. *CRC Handbook Series in Zoonoses, Section A: Bacterial, Rickettsial, and Mycotic Diseases*. Boca Raton, FL: CRC Press. pp. 515-597.
3. Gage KL, Ostfeld RS, Olson JG (1995) Nonviral vector-borne zoonoses associated with mammals in the United States. *J Mammal* 76: 695-715.
4. Gage KL, Kosoy MY (2005) Natural history of plague: perspectives from more than a century of research. *Annu Rev Entomol* 50: 505-528.
5. Rocke TE, Pussini N, Smith SR, Williamson J, Powell B, et al. (2010) Consumption of baits containing raccoon pox-based plague vaccines protects black-tailed prairie dogs (*Cynomys ludovicianus*). *Vector-Borne Zoonot* 10: 53-58.
6. Davis S, Begon M, De Bruyn L, Ageyev VS, Klassovskiy NL, et al. (2004) Predictive thresholds for plague in Kazakhstan. *Science* 304: 736-738.
7. Davis S, Trapman P, Leirs H, Begon M, Heesterbeek JAP (2008) The abundance threshold for plague as a critical percolation phenomenon. *Nature* 454: 634-637.
8. Stenseth NC, Samia NI, Viljugrein H, Kausrud KL, Begon M, et al. (2006) Plague dynamics are driven by climate variation. *Proc Natl Acad Sci U S A* 103: 13110-13115.
9. Anderson RM, May RM (1979) Population biology of infectious diseases. I. *Nature* 280: 361-367.
10. Anderson RM, May RM (1986) The invasion, persistence and spread of infectious diseases within animal and plant communities. *Phil Trans R Soc Lond B* 314: 533-570.
11. Keeling MJ, Rohani P (2008) *Modeling Infectious Diseases in Humans and Animals*. Princeton: Princeton University Press. 408 p.
12. Bacot AW, Martin CJ (1914) Observations on the mechanism of the transmission of plague by fleas. *J Hyg* 13: 423-439.
13. Webb CT, Brooks CP, Gage KL, Antolin MF (2006) Classic flea-borne transmission does not drive plague epizootics in prairie dogs. *Proc Natl Acad Sci U S A* 103: 6236-6241.
14. Eisen RJ, Bearden SW, Wilder AP, Monteneri JA, Antolin MF, et al. (2006) Early-phase transmission of *Yersinia pestis* by unblocked fleas as a mechanism explaining rapidly spreading plague epizootics. *Proc Natl Acad Sci U S A* 103: 15380-15385.

15. Eisen RJ, Wilder AP, Bearden SW, Monteneri JA, Gage KL (2007) Early-phase transmission of *Yersinia pestis* by unblocked *Xenopsylla cheopis* (Siphonaptera: Pulicidae) is as efficient as transmission by blocked fleas. *J Med Entomol* 44: 678-682.
16. Eisen RJ, Borchert JN, Holmes JL, Amatre G, Van Wyk K, et al. (2008) Early-phase transmission of *Yersinia pestis* by cat fleas (*Ctenocephalides felis*) and their potential role as vectors in a plague endemic region of Uganda. *Am J Trop Med Hyg* 78: 949-956.
17. Eisen RJ, Holmes JL, Schotthoefer AM, Vetter SM, Monteneri JA, et al. (2008) Demonstration of early-phase transmission of *Yersinia pestis* by the mouse flea, *Aetheca wagneri* (Siphonaptera: Ceratophyllidae), and implications for the role of deer mice as enzootic reservoirs. *J Med Entomol* 45: 1160-1164.
18. Wilder AP, Eisen RJ, Bearden SW, Monteneri JA, Tripp DW, et al. (2008) Transmission efficiency of two flea species (*Oropsylla tuberculata cynomuris* and *Oropsylla hirsuta*) involved in plague epizootics among prairie dogs. *EcoHealth* 5: 205-212.
19. Wilder AP, Eisen RJ, Bearden SW, Monteneri JA, Gage KL, et al. (2008) *Oropsylla hirsuta* (Siphonaptera: Ceratophyllidae) can support plague epizootics in black-tailed prairie dogs (*Cynomuris ludovicianus*) by early-phase transmission of *Yersinia pestis*. *Vector-Borne Zoonot* 8: 359-368.
20. Eisen RJ, Lowell JL, Monteneri JA, Bearden SW, Gage KL (2007) Temporal dynamics of early-phase transmission of *Yersinia pestis* by unblocked fleas: secondary infectious feeds prolong efficient transmission by *Oropsylla montana* (Siphonaptera: Ceratophyllidae). *J Med Entomol* 44: 672-677.
21. Salkeld DJ, Stapp P (2008) Prevalence and abundance of fleas in black-tailed prairie dog burrows: implications for the transmission of plague (*Yersinia pestis*). *J Parasitol* 94: 616-621.
22. Eisen RJ, Gage KL (2009) Adaptive strategies of *Yersinia pestis* to persist during inter-epizootic and epizootic periods. *Vet Res* 40. Available: <http://www.vetres.org/articles/vetres/pdf/2009/02/v08314.pdf>. Accessed 2011 May 3.
23. Thomas RE, Barnes AM, Quan TJ, Beard ML, Carter LG, et al. (1988) Susceptibility to *Yersinia pestis* in the northern grasshopper mouse (*Onychomys leucogaster*). *J Wildlife Dis* 24: 327-333.
24. Golov DA, Ioff AG (1928) On the question of the role of the rodent fleas in the southeastern part of the USSR and the epidemiology of plague. Proc. 1st All-Russian Anti-Plague Conf. Saratov, pp. 102-105. Saratov, Russia: Mikrob Central Antiplague Inst.
25. Sharets AS, Berendyev SA, Krasnikova LV, Tristan DF (1958) Effectiveness of the one shot marmot control. In: Trudy Sredneaziatskogo Protivochnunogo Instituta. Monogr. Almaty, Kazakhstan. pp.145-147.

26. Kartman L, Quan SF, Lechleitner RR (1962) Die-off of a Gunnison's prairie dog colony in central Colorado: II. Retrospective determination of plague infection in flea vectors, rodents, and man. *Zoonoses Res* 1: 201-224.
27. Bazanova LP, Maevskii MP (1996) The duration of the persistence of plague microbe in the body of flea *Citellophilus tesquorum altaicus*. *Med Parasitol* 2: 45-48.
28. Karimi PY (1963) Conservation naturelle de la peste dans le sol. *Bull Soc Pathol Exot Filiales* 56; 1183-1186.
29. Ber R, Mamroud E, Aftalion M, Tidhar A, Gur D, et al. (2003) Development of an improved selective agar medium for isolation of *Yersinia pestis*. *Appl Environ Microb* 69: 5787-5792.
30. Eisen RJ, Petersen JM, Higgins CL, Wong D, Levy CE, et al. (2008) Persistence of *Yersinia pestis* in soil under natural conditions. *Emerg Infect Dis* 14: 941-943.
31. Salkeld DJ, Salathé M, Stapp P, Jones JH (2010) Plague outbreaks in prairie dog populations explained by percolation thresholds of alternate host abundance. *Proc Natl Acad Sci U S A* 107: 14247-14250.
32. Gillespie DT (1977) Exact stochastic simulation of coupled chemical reactions. *J Phys Chem* 81: 2340-2361.
33. Tripp DW, Gage KL, Montenieri JA, Antolin MF (2009) Flea abundance on black-tailed prairie dogs (*Cynomys ludovicianus*) increases during plague epizootics. *Vector-Borne Zoonot* 9: 313-321.
34. Lang JD, Wills W (1991) Ecology of sylvatic plague in the San Jacinto Mountains of Southern California. *Bull Soc Vector Ecol* 16: 183-199.
35. Davis RM, Smith RT, Madon MB, Sitko-Cleugh E (2002) Flea, rodent, and plague ecology at Chuchupate Campground, Ventura County, California. *J Vector Ecol* 27: 107-127.
36. Blower SM, Dowlatabadi H (1994) Sensitivity and uncertainty analysis of complex models of disease transmission: an HIV model, as an example. *Int Stat Rev* 62: 229-243.
37. Collinge SK, Johnson WC, Ray C, Matchett R, Grensten J, et al. (2005) Landscape structure and plague occurrence in black-tailed prairie dogs on grasslands of the western USA. *Landscape Ecol* 20: 941-955.
38. Wimsatt J, Biggins DE (2009) A review of plague persistence with special emphasis on fleas. *J Vector Dis* 46: 85-99.
39. Craft ME, Volz E, Packer C, Meyers LA (2011) Disease transmission in territorial populations: the small-world network of Serengeti lions. *J R Soc Interface* 8: 776-786.

40. Sulkin SE (1962) Bat rabies: experimental demonstration of the “reservoiring mechanism.” *Am J Public Health* 52: 489-498.
41. George DB, Webb CT, Farnsworth M, O’Shea T, Bowen R, et al. (2011) Host and viral ecology determine bat rabies seasonality and maintenance. *Proc Natl Acad Sci U S A*. In press.
42. Gulland FMD, Koski M, Lowenstine LJ, Colagross A, Morgan L, et al. (1996) Leptospirosis in California sea lions (*Zalophus californianus*) stranded along the central California coast, 1981-1994. *J Wildlife Dis* 32: 572-580.
43. Wilson A, Darpel K, Mellor PS (2008) Where does bluetongue virus sleep in the winter? *PLoS Biol* 6: e210.
44. Nasci RS, Savage HM, White DJ, Miller JR, Cropp BC, et al. (2001) West Nile Virus in overwintering *Culex* mosquitoes, New York City, 2000. *Emerg Infect Dis* 7: 742-744.
45. Piesman, J, Sinsky, RJ (1988) Ability of *Ixodes scapularis*, *Dermacentor variabilis*, and *Amblyomma americanum* (Acari: Ixodidae) to acquire, maintain, and transmit Lyme disease spirochetes (*Borrelia burgdorferi*). *J Med Entomol* 25: 336-339.
46. May RM, Anderson RM (1979) Population biology of infectious diseases. II. *Nature* 280: 455-461.
47. Swinton J, Woolhouse MEJ, Begon ME, Dobson AP, Ferroglio E, et al. (2002) Microparasite transmission and persistence. In: Hudson PJ, Rizzoli A, Grenfell BT, Heesterbeek H, Dobson AP, editors. *The Ecology of Infectious Diseases*. New York: Oxford University Press. pp. 83-101.
48. Bartlett MS (1957) Measles periodicity and community size. *J R Stat Soc A* 120: 48-70.
49. Bartlett MS (1960) The critical community size for measles in the United States. *J R Stat Soc A* 123: 37-44.
50. Swinton J, Harwood J, Grenfell BT, Gilligan CA (1998) Persistence thresholds for phocine distemper virus infection in harbor seal *Phoca vitulina* metapopulations. *J Anim Ecol* 67: 54-68.
51. Begon M, Hazel SM, Telfer S, Bown K, Carslake D, et al. (2003) Rodents, cowpox virus, and islands: densities, numbers, and thresholds. *J Anim Ecol* 72: 343-355.
52. Engelthaler DM, Hinnebusch BJ, Rittner CM, Gage KL (2000) Quantitative competitive PCR as a technique for exploring flea-*Yersinia pestis* dynamics. *Am J Trop Med Hyg* 62: 552-560.
53. Lorange EA, Race BL, Sebbane F, Hinnebusch BJ (2005) Poor vector competence of fleas and the evolution of hypervirulence in *Yersinia pestis*. *J Infect Dis* 191: 1907-1912.

54. Hoogland JL (1995) *The Black-Tailed Prairie Dog*. Chicago: University of Chicago Press. 562 p.
55. Linsdale JM (1946) *The California Ground Squirrel*. Berkeley: University of California Press. 475 p.
56. Evans FC, Holdenried R (1943) A population study of the Beechey ground squirrel in central California. *J Mammal* 24: 231-260.
57. Cully JF, Williams ES (2001) Interspecific comparisons of sylvatic plague in prairie dogs. *J Mammal* 82: 894-905.
58. Williams JE, Moussa MA, Cavanaugh DC (1979) Experimental plague in the California ground squirrel. *J Infect Dis* 140: 618-621.
59. Quan TJ, Barnes AM, Carter LG, Tsuchiya KR (1985) Experimental plague in rock squirrels, *Spermophilus variegates* (Erxleben). *J Wildlife Dis* 21: 205-210.
60. Hartwell WV, Quan SF, Scott KG, Kartman L (1958) Observations on flea transfer between hosts: a mechanism in the spread of bubonic plague. *Science* 127: 814.
61. Eskey CR, Haas VH (1940) Plague in the western part of the United States. *Publ Health Bull* 254: 1-82.

Appendix 2.1: Alternate flea submodel which prevents the buildup of infectious, questing fleas.

In our original flea submodel, we assumed fleas must take a non-infectious blood meal to clear infection. Thus upon leaving a host, fleas maintained their current infection status indefinitely. We also developed an alternate version of the flea submodel that allowed fleas to clear infection without a feeding requirement (Eqs. S1-S6). This version of the flea submodel enabled the infectious questing flea reservoir to wane over time and allowed us to test the role of the questing flea reservoir on plague dynamics.

We defined the following additional parameters and their default values as: ε = rate at which fleas in EP1 transition to EP2 when not feeding = 0.125 [20]; ζ = rate at which fleas in EP2 clear infection when not feeding = 0.033 [52]. Default values were determined according to infectious periods seen in studies that maintained infectious flea stocks through continued blood meals. As such, these parameter values represent rates that may be much faster than those that would be observed in natural questing fleas that may enter a quiescent state when not feeding. All other parameters were given their default values (Tables 2.2 and 2.4).

Alternate Flea Submodel

$$\frac{dF_{SQ}}{dt} = \delta F_{SH} + r_F F_O \left(\frac{N}{1 + N + F_O} \right) - F_{SQ} \left[\mu_F + \left(1 - e^{-\frac{aN}{B}} \right) \right] + \zeta F_{LQ} \quad (S1)$$

$$\frac{dF_{SH}}{dt} = F_{SQ} \left(1 - e^{-\frac{aN}{B}} \right) - F_{SH} \left(\mu_F + \delta + \gamma \frac{I}{N} \right) + \theta_L F_{LH} \frac{(S + E + R)}{N} \quad (S2)$$

$$\frac{dF_{EQ}}{dt} = F_{EH} (\delta + \alpha) - F_{EQ} \left[\mu_F + \left(1 - e^{-\frac{aN}{B}} \right) \right] - \varepsilon F_{EQ} \quad (S3)$$

$$\frac{dF_{EH}}{dt} = F_{EQ} \left(1 - e^{-\frac{aN}{B}} \right) - F_{EH} \left[\mu_F + \delta + \alpha + \theta_E \frac{(S + E + R)}{N} \right] + \gamma F_{SH} \frac{I}{N} + \gamma F_{LH} \frac{I}{N} \quad (\text{S4})$$

$$\frac{dF_{LQ}}{dt} = F_{LH} (\delta + \alpha) - F_{LQ} \left[\mu_F + \left(1 - e^{-\frac{aN}{B}} \right) \right] + \varepsilon F_{EQ} - \xi F_{LQ} \quad (\text{S5})$$

$$\frac{dF_{LH}}{dt} = F_{LQ} \left(1 - e^{-\frac{aN}{B}} \right) + \theta_E F_{EH} \frac{(S + E + R)}{N} - F_{LH} \left[\mu_F + \delta + \alpha + \gamma \frac{I}{N} + \theta_L \frac{(S + E + R)}{N} \right] \quad (\text{S6})$$

Appendix 2.2: Parameter fitting and estimation.

Flea questing efficiency, a , and conversion efficiency, r_F , were fit to observed flea loads on California ground squirrels (observed = 28.4 [61]; model = 30.4). Because a and r_F had little impact on a previous prairie dog model [13] and are not well characterized in general [11], we assumed that these parameters were similar for all flea species but also tested their importance using sensitivity analysis. The transmission correction factor, B , was estimated from the home range sizes of hosts [13,55].

Appendix 2.3: Detailed prairie dog and California ground squirrel model outputs.

For the prairie dog parameters, the model predicted an extinction probability of 0.99 (95% CI [0.97, 1]) with an average time to extinction of 263 days (95% CI [204, 322]) and an epizootic time (i.e., time to reduce the host population to 1/10 of its carrying capacity) of 21.48 days (95% CI [21.13, 21.83]). No prairie dog colonies reached an enzootic state, and plague faded out in one of the 100 runs after only 6 days.

In the ground squirrel system, no extinctions were observed. The probability of enzootic persistence was 0.82 (95% CI [0.74, 0.90]) with 90.3% of individuals resistant to infection (95% CI [88.8, 91.8]). The probability of disease fade-out was 0.18 (95% CI [0.10, 0.26]) with an average time to fade-out of 538 days (95% CI [415, 661]).

CHAPTER 3

DISPERSAL STRATEGIES ALTER COEVOLUTIONARY TRAJECTORIES FOR HOST RESISTANCE AND PATHOGEN VIRULENCE IN A METAPOPOPULATION³

Summary

Host-pathogen interactions occur across a spectrum of spatial mixing patterns that range from well-mixed to within-population structure to metapopulation structure, and exploring quantitative trait coevolution of host resistance and pathogen virulence along this continuum has provided insights into the maintenance of highly virulent pathogens. However, expanding quantitative trait coevolution of resistance and virulence to the metapopulation scale has proven elusive due to a lack of theoretical tools to address this issue. Here, we focus on integrating quantitative trait coevolution into a metapopulation through a novel theoretical framework. This method combined a state-structured model that incorporated spatial structure with sensitivity analysis techniques in order to calculate selection gradients for both host resistance and pathogen virulence across a range of host and pathogen dispersal strategies. The results suggest that coevolutionary outcomes for host resistance and pathogen virulence in a metapopulation do not scale directly from those predicted under single population structures. Here, heterogeneous selection pressures promote a diversity of coevolutionary outcomes when host and pathogen

³Co-authors for this chapter include:

Colleen T. Webb

Department of Biology, Colorado State University, Fort Collins, CO, USA

Mike Boots

Centre for Ecology and Conservation, University of Exeter, Cornwall, UK

subpopulations are highly localized. These methods highlight the importance of ecological dynamics in understanding host and pathogen coevolution and also provide the first model of quantitative trait coevolution in a metapopulation.

Introduction

Numerous studies on the coevolution of host resistance and pathogen virulence have found a variety of potential coevolutionary outcomes (Anderson and May 1982; Bremermann and Pickering 1983; Levin and Pimental 1983; May and Anderson 1983; Bremermann and Thieme 1989). These results show that epidemiological feedbacks caused by the maximization of a pathogen's basic reproductive ratio, R_0 , can shape coevolutionary pressures and lead to the exclusion of avirulent pathogen strains (Anderson and May 1982; Bremermann and Pickering 1983; Levin and Pimental 1983; May and Anderson 1983; Bremermann and Thieme 1989). These outcomes, however, have been based on the assumption of a well-mixed host and pathogen population. For many host-pathogen systems, this assumption fails as spatial structure is known to affect disease dynamics. In these cases, spatial structure can range from within-population contact structures, as seen in chronic wasting disease in mule deer (*Odocoileus hemionus*; Farnsworth et al. 2006), canine distemper in African lions (*Panthera leo*; Craft et al. 2011), and bovine tuberculosis in European badgers (*Meles meles*; Vicente et al. 2007), to metapopulation dynamics like those observed for chytridiomycosis in boreal toads (*Bufo boreas*; Muths et al. 2003), and phocine distemper in harbour seals (*Phoca vitulin*; Swinton et al. 1998). Another disease, plague in black-tailed prairie dogs (*Cynomys ludovicianus*) caused by *Yersinia pestis*, exhibits maintenance that results from a mix of within population social structure that creates spatially distinct infection units (Salkeld et al. 2010), and between population dispersal

that results in pathogen persistence at a metapopulation scale (Snäll et al. 2008; George 2009). Thus, coevolution in a well-mixed population only addresses one end of a continuum of mixing patterns that potentially moves through spatial structure within a single host population to higher level metapopulation dynamics that govern between population dispersal.

Recent studies have expanded the evolution of pathogen virulence and host resistance to include a segment of this continuum: spatial structure within a single population. Here, local infection processes lead to the evolution of lower virulence (Boots and Sasaki 1999; Haraguchi and Sasaki 2000; Boots et al. 2004; Wild et al. 2009; Lion and Boots 2010). Furthermore, intermediate levels of spatial structure may select for higher transmission and virulence than predicted in well mixed populations (Kamo et al. 2007; Lion and Boots 2010). When costly host resistance is examined, local dispersal of the host generally selects for higher resistance, but the coevolutionary trajectories are modified based on the interaction between spatial structure of the host and pathogen (Best et al. 2011). The outcome of coevolution in these instances can then be viewed as a balance between ecological factors that structure the population, individual selective pressures that favor high fitness variants, and kin selection that results from local clustering of related hosts and pathogens (Wild et al 2009; Lion and Boots 2010; Best et al. 2011).

As host-pathogen interactions scale along the spatial structure continuum to include between population structures, however, spatially heterogeneous selective pressures and gene flow could dramatically affect the coevolution of resistance and virulence. Previous attempts to study coevolution at the metapopulation scale have relied on gene-for-gene (Thrall and Burdon 2002) or matching allele models (Gandon et al. 1996; Gandon 2002). Similar to the single-population models, these models showed that coevolutionary outcomes are affected by the interaction between host and pathogen dispersal (Thompson and Burdon 1992; Gandon et al.

1996; Gandon 2002; Thrall and Burdon 2002; Nuismer 2006). Specifically, local adaptation to the host when pathogen dispersal is relatively higher than host dispersal leads to higher virulence (Gandon et al. 1996; Gandon 2002; Nuismer 2006), while resistance to local pathogen populations increases when host dispersal is higher (Gandon et al. 1996; Gandon 2002).

Direct comparison across spatial scales using the previous studies is difficult, however, as the modeling approaches assume different genetic architectures. The metapopulation models assume that both resistance and virulence are determined by a small number of genes (Gandon et al. 1996; Gandon 2002; Thrall and Burdon 2002). This assumption is at odds with the more traditional assumption of polygenic determination of these traits (Sorci et al. 1997), which was used in studies within single, spatially-structured populations (Boots and Sasaki 1999; Boots et al. 2004; Lion and Boots 2010; Best et al. 2011) and well-mixed populations (Anderson and May 1982; Bremermann and Pickering 1983; Levin and Pimental 1983; May and Anderson 1983; Bremermann and Thieme 1989). Thus, to more fully understand coevolution along the continuum of spatial structures there is a need to scale up quantitative trait coevolution into a metapopulation framework. However, no methods exist to address this gap, and consequently, new theoretical tools are needed to expand the previous models of quantitative trait coevolution in a single, structured population.

Here, we study quantitative trait coevolution of host resistance and pathogen virulence in a metapopulation, and why highly virulent pathogens may persist both ecologically and evolutionarily in largely susceptible hosts that exhibit a metapopulation structure. To do this, we develop a novel mathematical framework. This approach builds on previous work by Metz & Gyllenberg (2001) and Gyllenberg & Metz (2001) looking at the evolution of single traits in metapopulations and also takes advantage of sensitivity analyses to calculate selection gradients

(Verdy and Caswell 2008). Our theoretical framework shows that coevolutionary outcomes in a metapopulation do not scale directly from those predicted in single, structured populations.

Sensitivities to genetic architecture are also discussed.

Methods

In general, our metapopulation modeling framework assumes equal connections between subpopulations (Figure 3.1; Levins 1969, 1970). Here, subpopulations are linked via independently dispersing hosts and pathogen particles (e.g., through the environment, vectors, or alternate hosts), and subpopulation dynamics are controlled via a simple susceptible-infected (SI) model (Figure 3.1). We link metapopulation and subpopulation dynamics by allowing a proportion of newborns to disperse and disease induced mortality to result in the release of independently dispersing infectious particles (Figure 3.1). From this structure, we can then specify fitness functions for the host and pathogen. Subsequently, we calculate selection gradients for resistance and virulence based on fitness and use an adaptive dynamics approach to determine coevolutionary trajectories based on incremental changes in resistance and virulence (Hofbauer and Sigmund 1990).

Metapopulation Model

We based our metapopulation model around the single-trait, evolutionary approach taken by Metz and Gyllenberg (2001) and Gyllenberg and Metz (2001). This approach tracks the number of subpopulations in each of a defined number of states. In the simplest case, a state would represent all subpopulations with the same number of individuals. Given our disease model, states are determined by the number of susceptible and infected hosts found in the

subpopulation. A single state in the metapopulation is denoted by $y_{(S,I)}$, where y is the number of subpopulations with S susceptible hosts and I infected hosts. The complete set of states is then defined to be all pairs of S and I such that $S + I \leq K$, where K is the carrying capacity of a subpopulation. We also add two dispersal states that track the number of susceptible migrants, D_S , and the number of independently dispersing infectious particles, D_I , in the metapopulation.

Because our metapopulation is composed of healthy and infected hosts, two sets of processes govern dynamics: demographic and disease processes. The demographic processes operating in the metapopulation are birth, death, emigration, and immigration. Each healthy individual within a subpopulation gives birth at rate, b_{obs} , which is a function of resistance (Equation 1). Healthy individuals have a constant natural mortality rate of μ . Emigration occurs at birth with a certain proportion, m_S , of newborns entering the susceptible migrant class. Susceptible migrants have an equal probability of settling in any subpopulation that is not at carrying capacity, which they encounter at rate f_S . Demographic processes are not explicitly regulated by density-dependence, but settlement of new individuals into a subpopulation, whether through local birth or immigration, cannot occur in a subpopulation at carrying capacity with additional individuals either dying immediately after birth or returning to the migrant pool.

The disease processes operating in the metapopulation are transmission, disease-induced host mortality and resultant production of independently dispersing pathogen particles. Here, transmission can occur either locally through the interaction with infectious individuals or globally through the interaction of susceptible hosts with an infectious migrant, where the host has a probability, p , of resisting infection and remaining susceptible. Also, because infectious migrants are not associated with a host, global infection processes do not increase the local subpopulation size. Within subpopulations, infected individuals suffer increased mortality due to

pathogen virulence, α . Upon the death of an infected host, a proportion, m_I , of the infection associated with the host enters the infectious migrant pool (e.g., individual pathogen particles or infectious vectors).

These assumptions lead us to the following model describing changes in the metapopulation (Equations 1-6):

$$\frac{dy_{(K,0)}}{dt} = -y_{(K,0)}\{K\mu + Kf_I(1-p)\beta_{obs}D_I\} + y_{(K-1,0)}\{(K-1)(1-m_s)b_{obs} + f_sD_s\} \quad (1)$$

⋮

$$\begin{aligned} \frac{dy_{(1,0)}}{dt} &= 2\mu y_{(2,0)} - y_{(1,0)}\{\mu + (1-m_s)b_{obs} + f_sD_s + f_I(1-p)\beta_{obs}D_I\} + y_{(1,1)}(\alpha + \mu) \\ &+ f_sD_s \sum_{i=0}^K \sum_{j=0}^{K-i} y_{(i,j)} \end{aligned} \quad (2)$$

⋮

$$\begin{aligned} \frac{dy_{(K-1,1)}}{dt} &= Kf_I(1-p)\beta_{obs}D_I y_{(K,0)} \\ &- y_{(K-1,1)}\{K\mu + \alpha + (K-1)f_I(1-p)\beta_{obs}D_I + (K-1)(1-p)\beta_{obs}\} \\ &+ y_{(K-2,1)}\{(K-2)(1-m_s)b_{obs} + f_sD_s\} \end{aligned} \quad (3)$$

⋮

$$\frac{dy_{(0,K)}}{dt} = y_{(1,K-1)}\{f_I(1-p)\beta_{obs}D_I + (K-1)(1-p)\beta_{obs}\} - y_{(0,K)}\{K\mu + K\alpha\} \quad (4)$$

$$\frac{dD_S}{dt} = m_S b_{obs} \sum_{i=0}^K \sum_{j=0}^{K-i} i y_{(i,j)} - \lambda_S D_S - f_S D_S \sum_{i=0}^{K-1} \sum_{j=0}^{K-1-i} y_{(i,j)} \quad (5)$$

$$\frac{dD_I}{dt} = m_I(\alpha + \mu) \sum_{i=0}^K \sum_{j=0}^{K-i} j y_{(i,j)} - \lambda_I D_I - f_I(1-p)\beta_{obs}D_I \sum_{i=0}^K \sum_{j=0}^{K-i} i y_{(i,j)} \quad (6)$$

where μ is the natural host mortality rate, α is the disease induced mortality rate, f_S is the rate at which susceptible migrants encounter local subpopulations, f_I is the rate at which infectious particles encounter local subpopulations, λ_S is the mortality rate of susceptible migrants, and λ_I is the decay rate of infectious particles (see Table 3.1).

Trade-off Assumptions

As is typical of many other studies of the evolution of resistance and virulence, we assumed simple trade-offs between resistance and reproduction and between virulence and transmission (Equations 7 and 8; Kamo et al. 2007; Best et al. 2011).

$$b_{obs} = b_{max} - \frac{(b_{max} - b_{min})p}{\{1 + \sigma(1-p)\}} \quad (7)$$

$$\beta_{obs} = \frac{\beta_{max}}{\ln 2} \ln(\alpha + 1) \quad (8)$$

Here, increased resistance, p , diverts energetic resources away from reproduction, denoted by b_{obs} , with weakly accelerating costs to reproduction from a maximum potential, b_{max} , down to a minimum, b_{min} , where σ controls the non-linearity in the trade-off function (Equation 7; Best et al. 2011). Increased virulence, α , results in quicker host death but also increases transmission, β_{obs} , non-linearly during the infectious period from no transmission to a maximum of β_{max} (Equation 8; Kamo et al. 2007; Best et al. 2011).

Defining fitness and trait evolution

Assuming that resistance and virulence are quantitative traits, we can then use basic quantitative genetics theory to derive fitness and the rate of evolution for each trait (Lande 1982). Specifically, consider the rate of evolution for the mean of a quantitative trait, \bar{z} , in a population of size N :

$$\frac{d\bar{z}}{dt} = \sigma_g^2 \frac{d\bar{r}}{d\bar{z}} \quad (9)$$

where σ_g^2 is the genetic variance of the trait, $d\bar{r}/d\bar{z}$ is the selection gradient, and \bar{r} describes the intrinsic rate of increase for the population, or

$$\bar{r} = \frac{1}{N} \frac{dN}{dt} \quad (10)$$

In our case, dN/dt can be found by summing the difference between birth rate and death rate in all subpopulations. Since we are considering both the rate of increase for the population as a whole (i.e., the fitness measure for resistance evolution) and for the infection (i.e., the fitness measure for virulence evolution), we refer to these rates as \bar{r}_H and \bar{r}_I respectively. We can write these as:

$$\bar{r}_H = \frac{1}{\sum_{i=0}^K \sum_{j=0}^{K-i} (i+j)y_{(i,j)}} \sum_{i=0}^K \sum_{j=0}^{K-i} y_{(i,j)} \{(1-m_S)b_{obs}i - \mu i - (\mu + \alpha)j + f_S D_S\} \quad (11)$$

$$\bar{r}_I = \frac{1}{\sum_{i=0}^K \sum_{j=0}^{K-i} j y_{(i,j)}} \sum_{i=0}^K \sum_{j=0}^{K-i} y_{(i,j)} \{(1-p)\beta_{obs}ij - (\mu + \alpha)j + f_I(1-p)\beta_{obs}iD_I\}. \quad (12)$$

Now, to calculate the rate of evolution for resistance and virulence, we must determine both the genetic variances and the selection gradients. In this study, due to the higher reproductive rate of pathogens relative to hosts, we assumed that $\sigma_{g,\alpha}^2 \gg \sigma_{g,p}^2$ (Table 3.1). When we calculate the selection gradients, $d\bar{r}_H/d\bar{p}$ and $d\bar{r}_I/d\bar{\alpha}$, we assume that $\bar{p} = p$ and $\bar{\alpha} = \alpha$ (i.e., all individuals have the same trait values). Also, notice that y and b_{obs} are functions of p , and y and β_{obs} are functions of α . Thus, taking the derivative of our fitness measures with respect to the traits and applying the chain rule, we have,

$$\begin{aligned}
\frac{d\bar{r}_H}{dp} &= \frac{1}{\sum_{i=0}^K \sum_{j=0}^{K-i} (i+j)y_{(i,j)}} \sum_{i=0}^K \sum_{j=0}^{K-i} \left(y_{(i,j)} \left\{ (1-m_S) \frac{db_{obs}}{dp} i + f_S \frac{dD_S}{dp} \right\} \right. \\
&\quad \left. + \frac{dy_{(i,j)}}{dp} \{ (1-m_S)b_{obs}i - \mu i - (\mu + \alpha)j + f_S D_S \} \right) \\
&\quad - \frac{\sum_{i=0}^K \sum_{j=0}^{K-i} \frac{dy_{(i,j)}}{dp} (i+j)}{\left(\sum_{i=0}^K \sum_{j=0}^{K-i} (i+j)y_{(i,j)} \right)^2} \sum_{i=0}^K \sum_{j=0}^{K-i} y_{(i,j)} \{ (1-m_S)b_{obs}i - \mu i - (\mu + \alpha)j + f_S D_S \}
\end{aligned} \tag{13}$$

$$\begin{aligned}
\frac{d\bar{r}_I}{d\alpha} &= \frac{1}{\sum_{i=0}^K \sum_{j=0}^{K-i} j y_{(i,j)}} \sum_{i=0}^K \sum_{j=0}^{K-i} \left(y_{(i,j)} \left\{ (1-p) \frac{d\beta_{obs}}{d\alpha} ij - j + f_I (1-p) \frac{d\beta_{obs}}{d\alpha} i D_I \right. \right. \\
&\quad \left. \left. + f_I (1-p) \beta_{obs} i \frac{dD_I}{d\alpha} \right\} + \frac{dy_{(i,j)}}{d\alpha} \{ (1-p)\beta_{obs}ij - (\mu + \alpha)j + f_I (1-p)\beta_{obs}i D_I \} \right) \\
&\quad - \frac{\sum_{i=0}^K \sum_{j=0}^{K-i} j \frac{dy_{(i,j)}}{d\alpha}}{\left(\sum_{i=0}^K \sum_{j=0}^{K-i} j y_{(i,j)} \right)^2} \sum_{i=0}^K \sum_{j=0}^{K-i} y_{(i,j)} \{ (1-p)\beta_{obs}ij - (\mu + \alpha)j + f_I (1-p)\beta_{obs}i D_I \}
\end{aligned} \tag{14}$$

It should be noted that the selection gradients (Equations 13 and 14) contain information about processes operating on multiple scales. These process include natural selection within a local subpopulation (Equations S1 and S4), environmental changes at the subpopulation level (i.e., subpopulation sorting; Equations S2 and S5), and gene flow (Equations S3 and S6). The second double sum, which is negative, in Equations 13 and 14, represents the component of selection that occurs at the metapopulation level.

Calculating subpopulation sorting terms

If we use vector notation for the metapopulation distribution vector (i.e., $\mathbf{y} = [y_{(S,I)} \text{ for } S \leq K \text{ and } I \leq K - S, D_S, D_I]$), and define $\boldsymbol{\theta}$ as a vector consisting of the parameters p and α , we can rewrite our model (Equations 3-8) in non-linear matrix notation as:

$$\frac{d\mathbf{y}}{dt} = \mathbf{A}[\mathbf{y}, \boldsymbol{\theta}]\mathbf{y} \quad (15)$$

where $\mathbf{A}[\mathbf{y}, \boldsymbol{\theta}]$ represents the non-linear matrix of coefficients. Our metapopulation sorting terms, $dy_{(i,j)}/dp$ and $dy_{(i,j)}/d\alpha$, can then be viewed as the sensitivity of the metapopulation distribution to $\boldsymbol{\theta}$. Because we assume ecological dynamics occur quickly relative to evolutionary dynamics (Lande 1982; Hofbauer and Sigmund 1990), we consider the equilibrium, $\hat{\mathbf{y}}$, of equation 15 when calculating the metapopulation sorting terms (i.e., $d\hat{y}_{(i,j)}/dp$ and $d\hat{y}_{(i,j)}/d\alpha$). We calculate these using the methods outlined in Verdy and Caswell (2008). Briefly,

$$\frac{d\hat{\mathbf{y}}}{d\boldsymbol{\theta}^T} = \left[-\mathbf{A} - (\hat{\mathbf{y}}^T \otimes \mathbf{I}) \frac{\partial \text{vec } \mathbf{A}}{\partial \hat{\mathbf{y}}^T} \right]^{-1} [\hat{\mathbf{y}}^T \otimes \mathbf{I}] \frac{\partial \text{vec } \mathbf{A}}{\partial \boldsymbol{\theta}^T} \quad (16)$$

where, T denotes the transpose; \mathbf{I} is the identity matrix; \otimes is the Kronecker product, and the vec operator stacks the columns of a matrix to form one column. The result of this equation is a two column matrix that gives the sensitivity of the equilibrium metapopulation distribution to the parameters of interest, p and α .

Model Analysis

We calculated the selection gradients for both resistance and virulence across a range of potential trait values (Table 3.1). This grid represents a selection surface that we used to predict coevolutionary trajectories from multiple initial values of host resistance and pathogen virulence. We did this by allowing resistance and virulence to change from the initial values according to increments determined by Equation 9, where the genetic variances for each trait, $\sigma_{g,p}^2$ and $\sigma_{g,\alpha}^2$, are given in Table 3.1. We allowed the traits to evolve on the surface in this fashion until a stable point was reached. This approach is in line with adaptive dynamics approaches in that the selection gradients at each point on the surface assume that the system is at equilibrium (Hofbauer and Sigmund 1990). Consequently, we are alternating the evolutionary component with ecological feedbacks as the system settles back to an equilibrium following perturbation by selection.

We then repeated this process across a range of host and pathogen dispersals, given by m_S and m_I (Table 3.1), to assess how asymmetries in host and pathogen dispersal impact coevolution. We also calculated the evolutionary processes found in the model (i.e., natural selection, subpopulation sorting, gene flow, and metapopulation-level selection) for both host resistance and pathogen virulence at all initial values and dispersal combinations.

Results

To understand how coevolution is affected by dispersal, we look at phenomenological patterns in selection as well as the mechanisms underlying these patterns. We first look at the patterns in selection gradients for host resistance and pathogen virulence. Although we considered a relatively large range of host and pathogen dispersals (Table 3.1), we present four

representative cases: 1) symmetric low dispersal (Figures 3.2C and 3.3C); 2) asymmetric low host – high pathogen dispersal (Figures 3.2D and 3.3D); 3) asymmetric high host – low pathogen dispersal (Figures 3.2A and 3.3A); and 4) symmetric high dispersal (Figures 3.2B and 3.3B).

In all cases, if hosts are initially highly resistant, the pathogen fails to persist in the population, and the resistance threshold necessary to exclude the pathogen increases as dispersal of the pathogen increases (i.e., light gray regions in Figure 3.3). In the absence of the pathogen, host resistance is selected against due to its reproductive costs as seen in the red areas of negative selection in Figure 3.2 associated with the light gray regions in Figure 3.3. Below this threshold, selection patterns vary with host and pathogen dispersal.

Case 1: Symmetric low dispersal

Here, the selection surfaces are dominated by a large region where resistance and virulence are selectively neutral (i.e., the region that is white in both Figure 3.2C and 3.3C). Below this neutral region, neither the host nor the pathogen persists as seen by the dark gray extinction region in Figures 3.2C and 3.3C. Above the neutral region, selection for both resistance and virulence is a mix of positive and negative pressures (i.e., the blue and red regions, respectively, of Figures 3.2C and 3.3C) that could lead to a coevolutionarily stable strategy (co-ESS), although none are observed (Figure 3.4C).

Case 2: Asymmetric low host – high pathogen dispersal

In this case, the neutral region is smaller than in case 1 (Figures 3.2D and 3.3D), and the metapopulation extinction region increases in size to include trait combinations where resistance is higher and virulence is lower (Figures 3.2D and 3.3D). Above the neutral region, the selection

gradients for resistance and virulence again vary between positive and negative with some areas along the neutral region promoting coevolution to the neutral region (Figures 3.2D and 3.3D), while others may promote a co-ESS although none are observed (Figure 3.4D).

Case 3: Asymmetric high host – low pathogen dispersal

Now, the selection surfaces for resistance and virulence change dramatically (Figures 3.2A and 3.3A). The selectively neutral region is relatively small and found at low resistance and high virulence values (Figures 3.2A and 3.3A), and metapopulation extinction only occurs for a small number of resistance-virulence combinations (Figures 3.2A and 3.3A). Above the neutral region, two coevolutionary outcomes are again apparent. First, a relatively large region of negative selection on resistance and positive selection on virulence pushes the system to the neutral region (Figures 3.2A and 3.3A). This basin is bordered by a region of positive selection on resistance (Figure 3.2A), which when coupled with a region of negative selection on virulence (Figure 3.2B), creates a coevolutionarily stable strategy (co-ESS) where resistance is intermediate and virulence is relatively low (i.e., red dots in Figure 3.4A).

Case 4: Symmetric high dispersal

When host and pathogen dispersal are high, the selectively neutral region is a narrow strip along the relatively large region of metapopulation extinction (Figures 3.2B and 3.3B). Above the neutral region, large regions of positive selection on resistance (Figure 3.2B) interact with large regions of negative selection on virulence (Figure 3.3B) to create two co-ESS's: one where resistance is high and virulence is low and one where resistance is slightly lower but virulence is intermediate (Figure 3.4B).

General trends in selection

Overall, several general trends emerge across these four cases. First, localized metapopulation structures, especially in the host, promote a diversity of coevolutionary outcomes as a result of the large neutral region (Cases 1 and 2). Neutral regions still exist with increasing dispersal, but now many more potential combinations of resistance and virulence are under selection, whether positive or negative, with the potential to coevolve to a co-ESS that is markedly different from the combinations found in the neutral region (Cases 3 and 4). In these cases where host dispersal is high, increasing pathogen dispersal results in the potential for increased resistance and/or increased virulence.

Evolutionary processes

The above results focused on the phenomenological patterns in selection. Now, we focus on the mechanistic underpinnings of these patterns by exploring the relative importance of the evolutionary processes captured by the model: natural selection, subpopulation sorting (i.e., local environmental change), gene flow, and metapopulation-level selection (Figures 3.5 and 3.6). First, natural selection in the host generally favors decreased resistance with the magnitude of selection decreasing with increasing host dispersal and increasing pathogen dispersal (Figure 3.5A). This selection on resistance is coupled with the negative natural selection pressures on virulence, which increases in magnitude with increasing pathogen dispersal but is relatively unaffected by host dispersal (Figure 3.6A).

Natural selection is generally balanced by the effect of local environmental changes (i.e., subpopulation sorting). Here, subpopulation sorting always favors increased virulence, although with the magnitude decreasing with pathogen dispersal (Figure 3.6B). For host resistance,

however, subpopulation sorting only opposes natural selection when host and pathogen dispersal are relatively low (Figure 3.5B). When pathogen dispersal increases, subpopulation sorting in the host coincides with natural selection for decreased virulence (Figure 3.5B). Increased host dispersal results in smaller subpopulation sorting terms regardless of the direction of selection.

In the pathogen population, gene flow, similar to subpopulation sorting, opposes natural selection on virulence (Figure 3.6C). The magnitude of the effect of gene flow in the pathogen increases with increasing pathogen dispersal with no effect of host dispersal (Figure 3.6C). In the host, the effect of gene flow on resistance also generally increases with increasing host dispersal (Figure 3.5C), but now the direction of the effect is determined by pathogen dispersal (Figure 3.5C). Low pathogen dispersal results in gene flow in the host that favors decreased resistance, while high pathogen dispersal favors increased resistance as a result of gene flow (Figure 3.5C).

Finally, the metapopulation-level component of selection is inconsequential in all cases when compared to natural selection, subpopulation sorting, and gene flow.

Discussion

Spatial mixing patterns in host-pathogen interactions vary along a continuum from well-mixed to within-population spatial structure to between-population mixing. Previous studies have differentiated evolutionary and coevolutionary outcomes in structured, single populations from the well mixed case while failing to scale further to the metapopulation level (Boots and Sasaki 1999; Haraguchi and Sasaki 2000; Boots et al. 2004; Lion and Boots 2010; Best et al. 2011). From our analysis, it is apparent that metapopulation structure determined through the interaction of host and pathogen dispersal between subpopulations affects the persistence of infectious pathogens and the consequent coevolution of host resistance and pathogen virulence.

In particular, predictions from a single population do not scale directly to determine coevolutionary outcomes in a metapopulation. Specifically, host and pathogen metapopulation structures where dispersal is symmetrically low favor a large selectively neutral region that creates the potential for high virulence. However, in a single population, local transmission in the face of completely local dispersal of the host favors decreased virulence (Boots and Sasaki 1999; Haraguchi and Sasaki 2000; Boots et al. 2004; Lion and Boots 2010; Best et al. 2011) and increased resistance (Best et al. 2011). The wider variety of resistance and virulence levels that experience low or no evolutionary pressure at low joint dispersal in a metapopulation could potentially be due to the greater spatial heterogeneity in selection pressures experienced by the highly structured host and pathogen subpopulations (Kerr et al. 2006). This spatial heterogeneity is generated by the balance between natural selection and subpopulation sorting (i.e., local environmental changes; Frank and Slatkin 1992) and is maintained by the relatively weak gene flow between subpopulations.

Despite these differences, as host dispersal increases, the metapopulation and single-population structures begin to show similar patterns as they both converge to the well-mixed case. In more well-mixed host metapopulations, we found coevolutionarily stable strategies with lower host resistance and pathogen virulence when transmission was local similar to the single population case (Boots and Sasaki 1999; Boots et al. 2004; Best et al. 2011). In this case, gene flow amongst host populations replaces natural selection as the primary evolutionary driver against resistance and potentially interrupts local adaptation at the subpopulation level due to the source-sink dynamics created by infection (Holt and Gaines 1992). This source-sink dynamic leads to increased demographic turnover in the host population as infected subpopulations with highly virulent strains go extinct favoring a coevolutionary stable strategy where virulence is

relatively low (Lion and Boots 2010). Thus, our results point to the convergence across spatial levels to a well-mixed scenario. However, metapopulation dynamics promote different ecological feedbacks on coevolution (e.g., population turnover and source-sink dynamics) that do not completely align with those found in single populations.

Although selection pressures fail to scale across spatial mixing patterns, our results point to the ability of some metapopulation effects to scale across genetic architectures. The large selectively neutral regions for quantitative traits we observed when dispersal was symmetrically low is similar to results from gene-for-gene models of coevolution in a metapopulation, where local dispersal promoted genetic diversity due to local adaptation (Thrall and Burdon 2002). However, the asymmetric adaptation (i.e., high resistance with low virulence or vice versa) previously observed under asymmetrical host and pathogen dispersal rates was only found in our model when the host was more global and the pathogen was local (Gandon et al. 1996; Gandon 2002). This difference may suggest that system-specific models should focus on one model or the other. We suggest plant diseases as ideal candidates for the gene-for-gene models (Thrall and Burdon 2003), while the quantitative trait approaches we presented may be useful across a broader range of host-pathogen systems with polygenic inheritance (Sorci et al. 1997). Despite this difference, the similarity in results between the two approaches is promising and suggests that metapopulation signatures in coevolutionary dynamics are strong allowing the different models of metapopulation coevolution to inform one another.

Returning to the example of plague in North America, differences in host dispersal may determine why some species like prairie dogs show little or no resistance to plague (Cully and Williams 2001), while others like the California ground squirrel (*Spermophilus beecheyi*), exhibit relatively high levels of resistance (Williams et al. 1979). In this case, both species

exhibit metapopulation-like structures, but inter-patch distances are much smaller in California ground squirrels leading to the potential for higher dispersal (Evans and Holdenried 1943; Dobson 1979; Stapp et al. 2004). In addition, the role of off-host flea reservoirs in plague dynamics (Buhnerkempe et al. 2011) coupled with the host specificity of many prominent plague fleas (Eskey and Haas 1940) suggests that pathogen dispersal may be small. Thus, plague in prairie dogs may be in the highly localized region for both host and pathogen (i.e., Case 1; Figures 3.2C and 3.3C) promoting neutrality, and as a consequence, the evolution of resistance will take longer with the potential for genetic drift to subsequently eliminate resistance. California ground squirrels on the other hand may move into the region where host dispersal is relatively higher (i.e., Case 3; Figures 3.2A and 3.3A) indicating that resistance may be evolutionarily stable and develop relatively quickly. However, no concomitant reduction in virulence has been observed in nature suggesting more plague specific models are needed. Other emerging infectious diseases in wildlife may also benefit from the metapopulation approach presented above. In particular, chytridiomycosis in amphibians may be an example of a system where host dispersal is relatively limited in relation to pathogen dispersal owing to the rapid spread of the pathogen (i.e., Case 2; Figures 3.2D and 3.3D; Muths et al. 2003). This may suggest that persistence is not possible supporting evidence of increased extinction risk (Muths et al. 2003). However, if persistence is possible, highly resistance hosts or relatively benign pathogens are the predicted outcome. To extend these and other examples beyond speculation though, more specific studies of the relative rates of dispersal of the host and pathogen would lead to better predictions of coevolutionary outcomes from more system-specific models.

Here, we presented, to our knowledge, the first model of quantitative trait coevolution in a metapopulation. This model allowed us to study the impact of host and pathogen dispersal

strategies on the coevolutionary trajectories of host resistance and pathogen virulence. However, more work is needed to understand how model assumptions interact with the metapopulation structure. In particular, the assumed form of the reproductive and transmission trade-offs associated with resistance and virulence could have a large effect on evolutionary outcomes (Kamo et al. 2007), as well as model structure in general (e.g., generation of the migrating infectious particles). Also, the simulation approach we used to estimate the selection surfaces may not be sufficient to identify all co-ESS's due to the coarse grain of resistance and virulence combinations explored (Kamo et al. 2007). This potential deficiency may explain the lack of co-ESS's when host dispersal is low (i.e., Cases 1 and 2) suggesting that a more analytical approach is needed (e.g., Haraguchi and Sasaki 2000; Lion and Boots 2010). Consequently, we view this work as the first-step to developing intuition on the role of metapopulation structure in coevolutionary processes, not only in the context of infectious diseases, but also across a variety of systems (e.g., competitive interactions or predator-prey dynamics). From this baseline, more system specific models can be developed to address how details of the ecological interactions may alter these general coevolutionary patterns.

Table 3.1: Model parameters and their values. Note that values given as intervals indicate the range of possible values studied.

Parameter	Description	Value(s)
m_S	Probability a newborn becomes a susceptible migrant	0.1, 0.25, 0.5, 0.75, 0.9
m_I	Proportion of infectious material that enters the infectious migrant pool upon disease induced mortality	0.1, 0.25, 0.5, 0.75, 0.9
p	Probability of resistance	[0,1] by 0.01
α	Virulence (i.e., disease induced mortality)	[0.01,1] by 0.01
K	Local carrying capacity	50
b_{obs}	Observed birth rate	$[b_{min}, b_{max}]$
b_{max}	Maximum possible birth rate	10
b_{min}	Minimum possible birth rate	2
β_{obs}	Observed transmission rate	$[0, \beta_{max}]$
β_{max}	Maximum possible transmission rate	0.25
μ	Natural host mortality rate	0.01
f_S	Rate at which susceptible migrants find habitable subpopulations	2.5
f_I	Rate at which infectious migrants find susceptible subpopulations	1.5
λ_S	Susceptible migrant mortality rate	0.005
λ_I	Infectious migrant mortality rate	0.005
$\sigma_{g,p}^2$	Genetic variance for resistance	0.001
$\sigma_{g,\alpha}^2$	Genetic variance for virulence	0.01

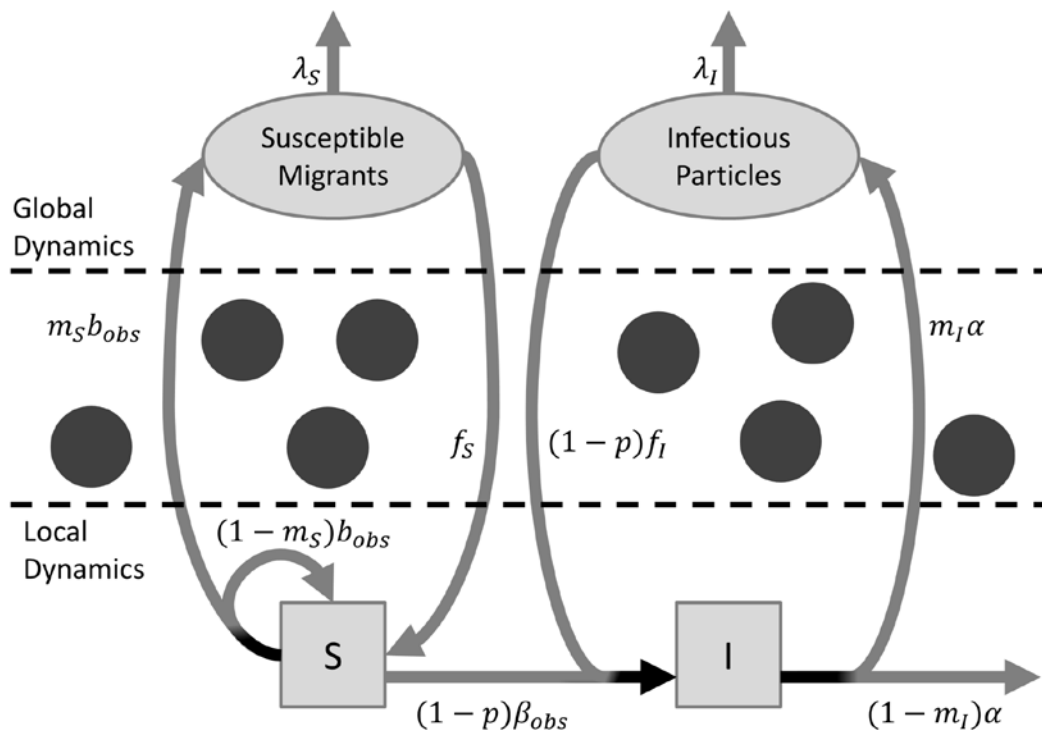


Figure 3.1: Box and arrow diagram of the model describing state changes in the metapopulation.

Parameters associated with transitions are given.

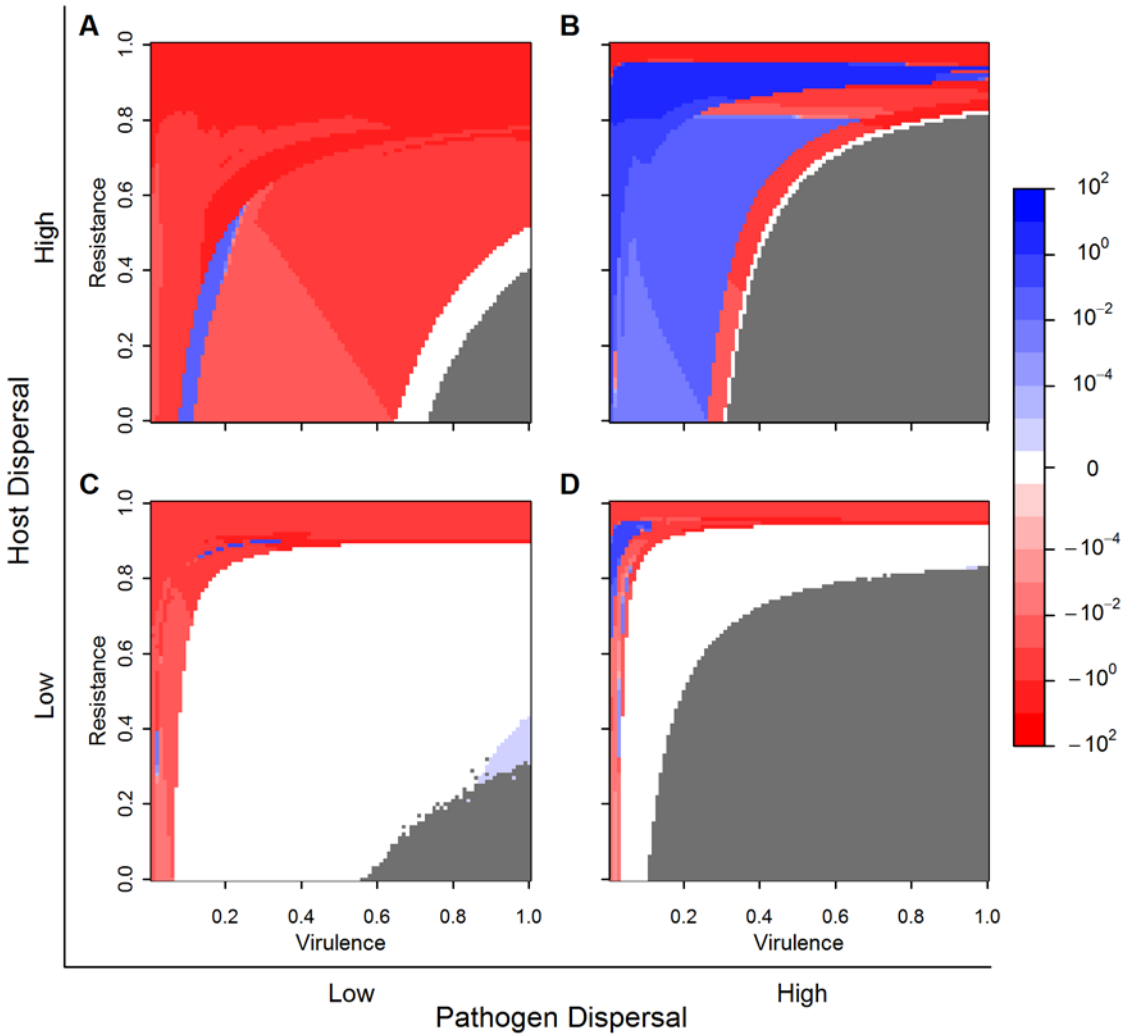


Figure 3.2: Selection gradient surface for host resistance across a range of host and pathogen dispersals. Red/blue values indicate negative/positive selection gradients which push the trait to lower/higher values. White indicates an approximately zero selection gradient. Dark grey denotes regions of parameter space where the host population failed to persist. A range of dispersal parameters were explored (Table 3.1), but here we present (A) $m_s = 0.9$ and $m_l = 0.1$, (B) $m_s = 0.9$ and $m_l = 0.5$, (C) $m_s = 0.1$ and $m_l = 0.1$, (D) $m_s = 0.1$ and $m_l = 0.5$.

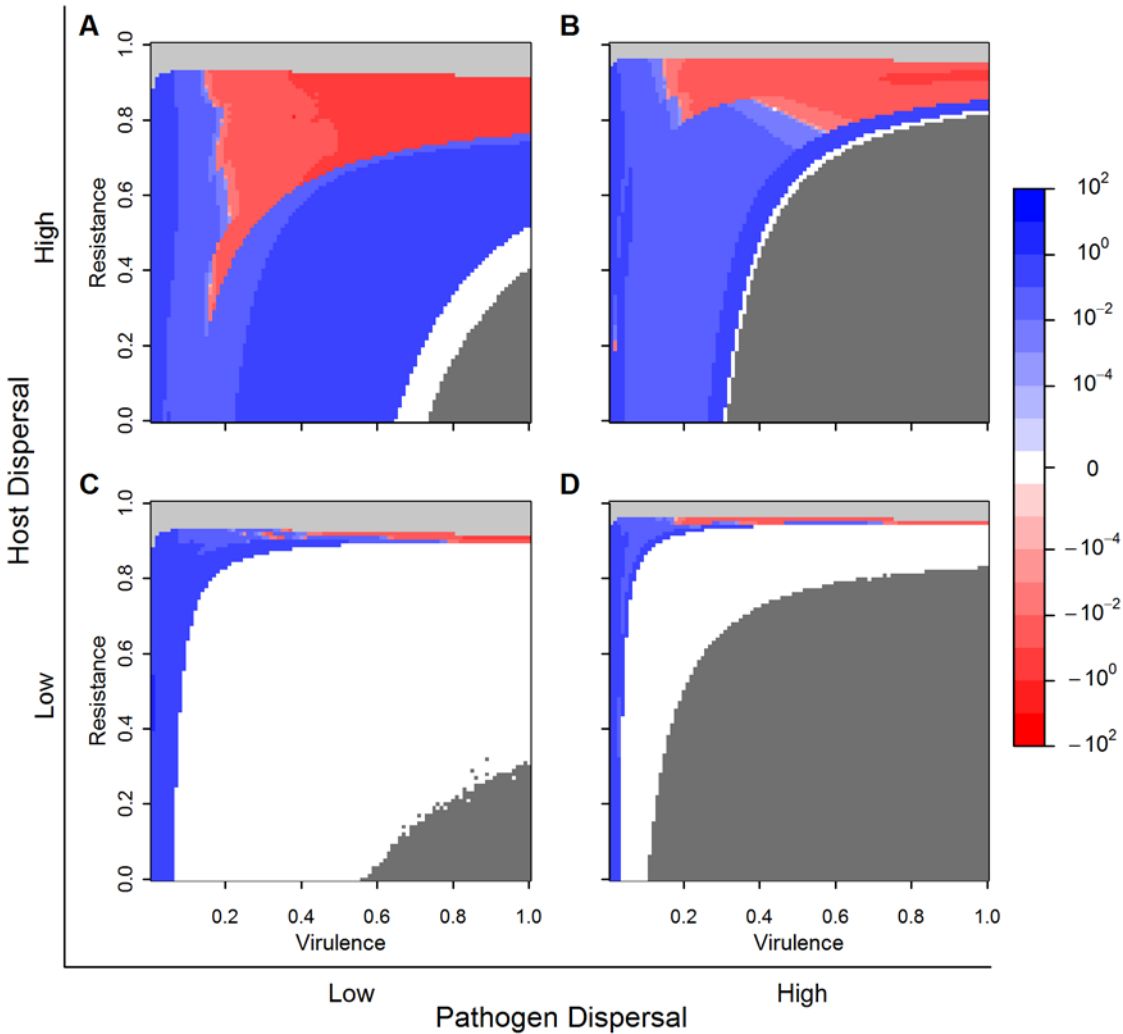


Figure 3.3: Selection gradient surface for pathogen virulence across a range of host and pathogen dispersals. Red/blue values indicate negative/positive selection gradients which push the trait to lower/higher values. White indicates an approximately zero selection gradient. Light grey denotes regions of parameter space the pathogen, but not the host, went extinct. Dark grey denotes regions of parameter space where the host population failed to persist. A range of dispersal parameters were explored (Table 3.1), but here we present (A) $m_s = 0.9$ and $m_l = 0.1$, (B) $m_s = 0.9$ and $m_l = 0.5$, (C) $m_s = 0.1$ and $m_l = 0.1$, (D) $m_s = 0.1$ and $m_l = 0.5$.

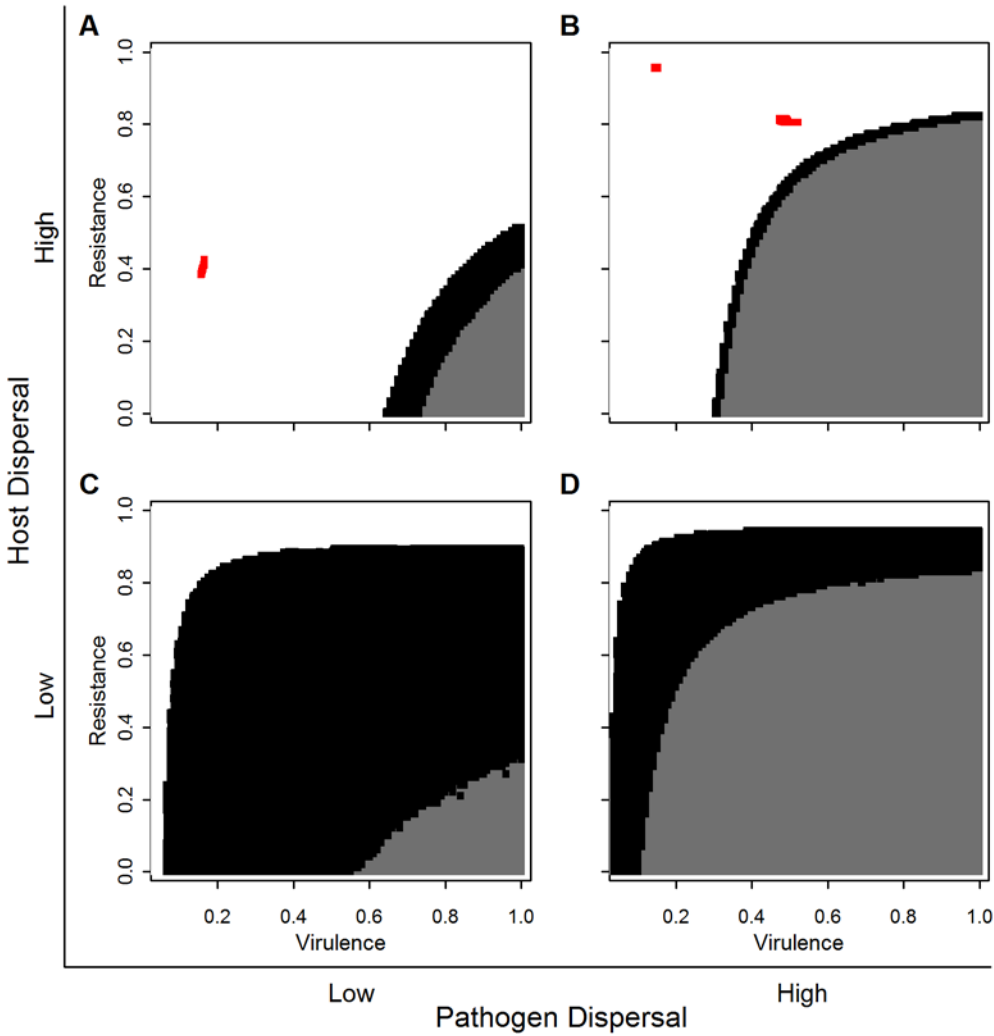


Figure 3.4: Coevolutionary outcomes for host resistance and pathogen virulence across a range of host and pathogen dispersal strategies. Red indicates coevolutionarily stable strategies (co-ESS's). Black indicates combinations of resistance and virulence that where coevolutionary pressures are approximately neutral. White indicates a coevolutionarily unstable combination of resistance and virulence. Grey indicates a combination of resistance and virulence that through coevolution result in the extinction of the metapopulation.

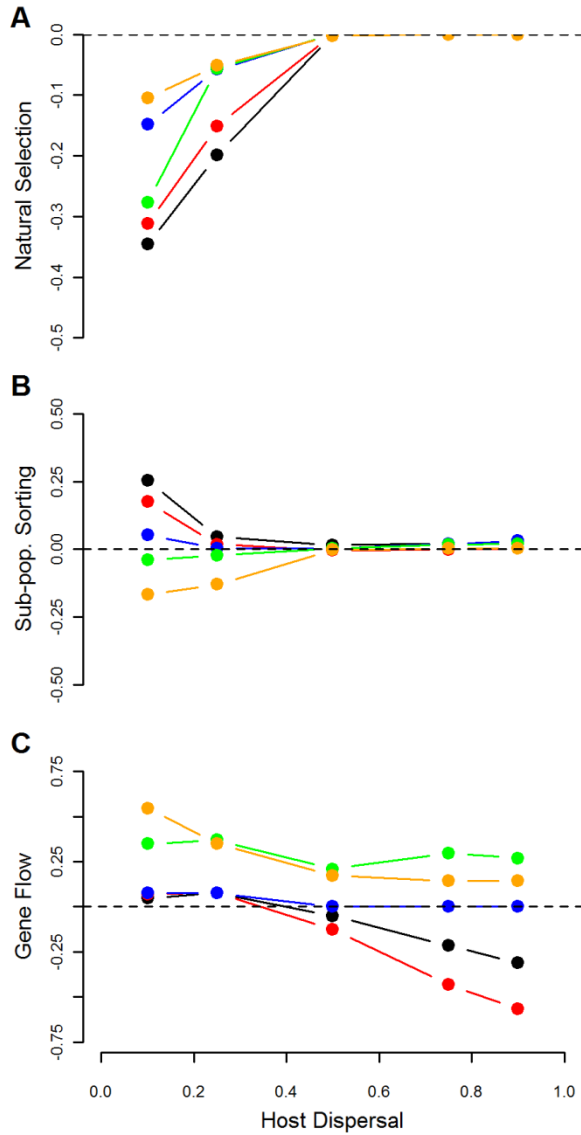


Figure 3.5: The components of selection on host resistance as a function of host and pathogen dispersal. These are divided into (A) natural selection, (B) sub-population sorting, and (C) gene flow. Lines are plotted over the range of host dispersal strategies with different line colors representing different pathogen dispersal strategies (Black – $m_I = 0.1$; Red – $m_I = 0.25$; Blue – $m_I = 0.5$; Green – $m_I = 0.75$; Orange – $m_I = 0.9$). Values plotted are the median value of the selection component across the entire coexistence region of the selection surface for a given host and pathogen dispersal combination.

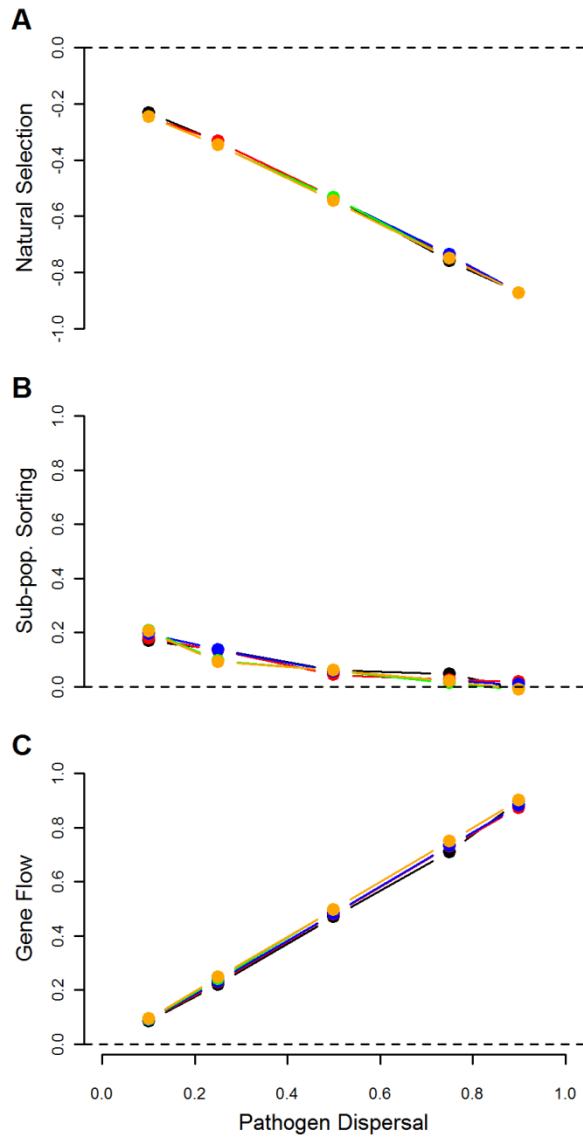


Figure 3.6: The components of selection on pathogen virulence as a function of pathogen and host dispersal. These are divided into (A) natural selection, (B) sub-population sorting, and (C) gene flow. Lines are plotted over the range of pathogen dispersal strategies with different line colors representing different host dispersal strategies (Black – $m_S = 0.1$; Red – $m_S = 0.25$; Blue – $m_S = 0.5$; Green – $m_S = 0.75$; Orange – $m_S = 0.9$). Values plotted are the median value of the selection component across the coexistence region of the entire selection surface for a given host and pathogen dispersal combination.

LITERATURE CITED

- Anderson, R.M., and R.M. May. 1982. Coevolution of hosts and pathogens. *Parasitology* 85: 411-426.
- Best, A., S. Webb, A. White, and M. Boots. 2011. Host resistance and coevolution in spatially structured populations. *Proceedings of the Royal Society B: Biological Sciences* 278: 2216-2222.
- Boots, M., and A. Sasaki. 1999. 'Small worlds' and the evolution of virulence: infection occurs locally and at a distance. *Proceedings of the Royal Society B: Biological Sciences* 266: 1933-1938.
- Boots, M., P.J. Hudson, and A. Sasaki. 2004. Large shifts in pathogen virulence relate to host population structure. *Science* 303: 842-844.
- Bremermann, H.J., and J. Pickering. 1983. A game-theoretical model of pathogen virulence. *Journal of Theoretical Biology* 100: 411-426.
- Bremermann, H.J., and H.R. Thieme. 1989. A competitive exclusion principle for pathogen virulence. *Journal of Mathematical Biology* 27: 179-190.
- Buhnerkempe, M.G., R.J. Eisen, B. Goodell, K.L. Gage, M.F. Antolin, and C.T. Webb. 2011. Transmission shifts underlie variability in population responses to *Yersinia pestis* infection. *PLoS One* 6: e22498.
- Craft, M.E., E. Volz, C. Packer, and L.A. Meyers. 2011. Disease transmission in territorial populations: the small-world network of Serengeti lions. *Journal of the Royal Society Interface* 8: 776-786.
- Cully, J.F. and E.S. Williams. 2001. Interspecific comparisons of sylvatic plague in prairie dogs. *Journal of Mammalogy* 82: 894-905.
- Dobson, F.S. 1979. An experimental study of dispersal in the California ground squirrel. *Ecology* 60: 1103-1109.
- Eskey, C.R. and V.H. Haas. 1940. Plague in the western part of the United States. *Public Health Bulletin* 254: 1-82.
- Evans, F.C. and R. Holdenried. 1943. A population study of the Beechey ground squirrel in central California. *Journal of Mammalogy* 24: 231-260.
- Farnsworth, M.L., J.A. Hoeting, N.T. Hobbs, and M.W. Miller. 2006. Linking chronic wasting disease to mule deer movement scales: a hierarchical Bayesian approach. *Ecological Applications* 16: 1026-1036.

- Frank, S.A., and M. Slatkin. 1992. Fisher's Fundamental Theorem of Natural Selection. *Trends in Ecology and Evolution* 7: 92-95.
- Gandon, S., Y. Capowiez, Y. Dubois, Y. Michalakis, and I. Olivieri. 1996. Local adaptation and gene-for-gene coevolution in a metapopulation model. *Proceedings of the Royal Society B: Biological Sciences* 263: 1003-1009.
- Gandon, S. 2002. Local adaptation and the geometry of host-parasite coevolution. *Ecology Letters* 5: 246-256.
- George, D. 2009. Pathogen persistence in wildlife populations: case studies of plague in prairie dogs and rabies in bats. Ph.D. Dissertation. Colorado State University: Fort Collins, CO.
- Gyllenberg, M. and J.A.J. Metz. 2001. On fitness in structured metapopulations. *Journal of Mathematical Biology* 43: 545-560.
- Haraguchi, Y., and A. Sasaki. 2000. The evolution of pathogen virulence and transmission rate in a spatially structured population. *Journal of Theoretical Biology* 203: 85-96.
- Hofbauer, J., and K. Sigmund. 1990. Adaptive dynamics and evolutionary stability. *Applied Mathematics Letters* 3: 75-79.
- Holt, R.D., and M.S. Gaines. 1992. Analysis of adaptation in heterogeneous landscapes: implications for the evolution of fundamental niches. *Evolutionary Ecology* 6: 433-447.
- Kamo, M., A. Sasaki, and M. Boots. 2007. The role of trade-off shapes in the evolution of parasites in spatial host populations: an approximate analytical approach. *Journal of Theoretical Biology* 244: 588-596.
- Kerr, B., C. Neuhauser, B.J.M. Bohannan, and A.M. Dean. 2006. Local migration promotes competitive restraint in a host-pathogen 'tragedy of the commons.' *Nature* 442: 75-78.
- Lande, R. 1982. A quantitative genetic theory of life history evolution. *Ecology* 63: 607-615.
- Levin, S., and D. Pimental. 1981. Selection of intermediate rates of increase in pathogen-host systems. *American Naturalist* 117: 308-315.
- Levins, R. 1969. Some demographic and genetic consequences of environmental heterogeneity for biological control. *Bulletin of the Entomological Society of America* 15: 237-240.
- Levins, R. 1970. Extinction. *Lectures on mathematics in the life sciences* 2: 75-107.
- Lion, S., and M. Boots. 2010. Are pathogens "prudent" in space? *Ecology Letters* 13: 1245-1255.

- May, R.M., and R.M. Anderson. 1983. Epidemiology and genetics in the coevolution of pathogens and hosts. *Proceedings of the Royal Society B: Biological Sciences* 219: 281-313.
- Metz, J.A.J. and M. Gyllenberg. 2001. How should we define fitness in structured metapopulation models? Including an application to the calculation of evolutionarily stable dispersal strategies. *Proceedings of the Royal Society B: Biological Sciences* 268: 499-508.
- Muths, E., P.S. Corn, A.P. Pessier, and D.E. Green. 2003. Evidence for disease-related amphibian decline in Colorado. *Biological Conservation* 110: 357-365.
- Nuismer, S. 2006. Parasite local adaptation in a geographic mosaic. *Evolution* 60: 24-30.
- Salkeld D.J., M. Salathé, P. Stapp, J.H. Jones. 2010. Plague outbreaks in prairie dog populations explained by percolation thresholds of alternate host abundance. *Proceedings of the National Academy of Sciences USA* 107: 14247-14250.
- Snäll, T., R.B. O'Hara, C. Ray, and S.K. Collinge. 2008. Climate-driven spatial dynamics of plague among prairie dog colonies. *American Naturalist* 171: 238-248.
- Sorci, G., A.P. Møller, and T. Boulinier. 1997. Genetics of host-parasite interactions. *Trends in Ecology and Evolution* 12: 196-200.
- Stapp, P., M.F. Antolin, and M. Ball. 2004. Patterns of extinction in prairie dog metapopulations: plague outbreaks follow El Niño events. *Frontiers in Ecology and the Environment* 2: 235-240.
- Swinton, J., J. Harwood, B.T. Grenfell, and C.A. Gilligan. 1998. Persistence thresholds for phocine distemper virus infection in harbor seal *Phoca vitulina* metapopulations. *Journal of Animal Ecology* 67: 54-68.
- Thompson, J.N., and J.J. Burdon. 1992. Gene-for-gene coevolution between plants and parasites. *Nature* 360: 121-125.
- Thrall, P.H., and J.J. Burdon. 2002. Evolution of gene-for-gene systems in metapopulations: the effect of spatial scale of host and pathogen dispersal. *Plant Pathology* 51: 169-184.
- Thrall, P.H., and J.J. Burdon. 2003. Evolution of virulence in a plant host-pathogen metapopulation. *Science* 299: 1735-1737.
- Verdy, A., and H. Caswell. 2008. Sensitivity analysis of reactive ecological dynamics. *Bulletin of Mathematical Biology* 70: 1634-1659.

- Vicente, J., R.J. Delahay, N.J. Walker, and C.L. Cheeseman. 2007. Social organization and movement influence the incidence of bovine tuberculosis in an undisturbed high-density badger *Meles meles* population. *Journal of Animal Ecology* 76: 348-360.
- Wild, G., A. Gardner, and S.A. West. 2009. Adaptation and the evolution of pathogen virulence in a connected world. *Nature* 459: 983-986.
- Williams, J.E., M.A. Moussa, and D.C. Cavanaugh. 1979. Experimental plague in the California ground squirrel. *Journal of Infectious Diseases* 140: 618-621.

Appendix 3.1: Calculation of evolutionary processes that make up the selection gradients

When splitting the selection gradient into separate evolutionary processes, we group terms from Equation 13 according to their biological interpretations. The natural selection component is composed of those terms that affect individual fitness directly (Equations S1 and S4). The subpopulation sorting component describes changes in the local environments and includes any subpopulation sorting terms that describe local, as opposed to global changes (Equations S2 and S5). Consequently, gene flow contains two effects: the effect of trait changes on gene flow itself (i.e., the global dynamics) and the interaction between the global dynamics and changing local dynamics (Equations S3 and S6).

$$\text{Natural Selection}_{Res} = \frac{1}{\sum_{i=0}^K \sum_{j=0}^{K-i} (i+j)y_{(i,j)}} \sum_{i=0}^K \sum_{j=0}^{K-i} \left(y_{(i,j)} (1 - m_s) \frac{db_{obs}}{dp} i \right) \quad (\text{S1})$$

$$\text{Subpop. Sorting}_{Res} = \frac{1}{\sum_{i=0}^K \sum_{j=0}^{K-i} (i+j)y_{(i,j)}} \sum_{i=0}^K \sum_{j=0}^{K-i} \left(\frac{dy_{(i,j)}}{dp} \{ (1 - m_s) b_{obs} i - \mu i - (\mu + \alpha) j \} \right) \quad (\text{S2})$$

$$\text{Gene Flow}_{Res} = \frac{1}{\sum_{i=0}^K \sum_{j=0}^{K-i} (i+j)y_{(i,j)}} \sum_{i=0}^K \sum_{j=0}^{K-i} \left(y_{(i,j)} f_s \frac{dD_s}{dp} + \frac{dy_{(i,j)}}{dp} f_s D_s \right) \quad (\text{S3})$$

$$\text{Natural Selection}_{Vir} = \frac{1}{\sum_{i=0}^K \sum_{j=0}^{K-i} j y_{(i,j)}} \sum_{i=0}^K \sum_{j=0}^{K-i} \left(y_{(i,j)} \left\{ (1 - p) \frac{d\beta_{obs}}{d\alpha} ij - j \right\} \right) \quad (\text{S4})$$

$$\text{Subpop. Sorting}_{vir} = \frac{1}{\sum_{i=0}^K \sum_{j=0}^{K-i} j y_{(i,j)}} \sum_{i=0}^K \sum_{j=0}^{K-i} \left(\frac{dy_{(i,j)}}{d\alpha} \{ (1-p)\beta_{obs}ij - (\mu + \alpha)j \} \right) \quad (\text{S5})$$

$$\text{Gene Flow}_{vir} \quad (\text{S6})$$

$$= \frac{1}{\sum_{i=0}^K \sum_{j=0}^{K-i} j y_{(i,j)}} \sum_{i=0}^K \sum_{j=0}^{K-i} \left(y_{(i,j)} \left\{ f_I(1-p) \frac{d\beta_{obs}}{d\alpha} i D_I + f_I(1-p) \beta_{obs} i \frac{dD_I}{d\alpha} \right\} + \frac{dy_{(i,j)}}{d\alpha} \{ f_I(1-p) \beta_{obs} i D_I \} \right)$$

CHAPTER 4

THE INTERACTION OF RESISTANCE-REPRODUCTION AND VIRULENCE-TRANSMISSION TRADE-OFFS, COEVOLUTION, AND DISPERSAL IN A METAPOPOPULATION⁴

Summary

Most theoretical studies on the evolution of pathogen virulence and host resistance have relied on trade-offs for increases in these traits. In particular, resistance comes at a cost of reproduction, and virulence, while increasing transmission, reduces the infectious period through increased host mortality. While many studies on the evolution of resistance and virulence have focused on well-mixed populations, the interaction between host and pathogen coevolution, spatial structure in a single population, and the functional forms of these trade-offs have also received considerable attention. Here, we expand spatial structure to include metapopulation dynamics in the host and pathogen and determine how the coevolutionary trajectories of resistance and virulence are affected by different trade-offs (i.e., accelerating, linear, and decelerating costs to reproduction and transmission) in a variety of metapopulation structures. The results suggest that the effect of trade-off shapes does not simply scale from single-population structure to metapopulation structure. In the metapopulation case, selection on

⁴Co-authors for this chapter include:

Colleen T. Webb

Department of Biology, Colorado State University, Fort Collins, CO, USA

Mike Boots

Centre for Ecology and Conservation, University of Exeter, Cornwall, UK

resistance is largely unaffected by changes from linear to accelerating cost trade-offs, while selection of virulence is unaffected by changes from linear to decelerating cost trade-offs, with the specific combination determining whether local structuring in the host can promote high levels of diversity through selective neutrality for resistance and virulence. Consequently, this work emphasizes that higher level spatial structure can change the sensitivities of coevolutionary trajectories to trade-off shapes which may further complicate estimation of trade-off shapes in natural systems.

Introduction

Studies on evolution in host-pathogen systems commonly assume trade-offs for host resistance and reproduction [1,2] and pathogen virulence and transmission [3], with the specific shapes of these trade-offs leading to a variety of evolutionary outcomes for resistance [1,4] and virulence [5-8]. Other studies on the coevolution of host resistance and parasite virulence have found that the interaction between evolutionary processes in host and pathogen populations and trade-off assumptions can have a considerable effect on coevolutionary trajectories [9,10]. All of these models assume well-mixed host populations but, other work has extended the evolution and coevolution of host resistance and pathogen virulence to more realistic cases where contact patterns in host populations are heterogeneous due to spatial structure within a single host population [11-15]. Here again, the functional forms of the trade-offs between virulence and transmission as well as resistance and reproduction can alter selection pressures in the system [16]. Specifically, localized transmission processes can promote an evolutionarily stable strategy (ESS) for virulence under a linear virulence-transmission trade-off [16]. This same functional trade-off form has not previously been shown to promote an ESS virulence value in well-mixed

populations [5, 16-18]. Thus, it is essential to understand the trade-offs that accompany host resistance and pathogen virulence in addition to the effect of spatial structure.

However, spatial structure is not only determined at the population level but can be a complex mix of within- and between-population dynamics (i.e., a metapopulation). Past attempts to incorporate metapopulation structure into the study of host-pathogen coevolution have found that the level of overlap between a host's and a pathogen's dispersal ability across subpopulations affects coevolutionary outcomes, but no costs to resistance and virulence were assumed [19-23]. More recently, a model of quantitative trait coevolution in a metapopulation has allowed the incorporation of trade-offs for host resistance and pathogen virulence (Buhnerkempe et al. unpublished manuscript). When resistance and virulence come at accelerating costs of reproduction and transmission, respectively, local dispersal strategies increase the diversity of potential coevolutionary outcomes (Buhnerkempe et al. unpublished manuscript). This is similar to results found in structured, single populations, but there is the potential for much greater diversity in virulence and resistance coevolutionary outcomes in the metapopulation context [15]. Because of the differences in coevolutionary pressures seen when scaling from within- to between-population spatial structure, it is not apparent how different trade-off functions will affect host-pathogen coevolution in a metapopulation.

Here, we analyze how different trade-offs between host resistance and reproduction and pathogen virulence and transmission affect coevolutionary trajectories in a metapopulation. To do this, we use the model of quantitative trait coevolution in a metapopulation described by Buhnerkempe et al. (unpublished manuscript). Three different functional forms for the trade-offs are considered: linear, decelerating, and accelerating. We then vary host and pathogen dispersal

strategies to test for an interaction between the ecological and epidemiological metapopulation structures and the shape of the trade-off.

Methods

Metapopulation Disease Model

For this study, we use the metapopulation disease model described by Buhnerkempe et al. (unpublished manuscript). Briefly, this simple susceptible-infected model assumes that transmission is a density-dependent process through either direct-contact within a subpopulation or through independently dispersing infectious particles (e.g., vectors). Transmission (β_{obs}) is determined by the trade-off with virulence, α . Exposed individuals resist infection with probability, p (i.e., resistance), and remain susceptible or become infectious, which results in disease-induced mortality at rate α (i.e., virulence). Death due to disease results in the release of a proportion, m_I , of the infection associated with the host as independently dispersing infectious particles (i.e., the pathogen's dispersal strategy).

Host population dynamics are not only regulated by disease, but by birth, death, and dispersal (Buhnerkempe et al. unpublished manuscript). Susceptible hosts give birth at rate b_{obs} , which is a monotonically decreasing function of host resistance, and have a natural mortality rate of μ . A proportion, m_S , of susceptible individuals disperse at birth (i.e., the host's dispersal strategy) and enter a susceptible migrant pool that consequently settles into available subpopulations at rate f_S .

Instead of modeling each patch explicitly, we model the number of patches (i.e., $y_{(S,I)}$) that contain a specific number of susceptibles, S , and infecteds, I , where the patch size is limited

by a carrying capacity, K (i.e., $S + I \leq K$; Buhnerkempe et al. unpublished manuscript; [24,25]).

Thus, changes in the metapopulation state distribution are governed by:

$$\begin{aligned}
\frac{dy_{(S,I)}}{dt} &= -y_{(S,I)}\{S(1 - m_S)b_{obs}1_{\{S+I < K\}} + S\mu + \beta_{obs}SI + I(\alpha + \mu) + f_S D_S 1_{\{S+I < K\}} \\
&+ \beta_{obs}Sf_I(1 - p)D_I\} + y_{(S-1,I)}\{(S - 1)(1 - m_S)b_{obs} + f_S D_S\} + y_{(S+1,I)}\{S\mu\} \\
&+ y_{(S+1,I-1)}\{\beta_{obs}(S + 1)(I - 1) + \beta_{obs}(S + 1)f_I(1 - p)D_I\} \\
&+ y_{(S,I+1)}\{(I + 1)(\alpha + \mu)\}
\end{aligned} \tag{1}$$

where $1_{\{S+I < K\}}$ is an indicator function that prevents birth and immigration into a subpopulation at carrying capacity. D_S and D_I are the susceptible migrants and independently dispersing infectious particles, respectively. These pools change according to:

$$\frac{dD_S}{dt} = m_S b_{obs} \sum_{i=0}^K \sum_{j=0}^{K-i} i y_{(i,j)} - \lambda_S D_S - f_S D_S \sum_{i=0}^{K-1} \sum_{j=0}^{K-1-i} y_{(i,j)} \tag{2}$$

$$\frac{dD_I}{dt} = m_I (\alpha + \mu) \sum_{i=0}^K \sum_{j=0}^{K-i} j y_{(i,j)} - \lambda_I D_I - f_I (1 - p) \beta_{obs} D_I \sum_{i=0}^K \sum_{j=0}^{K-i} i y_{(i,j)} \tag{3}$$

where λ_S and λ_I are the death rate of susceptible migrants and decay rate of infectious particles, respectively. For parameter values and descriptions see Table 4.1.

Selection Gradients

To define selection gradients, we first need to define the fitness functions that underlie resistance and virulence evolution. We define the fitness measure for resistance evolution to be the per capita growth rate across the entire metapopulation (i.e., the average of the difference between each individual's birth and death rates; Buhnerkempe et al. unpublished manuscript). The fitness measure for resistance evolution is then given by the per infectious individual increase in infection prevalence across the entire metapopulation (i.e., the average of the difference between each infected individual's transmission and death rates; Buhnerkempe et al. unpublished manuscript). We then take the derivatives of these fitness measures with respect to the associated trait (Equations 4-5; Buhnerkempe et al. unpublished manuscript).

$$\begin{aligned}
 \frac{d\bar{r}_H}{dp} = & \frac{1}{\sum_{i=0}^K \sum_{j=0}^{K-i} (i+j)y_{(i,j)}} \sum_{i=0}^K \sum_{j=0}^{K-i} \left(y_{(i,j)} \left\{ (1-m_S) \frac{db_{obs}}{dp} i + f_S \frac{dD_S}{dp} \right\} \right. \\
 & \left. + \frac{dy_{(i,j)}}{dp} \{ (1-m_S)b_{obs}i - \mu i - (\mu + \alpha)j + f_S D_S \} \right) \\
 & - \frac{\sum_{i=0}^K \sum_{j=0}^{K-i} \frac{dy_{(i,j)}}{dp} (i+j)}{\left(\sum_{i=0}^K \sum_{j=0}^{K-i} (i+j)y_{(i,j)} \right)^2} \sum_{i=0}^K \sum_{j=0}^{K-i} y_{(i,j)} \{ (1-m_S)b_{obs}i - \mu i - (\mu + \alpha)j + f_S D_S \}
 \end{aligned} \tag{4}$$

$$\begin{aligned}
\frac{d\bar{r}_I}{d\alpha} = & \frac{1}{\sum_{i=0}^K \sum_{j=0}^{K-i} j y_{(i,j)}} \sum_{i=0}^K \sum_{j=0}^{K-i} \left(y_{(i,j)} \left\{ (1-p) \frac{d\beta_{obs}}{d\alpha} ij - j + f_I(1-p) \frac{d\beta_{obs}}{d\alpha} i D_I \right. \right. \\
& \left. \left. + f_I(1-p) \beta_{obs} i \frac{dD_I}{d\alpha} \right\} + \frac{dy_{(i,j)}}{d\alpha} \{ (1-p) \beta_{obs} ij - (\mu + \alpha) j + f_I(1-p) \beta_{obs} i D_I \} \right) \\
& - \frac{\sum_{i=0}^K \sum_{j=0}^{K-i} j \frac{dy_{(i,j)}}{d\alpha}}{\left(\sum_{i=0}^K \sum_{j=0}^{K-i} j y_{(i,j)} \right)^2} \sum_{i=0}^K \sum_{j=0}^{K-i} y_{(i,j)} \{ (1-p) \beta_{obs} ij - (\mu + \alpha) j + f_I(1-p) \beta_{obs} i D_I \} \quad (5)
\end{aligned}$$

The derivatives in the selection gradients (i.e., $dy_{(i,j)}/dp$ and $dy_{(i,j)}/d\alpha$) were calculated using a sensitivity analysis for non-linear matrix population models (Buhnerkempe et al. unpublished manuscript; [26]).

Resistance and virulence trade-offs

We assume that investment in host resistance comes at a cost of decreased reproduction, and that increased virulence not only leads to increased host mortality but increased transmission as well. In this study, we consider three different types of trade-offs. First, we use trade-off functions where the reproductive costs accelerate with increasing resistance and the benefits to transmission decelerate with increasing virulence (i.e., accelerating cost trade-offs; Equations 6 and 7 respectively; Buhnerkempe et al. unpublished manuscript; [15,16]). Here, initial increases in resistance are relatively inexpensive in terms of reproduction loss, but further increases result in larger and larger forfeiture of reproductive potential. Similarly, initial increases in virulence result in relatively large gains in transmission, but subsequent increases see diminishing transmission returns. These trade-offs are given by:

$$b_{obs} = b_{max} - \frac{(b_{max} - b_{min})p}{\{1 + \delta(1 - p)\}} \quad (6)$$

$$\beta_{obs} = \frac{\beta_{max}}{\ln 2} \ln(\alpha + 1) \quad (7)$$

where b_{max} and b_{min} give the maximum and minimum reproductive potential respectively, and β_{max} describes the maximum possible transmission rate. We assume that a pathogen with no virulence is not transmitted. δ gives the strength of the non-linearity in the trade-off function.

We also consider the case where reproductive costs and transmission benefits are constant (i.e., linear cost trade-offs; [11,16]). This leads to the following linear trade-off functions for resistance and virulence:

$$b_{obs} = b_{max} - (b_{max} - b_{min})p \quad (8)$$

$$\beta_{obs} = \beta_{max}\alpha \quad (9)$$

The third trade-off assumes that resistance comes with decelerating reproductive costs and that the transmission benefits of virulence accelerate (i.e., decelerating cost trade-offs). In this case, the initial development of resistance is relatively more expensive than subsequent increases, and gains in transmission are relatively low for low virulence but increase with increasing virulence. These trade-off functions are given by:

$$b_{obs} = b_{max} - \frac{(b_{max} - b_{min})p}{\{1 - \delta(1 - p)\}} \quad (10)$$

$$\beta_{obs} = \frac{\beta_{max}}{e - 1} (e^\alpha - 1) \quad (11)$$

Model Analysis

For all three trade-off functions, we calculate the selection gradients over a range of resistance and virulence values to determine the joint selection surfaces. We then look for effects of spatial structure by calculating these selection surfaces over different combinations of host, m_S , and pathogen dispersal strategies, m_I .

Results

Accelerating cost trade-offs

As previously seen, accelerating costs to reproduction and transmission result in coevolutionarily stable strategies when host dispersal is high (i.e., co-ESS's represented by the black dots in Figures 4.1A-B and 4.2A-B; Buhnerkempe et al. unpublished manuscript). In particular, when host dispersal is high and pathogen dispersal is low, the co-ESS occurs at intermediate resistance and relatively low virulence with a small neutral region at low resistance and high virulence levels (Figures 4.1A and 4.2A). However, as pathogen dispersal increases, the co-ESS shifts to a higher resistance and virulence with an extremely narrow neutral region (Figures 4.1B and 4.2B). No co-ESS's are observed when host dispersal is low (Figures 4.1C-D and 4.2C-D). However, the neutral zones are large when host dispersal is low (Figures 4.1C-D

and 4.2C-D), with the largest neutral region found when pathogen dispersal is also low (Figures 4.1C and 4.2C).

Linear cost trade-offs

As opposed to the accelerating trade-offs, no co-ESS's exist when trade-offs are linear (Figures 4.3 and 4.4). The selection surfaces for resistance are qualitatively similar to those found in the accelerating case (Figure 4.3), but differences in selection on virulence prevent the development of a co-ESS (Figure 4.4). Here, regions of negative selection on virulence that were observed under the accelerating cost trade-offs (i.e., Figure 4.2) do not exist (Figure 4.4). Thus, virulence is always under positive selection outside of the neutral region, which when coupled with the generally negative selection on resistance, leads to the evolution of host resistance and pathogen virulence to the neutral regions (Figures 4.3 and 4.4). However, when the host and pathogen approach a well-mixed population, coevolution will favor high resistance and maximal virulence when the host is initially relatively resistant instead of coevolution to the neutral region (Figures 4.3B and 4.4B). The neutral zones show qualitatively similar patterns to those observed under accelerating cost trade-offs with the largest neutrality regions observed when host dispersal is low (Figures 4.3 and 4.4).

Decelerating cost trade-offs

Similar to the linear case, when host resistance and pathogen virulence are under decelerating cost trade-offs for reproduction and transmission, no co-ESS combination of traits exists (Figures 4.5 and 4.6). Now, host resistance shows no regions of neutrality, and selection is always negative (Figure 4.5). Pathogen virulence, on the other hand, still exhibits regions of

neutrality similar to the linear trade-off case (Figure 4.6). Regions of positive selection on virulence and negative selection on resistance push virulence into the neutral regions (Figures 4.5 and 4.6). However, negative selection on resistance ultimately results in either evolving no resistance or evolving to combinations of resistance and virulence that promote extinction in the metapopulation (Figures 4.5 and 4.6). When pathogen dispersal is low, a greater range of virulence values can persist when the host exhibits no resistance, but increasing pathogen dispersal shrinks this range resulting in the persistence of less virulent strains (Figures 4.5 and 4.6).

Discussion

Here, we have shown that coevolutionary outcomes are affected by the interaction between metapopulation structure in the host and pathogen and the functional form of reproductive and transmission trade-offs underlying resistance and virulence, respectively. When there are accelerating costs to reproduction and transmission for resistance and virulence, respectively, co-ESS's exist when host dispersal is high that promote intermediate to high resistance and low to intermediate virulence (Buhnerkempe et al. unpublished manuscript; [4,15,16]). We note, however, the difficulty in detecting ESS's using simulation techniques [16], and we predict that co-ESS's exist when host dispersal is low and are not detected due to the relatively coarse resolution used to estimate the selection surface (Table 4.1; Buhnerkempe et al. unpublished manuscript). Contrary to the results of the accelerating cost trade-offs, linear cost trade-offs, however, do not produce co-ESS's, a phenomenon that has also been seen in models of well-mixed populations [5,17,18]. Similarly, the pattern of all-or-nothing resistance that has been previously demonstrated in single well-mixed populations is recovered as the

metapopulation approaches the well-mixed assumption [4]. However, under this trade-off assumption, models of virulence evolution within a completely structured, single host population have seen that lower virulence evolves as transmission becomes increasing local [11,16]. At the metapopulation scale, changes in selection on virulence leave only the selectively neutral regions previously observed under the accelerating cost trade-offs. Consequently, lower virulence is not guaranteed with more local transmission under linear trade-offs, and in fact, local transmission allows for potentially higher virulence due to decreased extinction risks. This result supports the notion that metapopulation structure may affect coevolutionary outcomes in a fundamentally different way than single population structure (Buhnerkempe et al. unpublished manuscript; [15,27]).

Transitioning to trade-offs with decelerating costs reveals differing sensitivities to trade-off shapes for resistance and virulence. Under this trade-off assumption, the selectively neutral regions for resistance disappeared, and selection is always negative. Here, the heavy reproductive costs of developing even small amounts of resistance make resistance too costly to maintain despite the survival benefits. This pattern is drastically different from those observed under linear and accelerating cost trade-off functions. Under these trade-off assumptions, the increase in lifetime reproduction generated by increased survival outweighs the more immediate costs associated with single reproductive events. In comparison, selection on virulence is largely unaffected by the transition from linear to decelerating costs to transmission and is instead sensitive to the transition from accelerating to linear costs. This sensitivity can be understood by knowledge of the basic reproductive ratio of the pathogen (R_0). R_0 is affected by the ratio of the transmission rate to the inverse of the infectious period, and in this case, the inverse of the infectious period is exactly the virulence, while the transmission rate is determined by the trade-

off function used. Consequently, when the relationship between transmission and virulence is convex, this ratio will be larger than one favoring epidemic spread if the population was well-mixed, which leads to fundamentally different selection on virulence from the patterns observed under endemic maintenance (i.e., $R_0 = 1$ under linear trade-offs) and pathogen fade-out (i.e., $R_0 < 1$ under decelerating cost trade-offs). However, this ratio does not take into account constraints on transmission due to local availability of susceptibles [12,16], or the effects of gene flow on selection observed by Buhnerkempe et al. (unpublished manuscript). Thus, the maximization of R_0 observed in the well-mixed case may explain the sensitivity of selection patterns to the trade-off shapes but to truly understand coevolution of host resistance and pathogen virulence in a metapopulation, it is necessary to consider effects of dispersal. However, it is not necessary to completely differentiate between concave and convex trade-offs for both traits. Rather, resistance trade-offs only need to be identified to concave vs. linear, while virulence trade-offs should be estimated to distinguish between linear and convex functional forms.

Estimating the functional forms of these trade-offs in natural systems has proven difficult however. Empirical examples of reproductive costs to resistance are primarily limited to correlational studies comparing immune function in reproductive vs. non-reproductive individuals [28,29] or comparing parasite prevalence and immune function after manipulating brood size in birds [30,31]. Studies that look at the relationship between quantitative measures of resistance and reproduction are rare [32], and only one, to our knowledge, has used a controlled selection experiment to determine how reproduction changes with evolving resistance [33]. Although informative in identifying the existence of reproductive costs to resistance, these studies do not measure reproductive output across a range of possible resistance values making

determination of the functional form of the trade-off difficult. Similarly, many correlational studies have also shown that increasing virulence results in higher transmission (for a review see [3,34]). However, other studies of the effect of virulence on transmission have found functional forms for the trade-off with transmission saturating weakly at high levels of virulence [35,36]. Consequently, although there is some evidence for accelerating costs to transmission with increasing virulence, more empirical evidence is needed to generalize the functional form of these trade-offs across systems, especially for the resistance trade-off with reproduction.

Despite a lack of knowledge on specific trade-off shapes, this work has helped to identify how trade-off shapes interact with host and pathogen metapopulation structure to influence coevolution of resistance and virulence. Hypotheses on the underlying trade-offs can then be developed from the model to inform empirical studies of resistance and virulence trade-offs. Additionally, selection on the host and pathogen is sensitive to different trade-off shapes when metapopulation structure is considered helping to narrow the potential range of trade-off shapes that need to be explored in experimental studies. By incorporating different trade-off shapes not included in previous metapopulation studies (e.g., [20-22]), our modeling framework has helped to elucidate mechanisms that may lead to the coevolutionary stability of emerging infectious diseases in metapopulations where pathogen persistence is potentially enhanced.

Table 4.2: Description of model parameters and the values used in Model parameters. Note that values given as intervals indicate the range of possible values studied.

Parameter	Description	Value(s)
m_S	Probability a newborn becomes a susceptible migrant	0.1, 0.9
m_I	Proportion of infectious material that enters the infectious migrant pool upon disease induced mortality	0.1, 0.5
p	Probability of resistance	[0,1] by 0.05
α	Virulence (i.e., disease induced mortality)	[0.01,1] by 0.05
K	Local carrying capacity	50
b_{obs}	Observed birth rate	$[b_{min}, b_{max}]$
b_{max}	Maximum possible birth rate	10
b_{min}	Minimum possible birth rate	2
β_{obs}	Observed transmission rate	$[0, \beta_{max}]$
β_{max}	Maximum possible transmission rate	0.25
μ	Natural host mortality rate	0.01
f_S	Rate at which susceptible migrants find habitable subpopulations	2.5
f_I	Rate at which infectious migrants find susceptible subpopulations	1.5
λ_S	Susceptible migrant mortality rate	0.005
λ_I	Infectious migrant mortality rate	0.005
δ	Strength of non-linearity in accelerating and decelerating cost of resistance trade-offs	0.1

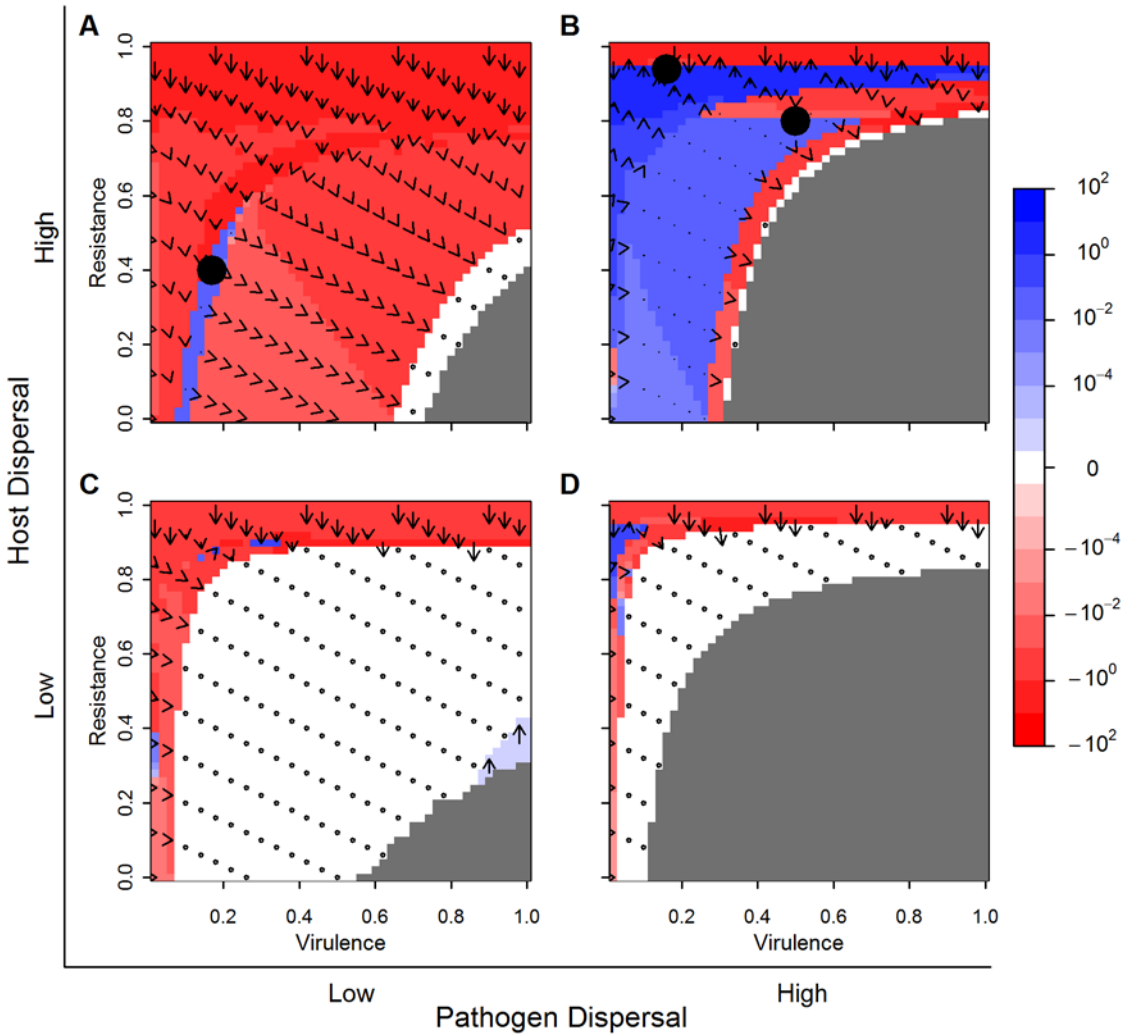


Figure 4.1: Selection gradients and coevolutionary trajectories for host resistance under accelerating costs to reproduction. Red/blue values indicate negative/positive selection. White indicates an approximately zero gradient. Dark grey denotes host extinction. Arrows give the coevolutionary trajectories across the surface with lengths scaled by the strength of selection. The large, black circles represent co-ESS's as estimated in Buhnerkempe et al. (unpublished manuscript). Metapopulation structures are defined by: (A) $m_s = 0.9$ and $m_I = 0.1$, (B) $m_s = 0.9$ and $m_I = 0.5$, (C) $m_s = 0.1$ and $m_I = 0.1$, (D) $m_s = 0.1$ and $m_I = 0.5$.

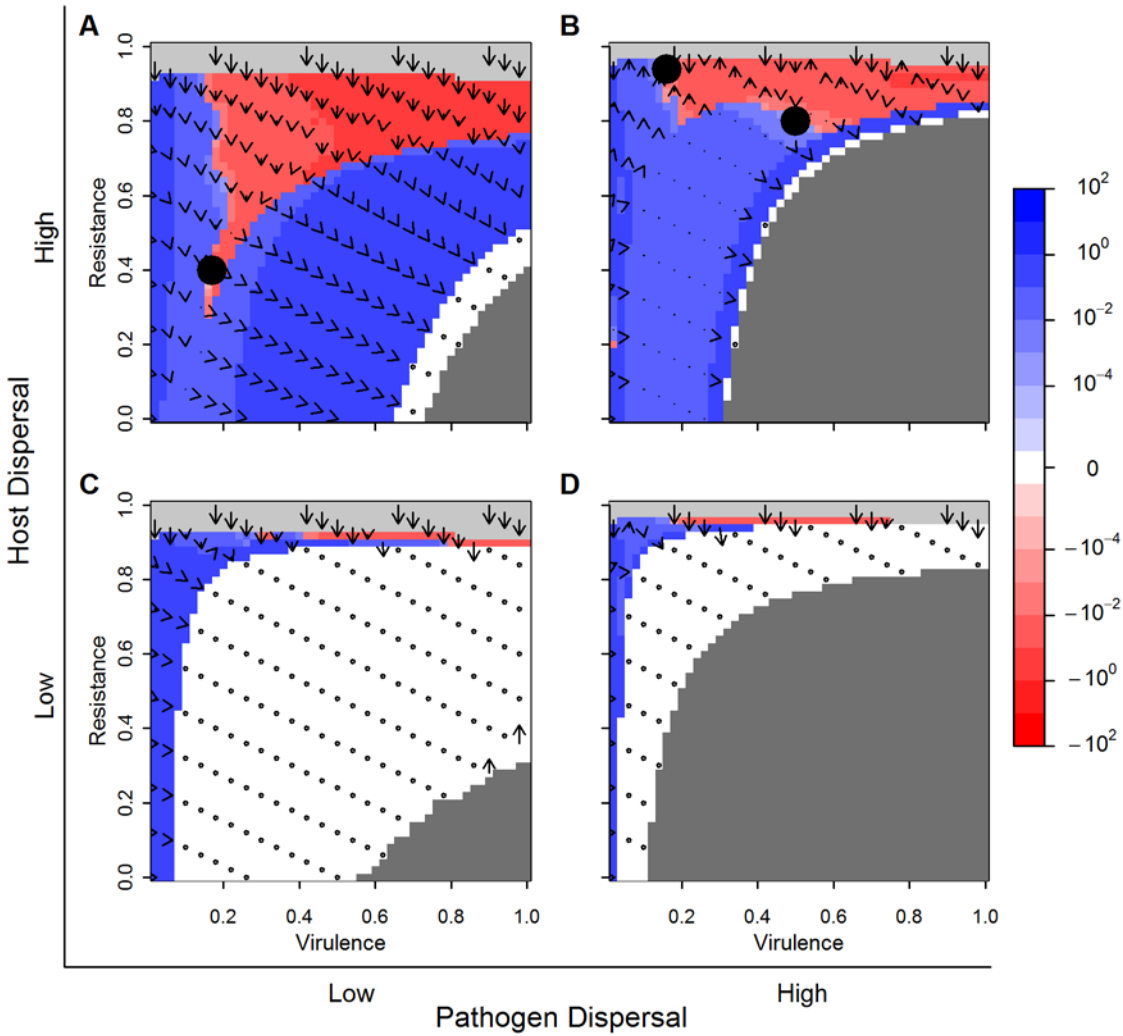


Figure 4.2: Selection gradients and coevolutionary trajectories for pathogen virulence under accelerating costs to transmission. Red/blue values indicate negative/positive selection. White indicates an approximately zero gradient. Dark and light grey denote host and pathogen extinction respectively. Arrows give the coevolutionary trajectories on the surface with lengths scaled by the strength of selection. The large, black circles represent co-ESS's estimated in Buhnerkempe et al. (unpublished manuscript). Metapopulation structures are defined by: (A)

$m_s = 0.9$ and $m_I = 0.1$, (B) $m_s = 0.9$ and $m_I = 0.5$, (C) $m_s = 0.1$ and $m_I = 0.1$, (D) $m_s = 0.1$ and $m_I = 0.5$.

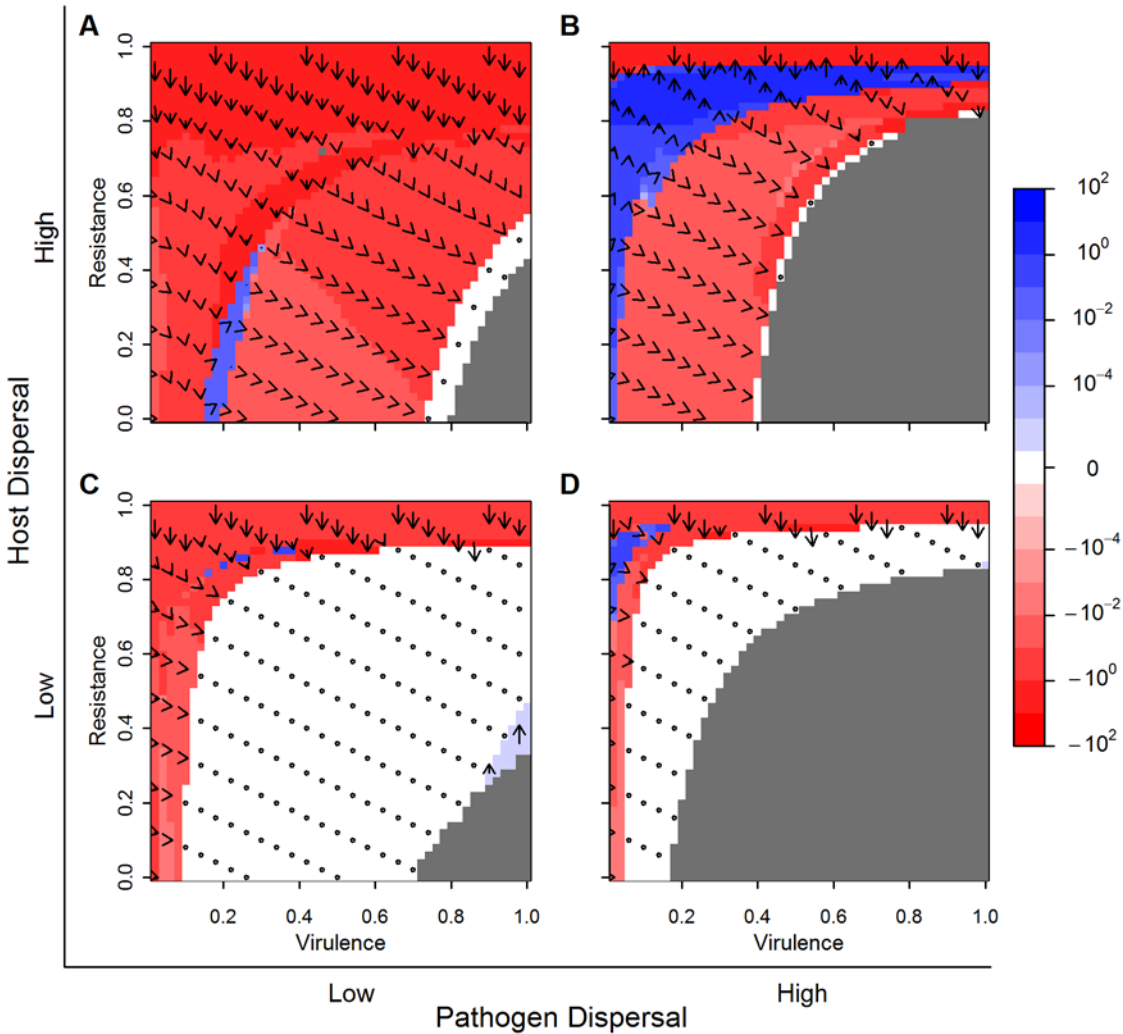


Figure 4.3: Selection gradients and coevolutionary trajectories for host resistance under linear increases in costs to reproduction. Red/blue values indicate negative/positive selection. White indicates an approximately zero gradient. Dark grey denotes host extinction. Arrows give the coevolutionary trajectories across the surface with lengths scaled by the strength of selection. For these trade-offs, there are no co-ESS's. Metapopulation structures are defined by: (A) $m_s = 0.9$ and $m_l = 0.1$, (B) $m_s = 0.9$ and $m_l = 0.5$, (C) $m_s = 0.1$ and $m_l = 0.1$, (D) $m_s = 0.1$ and $m_l = 0.5$.

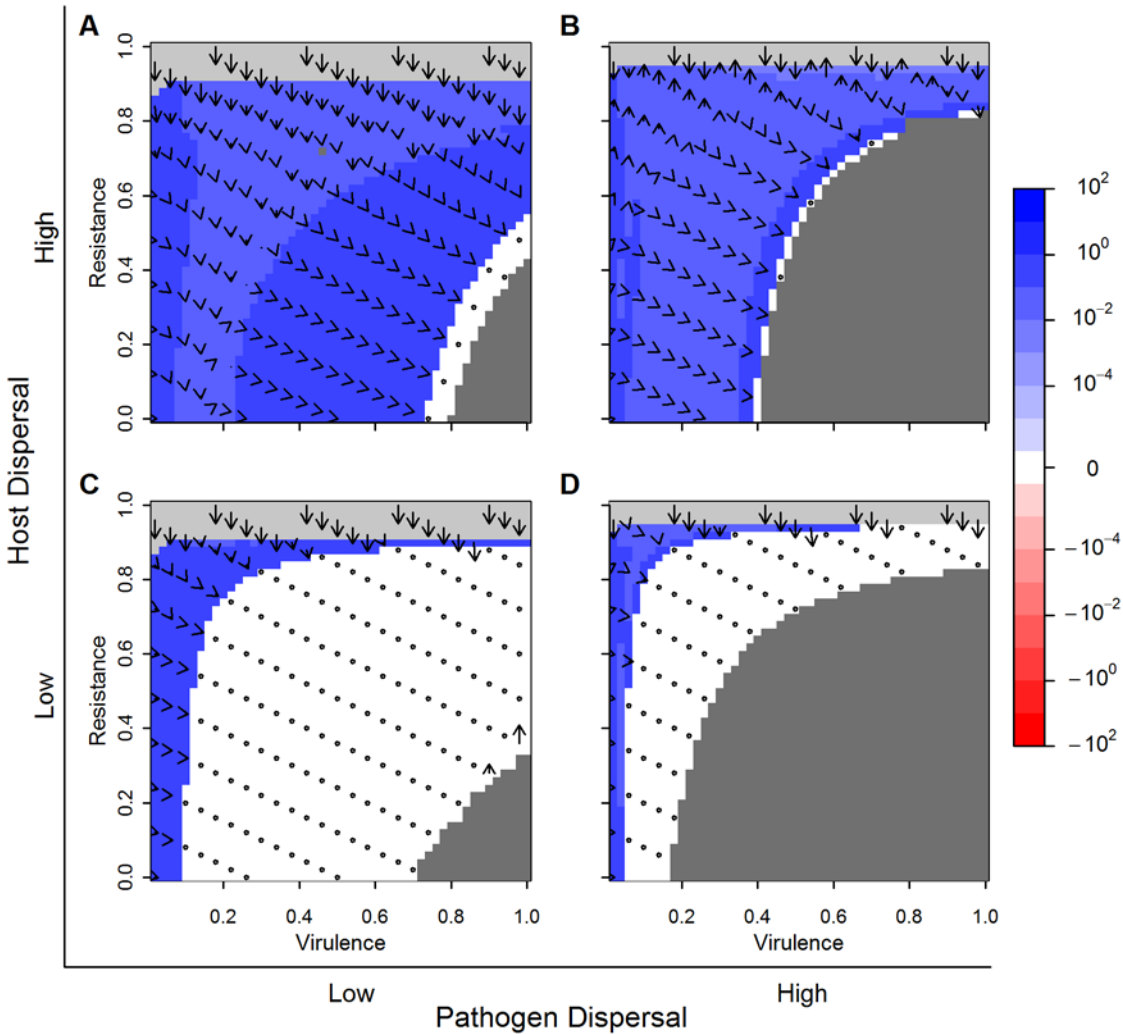


Figure 4.4: Selection gradients and coevolutionary trajectories for pathogen virulence under linear increases in costs to transmission. Red/blue values indicate negative/positive selection. White indicates an approximately zero gradient. Dark and light grey denote host and pathogen extinction respectively. Arrows give the coevolutionary trajectories across the surface with lengths scaled by the strength of selection. For these trade-offs, there are no co-ESS's. Metapopulation structures are defined by: (A) $m_s = 0.9$ and $m_I = 0.1$, (B) $m_s = 0.9$ and $m_I = 0.5$, (C) $m_s = 0.1$ and $m_I = 0.1$, (D) $m_s = 0.1$ and $m_I = 0.5$.

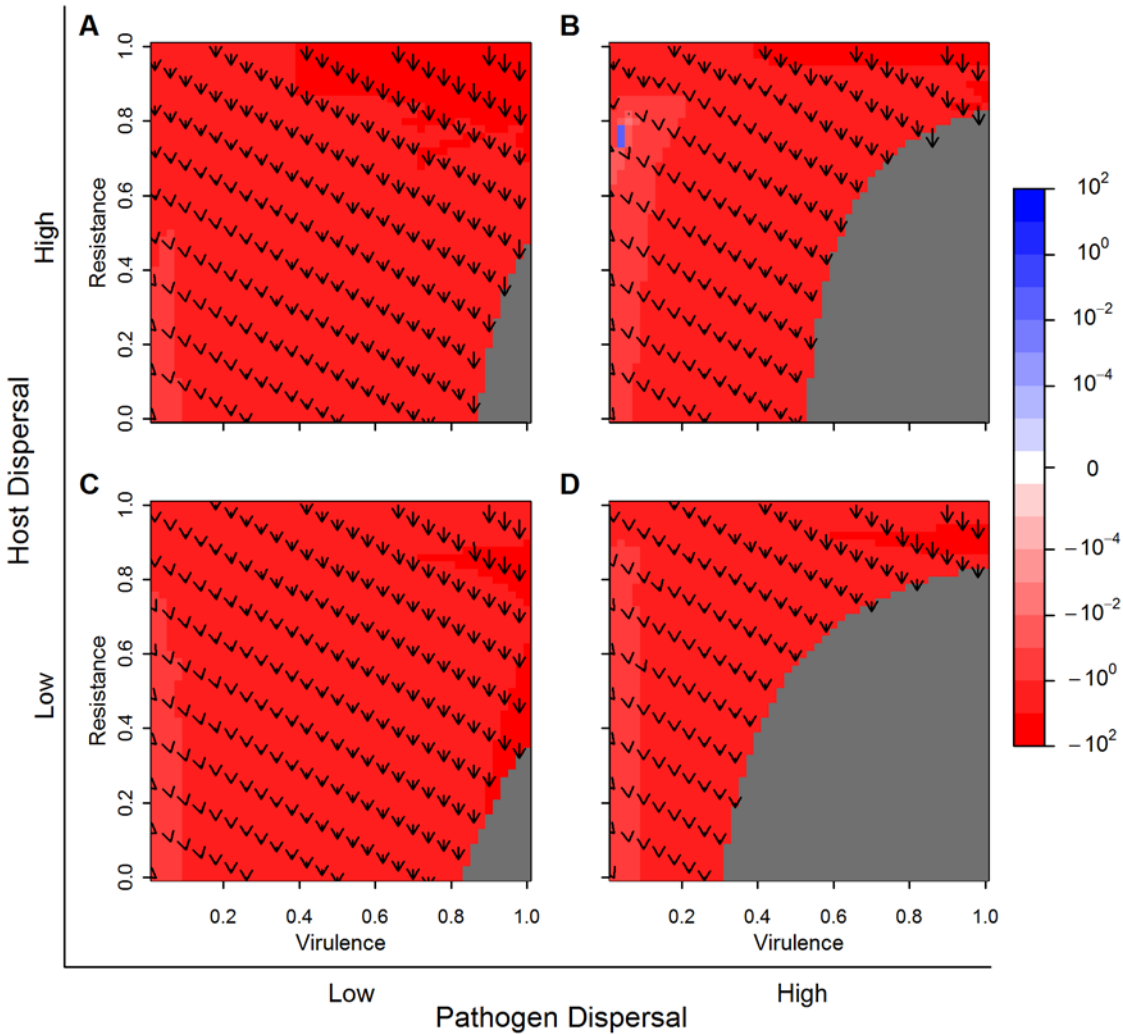


Figure 4.5: Selection gradients and coevolutionary trajectories for host resistance underdecelerating costs to reproduction. Red/blue values indicate negative/positive selection. White indicates an approximately zero gradient. Dark grey denotes host extinction. Arrows give the coevolutionary trajectories across the surface with lengths scaled by the strength of selection. For these trade-offs, there are no co-ESS's. Metapopulation structures are defined by: (A) $m_S = 0.9$ and $m_I = 0.1$, (B) $m_S = 0.9$ and $m_I = 0.5$, (C) $m_S = 0.1$ and $m_I = 0.1$, (D) $m_S = 0.1$ and $m_I = 0.5$.

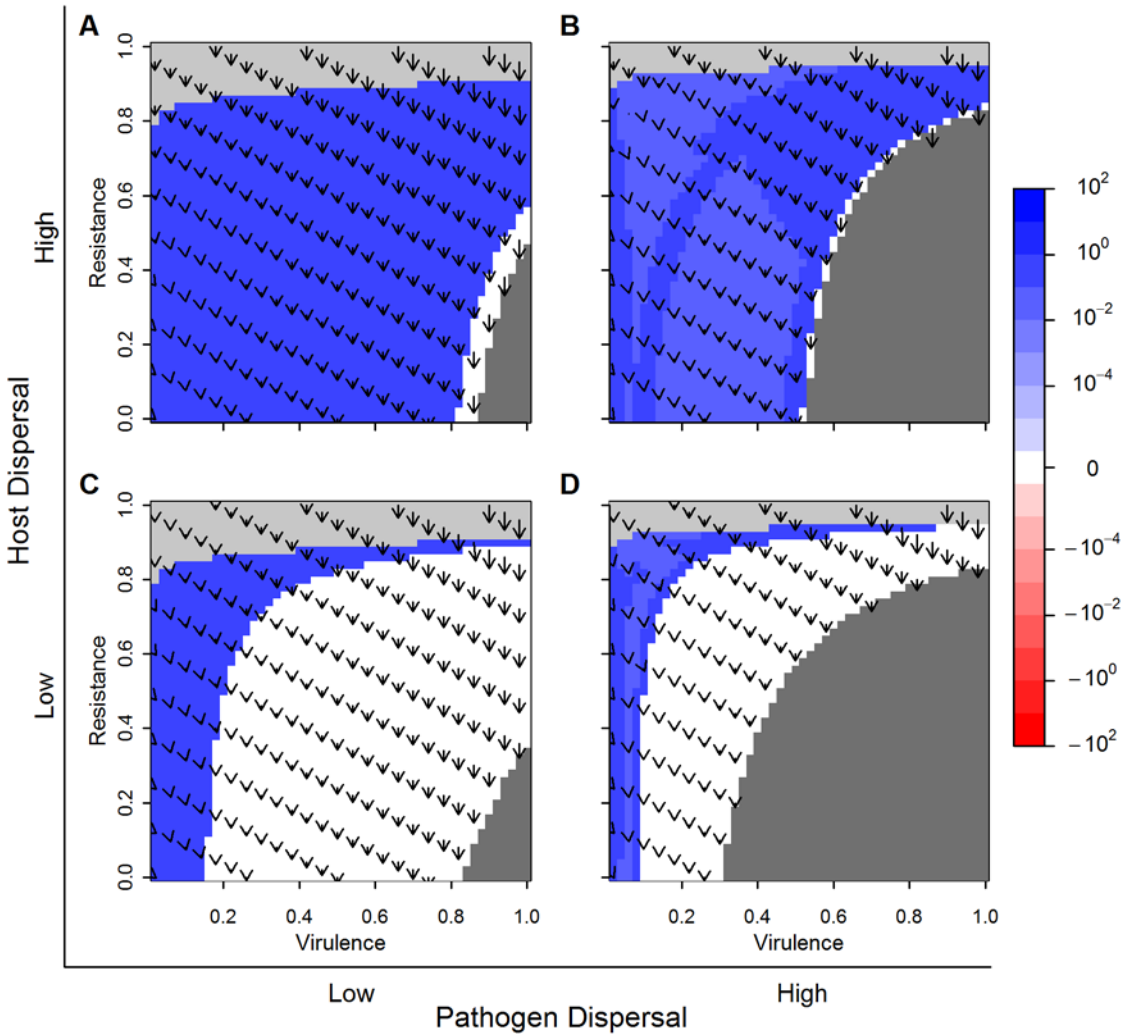


Figure 4.6: Selection gradients and coevolutionary trajectories for pathogen virulence under decelerating costs to transmission. Red/blue values indicate negative/positive selection. White indicates an approximately zero gradient. Dark and light grey denote host and pathogen extinction respectively. Arrows give the coevolutionary trajectories across the surface with lengths scaled by the strength of selection. For these trade-offs, there are no co-ESS's. Metapopulation structures are defined by: (A) $m_s = 0.9$ and $m_I = 0.1$, (B) $m_s = 0.9$ and $m_I = 0.5$, (C) $m_s = 0.1$ and $m_I = 0.1$, (D) $m_s = 0.1$ and $m_I = 0.5$.

LITERATURE CITED

- [1] Bowers, R.G., M. Boots, M. Begon, Life-history trade-offs and the evolution of pathogen resistance: competition between host strains, *Proc. R. Soc. B* 257 (1994) 247-253.
- [2] Boots, M., Y. Haraguchi, The evolution of costly resistance in host-parasite systems, *Am. Nat.* 153 (1999) 359-370.
- [3] Alizon, S., A. Hurford, N. Mideo, M. Van Baalen, Virulence evolution and the trade-off hypothesis: history, current state of affairs and the future, *J. Evolution. Biol.* 22 (2009) 245-259.
- [4] Boots, M., Y. Haraguchi, The evolution of costly resistance in host-parasite systems, *Am. Nat.* 153 (1999) 359-370.
- [5] Anderson, R.M., R.M. May, Coevolution of hosts and pathogens, *Parasitology* 85 (1982) 411-426.
- [6] May, R.M., R.M. Anderson, Epidemiology and genetics in the coevolution of pathogens and hosts, *Proc. R. Soc. B* 219 (1983) 281-313.
- [7] Bremermann, H.J., J. Pickering, A game-theoretical model of pathogen virulence, *J. Theor. Biol.* 100 (1983) 411-426.
- [8] Ganusov, V.V., R. Antia, Trade-offs and the evolution of virulence of micropathogens: do details matter?, *Theor. Pop. Biol.* 64 (2003) 211-220.
- [9] Koella, J.C., C. Boëte, A model for the coevolution of immunity and immune evasion in vector-borne diseases with implications for the epidemiology of malaria, *Am. Nat.* 161 (2003) 698-707.
- [10] Best, A., A. White, M. Boots, The implications of coevolutionary dynamics to host-parasite interactions, *Am. Nat.* 173 (2009) 779-791.
- [11] Boots, M., A. Sasaki, 'Small worlds' and the evolution of virulence: infection occurs locally and at a distance, *Proc. R. Soc. B* 266 (1999) 1933-1938.
- [12] Haraguchi, Y., A. Sasaki, The evolution of pathogen virulence and transmission rate in a spatially structured population, *J. Theor. Biol.* 203 (2000) 85-96.
- [13] Boots, M., P.J. Hudson, A. Sasaki, Large shifts in pathogen virulence relate to host population structure, *Science* 303 (2004) 842-844.
- [14] Lion, S., M. Boots, Are pathogens "prudent" in space?, *Ecol. Lett.* 13 (2010) 1245-1255.

- [15] Best, A., S. Webb, A. White, M. Boots, Host resistance and coevolution in spatially structured populations, *Proc. R. Soc. B* 278 (2011) 2216-2222.
- [16] Kamo, M., A. Sasaki, M. Boots, The role of trade-off shapes in the evolution of parasites in spatial host populations: an approximate analytical approach, *J. Theor. Biol.* 244 (2007) 588-596.
- [17] van Baalen, M., M.W. Sabelis, The dynamics of multiple infection and the evolution of virulence, *Am. Nat.* 146 (1995) 881-910.
- [18] Frank, S, Models of parasite virulence, *Q. Rev. Biol.* 71 (1996) 37-78.
- [19] Thompson, J.N., J.J. Burdon, Gene-for-gene coevolution between plants and parasites, *Nature* 360 (1992) 121-125.
- [20] Gandon, S., Y. Capowiez, Y. Dubois, Y. Michalakis, I. Olivieri, Local adaptation and gene-for-gene coevolution in a metapopulation model, *Proc. R. Soc. B* 263 (1996) 1003-1009.
- [21] Gandon, S., Local adaptation and the geometry of host-parasite coevolution, *Ecol. Lett.* 5 (2002) 246-256.
- [22] Thrall, P.H., J.J. Burdon, Evolution of gene-for-gene systems in metapopulations: the effect of spatial scale of host and pathogen dispersal, *Plant Pathol.* 51 (2002) 169-184.
- [23] Nuismer, S., Parasite local adaptation in a geographic mosaic, *Evolution* 60 (2006) 24-30.
- [24] Metz, J.A.J., M. Gyllenberg, How should we define fitness in structured metapopulation models? Including an application to the calculation of evolutionarily stable dispersal strategies, *Proc. R. Soc. B* 268 (2001) 499-508.
- [25] Gyllenberg, M., J.A.J. Metz, On fitness in structured metapopulations, *J. Math. Biol.* 43 (2001) 545-560.
- [26] Verdy, A., H. Caswell, Sensitivity analysis of reactive ecological dynamics, *B. Math. Biol.* 70 (2008) 1634-1659.
- [27] Lion, S., M. van Baalen, Self-structuring in spatial evolutionary ecology, *Ecol. Lett.* 11 (2008) 277-295.
- [28] Festa-Bianchet, M, Individual differences, parasites, and the costs of reproduction for bighorn ewes (*Ovis canadensis*), *J. Anim. Ecol.* 58 (1989) 785-795.
- [29] Adamo, S.A., M. Jensen, M. Younger, Changes in lifetime immunocompetence in male and female *Gryllus texensis* (formerly *G. integer*): trade-offs between immunity and reproduction, *Anim. Behav.* 62 (2001) 417-425.

- [30] Gustafsson, L., D. Nordling, M.S. Andersson, B.C. Sheldon, A. Qvarnström, Infectious diseases, reproductive effort and the cost of reproduction in birds, *Philos. Trans. R. Soc. B.* 346 (1994) 323-331.
- [31] Norris, K., M. Anwar, A.F. Read, Reproductive effort influences the prevalence of haematozoan parasites in great tits, *J. Anim. Ecol.* 63 (1994) 601-610.
- [32] Gwynn, D.M., A. Callaghan, J. Gorham, K.F.A. Walters, M.D.E. Fellowes, Resistance is costly: trade-offs between immunity, fecundity and survival in the pea aphid, *Proc. R. Soc. B* 272 (2005) 1803-1808.
- [33] Boots, M., M. Begon, Trade-offs with resistance to a granulosis virus in the Indian meal moth, examined by a laboratory evolution experiment, *Funct. Ecol.* 7 (1993) 528-534.
- [34] Lipsitch, M., E.R. Moxon, Virulence and transmissibility of pathogens: what is the relationship?, *Trends Microbiol.* 5 (1997) 31-37.
- [35] Fraser, C., T.D. Hollingsworth, R. Chapman, F. de Wolf, W.P. Hanage, Variation in HIV-1 set-point viral load: epidemiological analysis and an evolutionary hypothesis, *PNAS* 104 (2007) 17441-17446.
- [38] de Roode, J.C., A.J. Yates, S. Altizer, Virulence-transmission trade-offs and population divergence in virulence in a naturally occurring butterfly parasite, *PNAS* 105 (2008) 7489-7494.

CHAPTER 5

GENERAL CONCLUSIONS

In this dissertation, I have explored ecological and evolutionary mechanisms underlying the persistence of highly virulent pathogens. As outlined in Chapter 1, the primary aims of this dissertation were to study the role of metapopulation structure in enabling the continued maintenance of virulent pathogens in highly susceptible hosts. Consequently, it is vital to understand how different transmission mechanisms alter the dispersal and spatial structure of the pathogen relative to the host and create coevolutionary outcomes that may not be observed in models of a well-mixed host-pathogen population.

Chapter 2 uses plague in North America as an example to study the role of different transmission mechanisms in a system where metapopulation structure is believed to lead to regional persistence of a highly virulent pathogen (Snäll et al. 2008; George 2009). By developing a mechanistic model of plague dynamics parameterized for an epizootic host (i.e., black-tailed prairie dogs) and an enzootic host (i.e., California ground squirrels), I have shown that species-specific responses to *Y. pestis* infection at the single population level can be driven by shifts in transmission dynamics. In particular, epizootic dynamics require large amounts of on-host cycling of fleas to maintain continuous transmission chains in the local population. Enzootics, however, rely on an off-host, questing flea reservoir to sustain *Y. pestis* infection in the population. As a consequence of this reservoir, the pathogen is not dependent on its host for movement between local populations, and spatial structure in the pathogen may differ considerably from that of the host.

To study how host and pathogen dispersal strategies interact to determine coevolutionary maintenance of the highly virulent plague bacterium within highly susceptible hosts, it is necessary to model quantitative trait coevolution in a metapopulation. However, until this point, no such modeling framework existed to address this issue. In Chapter 3, I developed a novel modeling approach to coevolution in a metapopulation. This work points to the role interactions between host and pathogen dispersal strategies play in shaping coevolution of host resistance and pathogen virulence. As speculated in Chapter 3, prairie dogs and *Y. pestis* may have highly localized metapopulation structures when compared to species like the California ground squirrel promoting neutrality in selection for host resistance and pathogen virulence in prairie dogs, and as a consequence, the evolution of resistance will take longer with the potential for genetic drift to subsequently eliminate resistance. In addition, we observed in Chapter 4 how life-history trade-offs in both the host and pathogen may affect coevolutionary outcomes. Specifically, metapopulation structure in the host and pathogen can interact with the functional form of these trade-offs resulting in vastly different coevolutionary trajectories. Measuring the shape of resistance and virulence trade-offs in natural systems has proven difficult, and no work has been done on plague in North America to inform these trade-offs. Consequently, this modeling framework can provide hypotheses on the relationship between resistance and reproduction and virulence and transmission. We speculate that both resistance and virulence show accelerating cost trade-off functions in the plague system.

However, plague does not fit ideally within the current theoretical model. Specifically, *Y. pestis* in hosts with higher dispersal, like California ground squirrels, is predicted to potentially develop decreased virulence, which is not observed in natural systems. Thus, to provide a more complete understanding of why the plague bacterium has remained highly virulent with host

species that are highly variable in their response, the theory developed in Chapters 3 and 4 needs to be adapted to include system-specific details. In particular, Chapter 3 assumes equal connections between all subpopulations, but the explicit spatial arrangement of populations is likely to play a large role in host dispersal and plague dynamics (George 2009). Additionally, although Chapter 2 established that pathogen dispersal can be separated from dispersal of a specific host, the actual mechanism underlying such dispersal may be important for determining the spatial pattern and scale of between population spread of *Y. pestis*. In particular, multiple carnivore species are thought to transport infected fleas between host subpopulations (Gage et al. 1994) and may act as reservoirs for the plague bacterium themselves (Salkeld and Stapp 2006). The role of carnivores is in contrast to the typical assumption of alternate, small mammal host species acting as a reservoir for *Y. pestis* (e.g., grasshopper mice, *Onychomys leucogaster*; Thomas 1988; Gage and Kosoy 2005). Movement of fleas via carnivores would result in longer distance dispersal patterns than the more wave-like spread that might be expected under movement by other small mammals.

Incorporation of the biological realisms specific to plague in North America quickly increases the complexity of the model beyond what the framework in Chapter 3 was designed to explore. Future attempts to model coevolution of *Y. pestis* in spatially structured host species will most likely require an individual-based modeling approach. This approach allows for explicit designation of the spatial structure in the host and corresponding dispersal patterns. Movement of fleas can then be overlaid on this landscape with different spread patterns representing different transport hypotheses (e.g., carnivores vs. alternate, small mammal hosts). Different trade-off hypotheses can also be incorporated to gain a more complete understanding of host resistance and *Y. pestis* virulence and their coevolution. Although the complexities involved in such a

system-specific model can potentially hamper interpretation, the intuition gained through the theoretical developments in Chapters 3 and 4 should serve to guide model analysis and subsequent empirical tests of hypotheses identified through continued modeling efforts.

LITERATURE CITED

- Snäll, T., R.B. O'Hara, C. Ray, and S.K. Collinge. 2008. Climate-driven spatial dynamics of plague among prairie dog colonies. *American Naturalist* 171: 238-248.
- George, D. 2009 Pathogen persistence in wildlife populations: Case studies of plague in prairie dogs and rabies in bats. PhD Thesis, Colorado State University.
- Gage, K.L., J.A. Montenieri, and R.E. Thomas. 1994. The role of predators in the ecology, epidemiology, and surveillance of plague in the United States. *Proceedings of the 16th Vertebrate Pest Conference 1994*. Pgs. 200-206.
- Salkeld, D.J., and P. Stapp. 2006. Seroprevalence rates and transmission of plague (*Yersinia pestis*) in mammalian carnivores. *Vector-Borne and Zoonotic Diseases* 6: 231-239.
- Thomas, R.E. 1988. A review of flea collection records from *Onychomys leucogaster* with observations on the role of grasshopper mice in the epizootology of wild rodent plague. *Great Basin Naturalist* 48: 83-95.
- Gage, K.L., and M.Y. Kosoy. 2005. Natural history of plague: perspectives from more than a century of research. *Annual Review of Entomology* 50: 505-528.